

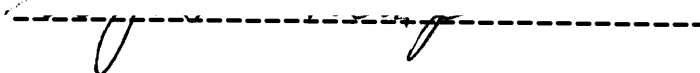
AN ABSTRACT OF THE THESIS OF

Hiraz Kekobad Medhora for the degree of Master of  
-----  
Science in Forest Products presented on January 8, 1987.  
-----

Title: Reaction Kinetic Study and Determination of  
-----  
Controlling Resistances during Alkaline Sulfite/  
-----  
Anthraquinone Pulping Process.  
-----

Signature redacted for privacy.

Abstract Approved :

A handwritten signature in black ink, appearing to be a stylized name, is written over a horizontal dashed line.

A survey of the pulping literature indicated that although the kinetics of the Kraft Pulping process has been studied in detail , very few studies have been reported for Alkaline Sulfite / Anthraquinone (ASAQ) pulping process. There is no existing rate model for this pulping process. Hence, the objectives of this thesis were to obtain a kinetic rate data and to determine the controlling resistances for this process.

Delignification rate data were obtained using a softwood - chip mixture containing balsam, spruce, and northern pine. Time, temperature, and chip size were chosen as the independent variables in this study. The concentrations of pulping chemicals were kept constant during the cooks. The rate data obtained was then analyzed using different techniques to establish

the controlling resistances during this process.

From the results obtained, it was concluded that during this process, ASAQ delignification occurs in the mixed regime with internal diffusion resistance and chemical reaction resistance controlling the rate of reaction. The internal diffusion resistance is the prominent resistance for most of the chip sizes used in this study. The smallest chip size, however, shows that chemical reaction resistance is prominent in this case. Since the chips used in this study are smaller than the commercial chips, we expect that the rate of delignification for commercial pulping is controlled mainly by internal diffusion although the delignification reaction itself becomes important for the smaller chips, and at higher conversions.

Reaction Kinetic Study and  
Determination of Controlling Resistances  
During Alkaline Sulfite/Anthraquinone Pulping

by

Hiraz Kekobad Medhora

A THESIS

submitted to

Oregon State University

in partial fulfillment of

the requirements for the

degree of

Master of Science

Completed January 8, 1987

Commencement June 1987

APPROVED:

Signature redacted for privacy.

-----  
Professor of Forest Products in charge of major

Signature redacted for privacy.

-----  
Head of Department of Forest Products

Signature redacted for privacy.

-----  
Dean of Graduate School

Date thesis is presented

January 8, 1987  
-----

Typed by

Hiraz Kekobad Medhora  
-----

## ACKNOWLEDGEMENTS

I would like to express my heartfelt thanks and appreciation to Dr. W. J. Frederick, Jr. for his skillful guidance, advice, support and inspiration during this Master's thesis study.

I am grateful to the members of my advisory committee for their suggestions and consultations.

I wish to thank Mr. Jerry Hull (Exptl. Biol. Tech., Forest Research Lab) for his technical assistance in performing the experimental part of my study and for the maintenance of the experimental equipment.

I would also like to thank my parents and my entire family who were a constant source of inspiration and encouragement during this work.

Finally, I would like to express my deepest gratitude to Dr. Al Wong (Arbokem, Inc.) for financial support for this research project, which gave me an excellent opportunity to pursue my chosen field of interest.

## TABLE OF CONTENTS

CHAPTER	PAGE
INTRODUCTION .....	1
1. PULPING TECHNOLOGY .....	1
2. PULPING RATE STUDIES .....	7
THEORY SECTION .....	13
EXPERIMENTAL DESIGN SECTION .....	44
EXPERIMENTAL PROCEDURES SECTION .....	50
WOOD SUPPLY .....	50
PULPING EXPERIMENTS .....	51
PULP ANALYSIS .....	56
RESULTS SECTION .....	59
CONCLUSIONS .....	88
BIBLIOGRAPHY .....	89
APPENDIX	
1.SAMPLE CALCULATIONS .....	92

## LIST OF FIGURES.

FIGURE	PAGE
1. Refining energy inputs and pulp properties for kraft versus alkaline sulfite anthraquinone pulps.	5
2. Plot of soluble reactant concentration versus position to show steady state concentration profiles for the different resistances controlling the overall rate of reaction.	19
3. Plot of effective diffusivity ( $D/D_0$ ) versus yield for pulped wood at pH 13.2.	34
4. Plot of $E_{ax}$ , $E_{ay}$ , and $E_{az}$ versus $(Dt/a^2)$ drawn on the basis of the solution of unsteady state diffusion equation for a slab, cylinder, and spherical geometries.	39
5. Calibration curve between kappa number and lignin (% on pulp) of pulps.	58
6. Plot of $f(X_c, X_a)$ versus $t/t_a$ of Wilder & Daleski's delignification rate data.	64
7. Plot of $f(X_c, X_a)$ versus $t/t_a$ ; Olm and Tistad's delignification rate data; temperature = $313^{\circ}\text{K}$ .	66
8. Plot of $f(X_c, X_a)$ versus $t/t_a$ ; $d_e=0.72$ cms; all geometries; finite heat-up method of pulping.	68
9. Plot of $f(X_c, X_a)$ versus $t/t_a$ ; $d_e=0.28$ cms; long cylinder geometry; finite heat-up method of pulping.	69
10. Plot of $f(X_c, X_a)$ versus $t/t_a$ ; $d_e=0.72$ cms; all geometries; isothermal method of pulping.	70
11. Plot of $f(X_c, X_a)$ versus $t/t_a$ ; $d_e=0.11$ cms; operating temperature = $435^{\circ}\text{K}$ ; isothermal method of pulping; spherical geometry.	71
12. Plot of $f(X)$ versus $t/R^2$ ; $d_e=0.72$ cms.	75
13. Plot of $f(X)/\text{Effective Diffusivity}$ versus $t/R^2$ ; $d_e=0.72$ cms.	76

LIST OF FIGURES (contd.)

	FIGURE	PAGE
14.	Plot of $f(X)/\text{Effective Diffusivity}$ versus $t/R^2$ ; $d_e=0.43$ cms.	77
15.	Plot of $f(X)/\text{Effective Diffusivity}$ versus $t/R^2$ ; $d_e=0.28$ cms.	78
16.	Plot of $f(X)/\text{Effective Diffusivity}$ versus $t/R^2$ ; $d_e=0.20$ cms.	79
17.	Plot of $f(X)/\text{Effective Diffusivity}$ versus $t/R^2$ ; $d_e=0.11$ cms.	80
18.	Plot of $\ln(1/t_n)$ , where ( $n = 13.50\%$ ) versus $1/T$ for calculation of activation energy of Olm and Tistad's delignification rate data.	83
19.	Plot of $\ln(1/t_n)$ , where ( $n = 56.8\%$ , $38.8\%$ , and $24.4\%$ ) versus $1/T$ for calculation of activation energy. Isothermal method of Pulping data; $d_e=0.28$ cms.	84



LIST OF TABLES.

TABLE	PAGE
1. "Shrinking Core" Heterogenous Reaction models for various geometries, $f(X_c, X_a)$ (10).	27
2. Effective diffusivity ( $D/D_0$ ) values in the longitudinal, radial, and tangential directions for various wood species.	37
3. Average values of the size measurements of five chip sizes used in the experiments.	52
4. Lignin contents of the five chip sizes used in this study.	53
5. Typical moisture content data for chips stored at 50 % R.H., and 72 <sup>o</sup> F.	54
6. Estimated Biot Numbers at the beginning and at the end of the cooks. Isothermal method of pulping.	60
7. Table of Damkohler numbers at the beginning and at the end of the cooks. Isothermal method of pulping.	62
8. Table of mean square regression ( $r^2$ ) values for $f(x)/D/D_0$ versus $t/R^2$ in figures 12-17.	81
9. Table of activation energy values (k cal) of various chip sizes and at various lignin, L(% on wood).	86
A-1. Pulping data # 1 of "Finite Heat-Up method of pulping"; Maximum Temperature = 438 <sup>o</sup> K; Time at maximum temperature = 0 minutes.	104
A-2. Pulping data # 2 of "Finite Heat-Up method of pulping"; Maximum Temperature = 438 <sup>o</sup> K; Time at maximum temperature = 20 minutes.	105
A-3. Pulping data # 3 of "Finite Heat-Up method of pulping"; Maximum Temperature = 438 <sup>o</sup> K; Time at maximum temperature = 60 minutes.	106
A-4. Pulping data # 4 of "Finite Heat-Up method of pulping"; Maximum Temperature = 438 <sup>o</sup> K; Time at maximum temperature = 180 minutes.	107

LIST OF TABLES (contd.)

	TABLE	PAGE
A-5.	Pulping data # 1 of "Isothermal Method of pulping"; Constant Temperature = 435 <sup>0</sup> K; Time at constant temperature = 10 minutes.	108
A-6.	Pulping data # 2 of "Isothermal Method of pulping"; Constant Temperature = 435 <sup>0</sup> K; Time at constant temperature = 20 minutes.	109
A-7.	Pulping data # 3 of "Isothermal method of pulping"; Constant Temperature = 435 <sup>0</sup> K; Time at constant temperature = 30 minutes.	110
A-8.	Pulping data # 4 of "Isothermal method of pulping"; Constant Temperature = 435 <sup>0</sup> K; Time at constant temperature = 60 minutes.	111
A-9.	Pulping data # 5 of "Isothermal method of pulping"; Constant Temperature = 444 <sup>0</sup> K; Time at constant temperature = 10 minutes.	112
A-10.	Pulping data # 6 of "Isothermal method of pulping"; Constant Temperature = 444 <sup>0</sup> K; Time at constant temperature = 20 minutes.	113
A-11.	Pulping data # 7 of "Isothermal method of pulping"; Constant Temperature = 444 <sup>0</sup> K; Time at constant temperature = 30 minutes.	114
A-12.	Pulping data # 8 of "Isothermal method of pulping"; Constant Temperature = 444 <sup>0</sup> K; Time at constant temperature = 60 minutes.	115
A-13.	Pulping data # 9 of "Isothermal method of pulping"; Constant Temperature = 453 <sup>0</sup> K; Time at constant temperature = 10 minutes.	116
A-14.	Pulping data # 10 of "Isothermal method of pulping"; Constant Temperature = 453 <sup>0</sup> K; Time at constant temperature = 20 minutes.	117
A-15.	Pulping data # 11 of "Isothermal method of pulping"; Constant Temperature = 453 <sup>0</sup> K; Time at constant temperature = 30 minutes.	118
A-16.	Pulping data # 12 of "Isothermal method of pulping"; Constant Temperature = 453 <sup>0</sup> K; Time at constant temperature = 75 minutes.	119
A-17.	Lignin versus Kappa calibration.	120

LIST OF TABLES (contd.)

	TABLE	PAGE
A-18.	Shrinking Core Models data for the analysis of Wilder & Daleski's delignification rate data; Temperature of pulping= 423 <sup>0</sup> K; Refernce time, t <sub>a</sub> =105 minutes.	121
A-19.	Shrinking Core Models for the analysis of Olm and Tistad's delignification rate data ; Operating Temperature = 313 <sup>0</sup> K; ta = 14 minutes.	122
A-20.	Shrinking Core Models for the analysis of the finite heat-Up Method of pulping data; chip size de=0.72 cms; Temperature=438 <sup>0</sup> K; ta=180 minutes.	123
A-21.	Shrinking Core Models for the analysis of the Isothermal method of pulping data; chip size, de=0.43 cms; Temperature=438 <sup>0</sup> K; Long Cylinder Geometry; t <sub>a</sub> = 180 minutes.	124
A-22.	Shrinking Core Models for the analysis of the Isothermal method of pulping data; chip size, de=0.72 cms; Temperature=444 <sup>0</sup> K; ta=60 minutes; t <sub>o</sub> =10 minutes.	125
A-23.	Shrinking Core Models for the analysis of the Isothermal method of Pulping data; chip size, de=0.11 cms; Temperature=435 <sup>0</sup> K; Spherical geometry; ta=60 minutes; to=10 minutes;	126
A-24.	Table # 1 of "Accounting for time variable diffusivity". Isothermal method of pulping; chip size, de=0.72 cms; R <sup>2</sup> =0.13 cm <sup>2</sup> .	127
A-25.	Table # 2 of " Accounting for time variable diffusivity"; Isothermal method of pulping; chip size, de=0.72 cms; R <sup>2</sup> =0.13 cm <sup>2</sup> .	128
A-26.	Table # 3 of "Accounting for time variable diffusivity"; Isothermal method of pulping; chip size, de=0.43 cms; R <sup>2</sup> =0.0.046 cm <sup>2</sup> .	129
A-27.	Table # 4 of "Accounting for time variable diffusivity"; Isothermal method of pulping; chip size, de=0.28 cms; R <sup>2</sup> =0.020 cm <sup>2</sup> .	130

LIST OF TABLES (contd.)

	TABLE	PAGE
A-28.	Table # 5 of "Accounting for time variable diffusivity"; Isothermal method of pulping; chip size, $d_e=0.20$ cms; $R^2=0.010$ cm <sup>2</sup> .	131
A-29.	Table # 6 of "Accounting for time variable diffusivity"; Isothermal method of pulping; chip size, $d_e=0.11$ cms; $R^2=0.003$ cm <sup>2</sup> .	132
A-30.	Table to calculate Activation Energies of Olm and Tistad's delignification rate data.(23).	133
A-31.	Table to calculate Activation Energies of the isothermal Method of Pulping data; Chip size, $d_e = 0.28$ cms.	134

## NOMENCLATURE

- $A$  = Arrhenius' pre - exponential factor,  $(\text{mass})^{n-1}(\text{time})$
- $A_s$  = Surface area of solid phase,  $(\text{length})^2$
- $b$  = Stoichiometric coefficient for solid phase reactant
- $C_{a,b}$  = Concentration of constituent "a" in the bulk fluid,  $(\text{mass}/\text{length}^3)$
- $C_{a,g}$  = Concentration of constituent "a" in the bulk phase,  $(\text{mass}/\text{length}^3)$
- $C_{a,i}$  = Concentration of constituent "a" at the center of solid,  $(\text{mass}/\text{length}^3)$ .
- $C_{a,s}$  = Concentration of constituent "a" at the solid interface,  $(\text{mass}/\text{length}^3)$
- $C^*$  = Characteristic Concentration of constituent "a" (usually initial or bulk concentration)  $(\text{mass}/(\text{length}^3 \cdot \text{time}))$ .
- $C_{p,b}$  = Concentration of the delignifying agent in the bulk phase,  $(\text{mass}/\text{length}^3)$
- $D$  = diffusivity of  $[\text{OH}]^-$  in the liquor within the porous solid,  $(\text{length}^2/\text{time})$
- $D_0$  = diffusivity of  $[\text{OH}]^-$  in the same liquor in the absence of a porous solid,  $(\text{length}^2/\text{time})$
- $D_a$  = diffusivity of constituent "a",  $(\text{length}^2/\text{time})$
- $-dL/dt$  = overall rate of disappearance (delignification), or conversion of part of solid phase (lignin).
- $(-dL/dt)_{\text{init.}}$  = rate of delignification during the initial period,  $(\% \text{ on wood})/\text{mins}$
- $(-dL/dt)_{\text{fin.}}$  = rate of delignification during the final period,  $(\% \text{ on wood})/\text{mins}$
- $(D_k)_{\text{init.}}$  = Damkohler number during initial period of delignification.
- $(D_k)_{\text{fin.}}$  = Damkohler number during final period of delignification.

$d_e$  = equivalent diameter (length)  
 $E_a$  = Arrhenius' Activation energy, (energy/mass)  
 $E_{ax}$ ,  $E_{ay}$ ,  $E_{az}$  = Solutions to Fick's Second law of diffusion for the x, y, and z directions.  
 $k$  = reaction rate constant, ( $\text{time}^{-1}$ )  
 $k_B$  = bulk to surface mass transfer coefficient, (length/time)  
 $k_L$  = convective mass transfer coefficient, (length/time)  
 $k_S$  = mass transfer coefficient in solid phase, (length/time)  
 $l$  = diffusion path length, (length)  
 $L$  = Residual lignin content (% on wood) in the solid phase after time  $t$  (mins).  
 $L_0$  = Initial lignin content (% on wood) in the solid phase.  
 $(L)_{\text{init.}}$  = average lignin content in solid phase during initial period of delignification (% on wood).  
 $(L)_{\text{fin.}}$  = average lignin content in solid phase during final period of delignification (% on wood).  
 $(N_a)_r$  = mass flux due to chemical reaction, ( $\text{mass}/(\text{length}^2 \cdot \text{time})$ ).  
 $(N_a)_d$  = diffusive mass flux, ( $\text{mass}/(\text{length}^2 \cdot \text{time})$ ).  
 $N_L$  = moles of lignin in the solid phase, disappearing with time, ( $\text{mass}/\text{length}^2 \cdot \text{time}$ )  
 $(N_a)_c$  = Convective mass flux, ( $\text{mass}/(\text{length}^2 \cdot \text{time})$ )  
 $[\text{OH}]^-$  = hydroxyl ion concentration in liquor, ( $\text{mass}/\text{volume}$ )  
 $q_c$  = convective mass transport rate, (mass/time)  
 $q_d$  = diffusive mass transport rate, (mass/time)  
 $q_r$  = rate of reaction of constituent "a", (mass/time)  
 $R$  = outer radius of fiber, (length); as it appears in equation (14).

$R$  = Gas constant (1.987 cal/g-mole  $^{\circ}K$ ); as it appears in equation (34).

$r_c$  = radius of unreacted core, (length).

$r_a$  = radius of the Shrinking Core, (length); corresponding to a reference time ( $t_a$ ).

$R_e$  = Reynold's number.

$S_c$  = Schmidt number.

$t$  = time, (time units)

$t_a$  = reference time, (time units).

$U_a$  = reaction rate per unit volume, (mass/(length<sup>3</sup>\*time))

$\rho_B$  = density of liquor in bulk phase, (mass/length<sup>3</sup>)

$\rho_L$  = density of liquor in the fiber, (mass/length<sup>3</sup>)

$x, y, z$  = reaction orders with respect to various chemicals used for preparation of liquor.

$X_c$  = Fractional conversion,  $(L_0 - L)/L_0$ , (%).

$\pi$  = 3.1417.

# Reaction Kinetic Study and Determination of Controlling Resistances during Alkaline Sulfite/Anthraquinone Pulping process.

## INTRODUCTION

### 1. PULPING TECHNOLOGY:

Pulping is a process by which wood is reduced to a fibrous mass. The existing commercial processes are generally classified as mechanical, chemical, or semi-chemical (i.e. combined, chemical and mechanical) (1).

The objective of chemical pulping is to degrade and dissolve the lignin and leave behind most of the cellulose and hemicellulose (some of the other components of wood) in the form of intact fibers. In commercial chemical pulping processes, the wood chips are cooked with appropriate chemicals in an aqueous solution at elevated temperature and pressure. The two principal methods are the (alkaline) kraft process and the (acidic) sulfite process. The kraft process involves cooking the wood chips in a solution of Sodium Hydroxide (NaOH) and Sodium Sulfide ( $\text{Na}_2\text{S}$ ). In the sulfite process, a mixture of sulfurous acid ( $\text{H}_2\text{SO}_3$ ) and a bisulfite ( $\text{MHSO}_3$ ,  $\text{M} = \text{Na}^+, \text{NH}_3^+, 1/2 \text{Ca}^{++}$ ) is used to attack and solublize the lignin.

The kraft process is the predominant pulping



process in North America. It accounts for 52 % of all the pulp produced (1). The reason it is predominant is that it produces strong pulp, and can pulp any kind of wood species. The principal disadvantages are the capital cost for a kraft pulp mill and its association with malodorous gases, principally  $H_2S$  and organic sulfides, which causes environmental concern. Kraft pulps are also difficult to bleach.

The sulfite pulping process ranks second to the kraft process, accounting for 10 % of all pulp. It is more selective than kraft, yielding 1-3 % more fiber per mass of wood pulped at the same residual lignin content. Sulfite pulps are also easier to bleach. They are weaker pulps generally, and the process is limited to non-resinous softwoods. While sulfite pulping process was a predominant process till 1930, the above mentioned disadvantages have led to its replacement by kraft (1).

The full range of sulfite pulping includes acid, bisulfite, neutral sulfite and alkaline sulfite pulping processes. In the acid sulfite pulping, any pH within the range of 1.5 - 4.0 can be achieved by controlling the ratio of free and combined  $SO_2$ . True bisulfite pulping (equal amounts of free and combined  $SO_2$ ) would be carried out at a pH of 4 - 5. In the neutral sulfite pulping process, the cooking liquor is composed of  $Na_2SO_3$  and  $Na_2CO_3$ , and the cold pH of the liquor

is less than 10. In the alkaline sulfite pulping process, the cooking liquor is composed of NaOH and Na<sub>2</sub>SO<sub>3</sub>, with the cold pH of the liquor between 10 and 13.5 (2).

In the field of alkaline sulfite pulping, two areas have been explored:

a). The original alkaline sulfite pulping process

(3) was a strong alkaline cook with about equal portions of sodium sulfite and caustic soda at an initial pH similar to kraft and soda liquors. The strong alkaline cook is useful for pulping even without anthraquinone because the alkali concentration provides sufficient force for pulping, but with the application of anthraquinone, benefits are seen in yield and cooking rate.

b). The second area explored was pulping at a charge of 80 - 95 % sulfite, a lower level of alkalinity, and with anthraquinone as an additive needed for obtaining a practical rate of cooking and kraft - like quality (4). This process, using a high charge of sulfite and correspondingly less alkali, cooks very slowly in the absence of accelerators like anthraquinone, but when anthraquinone is added, the pulping rate, yield, and pulp properties improve substantially.

On comparing ASAQ with the Sulfite pulping process, it has been shown that (2) the use of

anthraquinone in alkaline sulfite cooking reduces the active chemical charge by 15 - 30 % , and the heat consumption in the ASAQ process was less than in sulfite cooking process. The paper making properties of oven - dry ASAQ pulps and the sulfate pulps were the same (2).

Alkaline Sulfite pulping offers an advantage over kraft pulps at high yields. It has been shown that ASAQ softwood pulp loses none or very little of its strength when the yield is increased above 60 % or even 70 % (6). Figure 1 shows that a kraft pulp at 57 % yield has slightly lower tear, slightly higher breaking length and the same burst strength, all at half the refiner energy consumed. When compared with an alkaline sulfite pulp at 64 % yield from the same wood species, the ASAQ pulp was found to bleach much more easily than kraft pulps.

When comparing ASAQ with kraft pulps, a major advantage of ASAQ is the possibility of eliminating the causticizing process from the flow sheet (7). This would reduce the costs of equipment and maintenance.

The first full scale production of ASAQ pulps in the world started at Valkeakoski plant of United Paper Mills in Finland in 1981 at a rate of 80,000 tons/yr. A case study was conducted for converting the Joutseno kraft mill in Finland into an ASAQ mill (8).

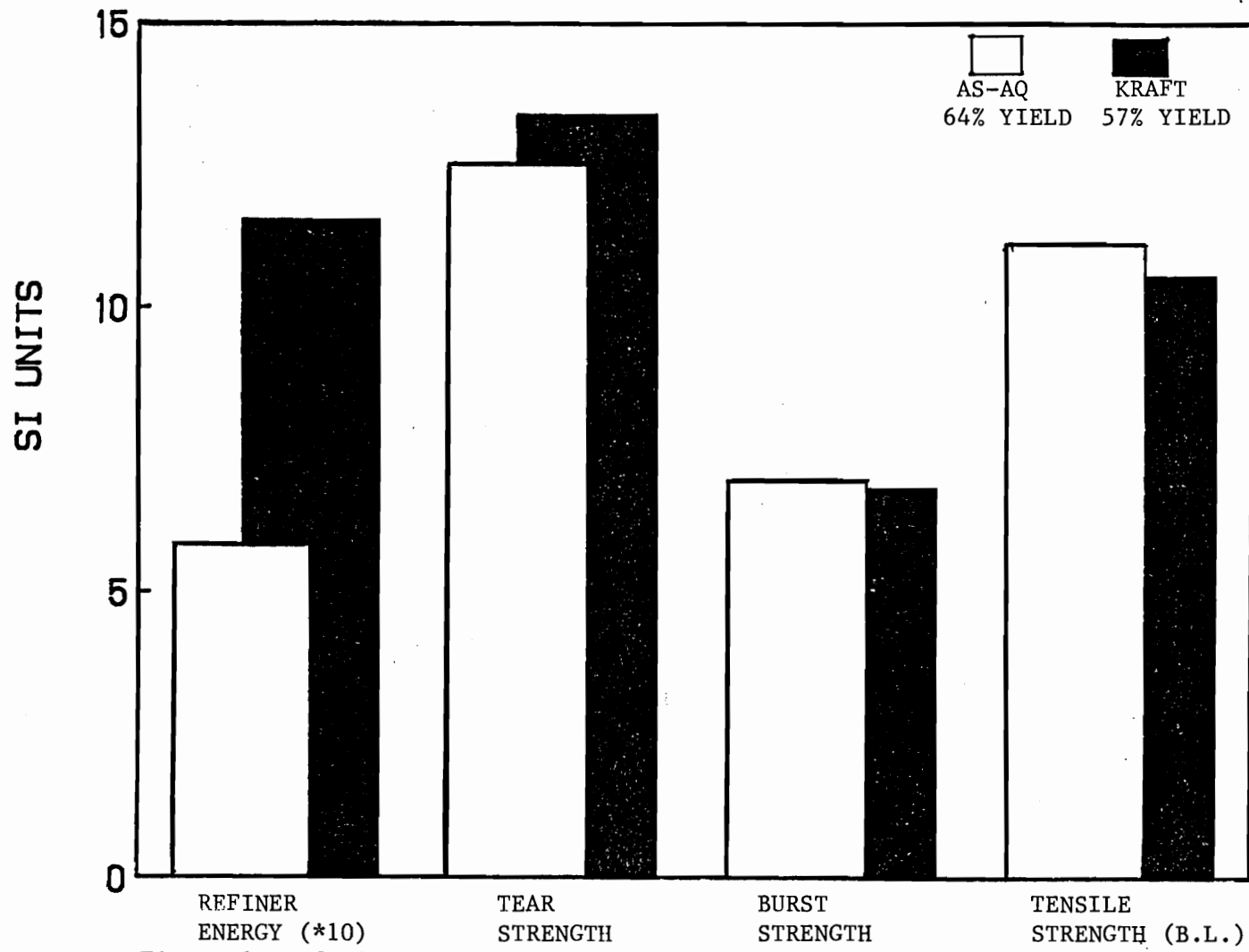


Figure 1. Refining Energy inputs and pulp properties for kraft versus alkaline sulfite anthraquinone pulps.

A comparison of the two processes showed that the ASAQ pulping process would result in savings in major areas including wood, bleaching, and fixed costs, but is more costly regarding chemicals, particularly the essential anthraquinone, and energy.

## 2. PULPING RATE STUDIES.

Studies of ASAQ pulping to date have been directed at comparing the overall pulping rates, bleaching abilities, and pulp properties to those of kraft pulping. There have been no pulping rate data reported that can help us in developing delignification rate models.

The two important uses of rate models are designing delignification reactors and optimizing the pulping process. A long - term objective of pulping rate studies is to develop a reactor design model capable of predicting yield, Kappa , etc. as a function of wood species and the pulping conditions. As a first step toward accomplishing this objective, we must know what controls the rate of delignification during the process.

To develop a delignification rate model, one needs to a) formulate a rate model, which accurately describes the experimental observations made in pulping studies, b) obtain experimental data to permit calculations of various parameters of the model, and, c) verify the model. The formulation of a satisfactory rate equation follows from trial and error attempts to fit experimental results to mathematical models, representing individual steps or combination of the various possible steps (9). The key to optimum

design for multiple reactions is proper contacting and proper flow patterns of fluids within the reactors. These requirements are determined by the stoichiometry and the observed kinetics (10).

The kinetics of a chemical reaction will be directed at developing rate equations in a useful form for design and analysis of the pulping reactors (9). The rate of a chemical reaction is defined as the rate of consumption of reactants or production of products, and/or as the rate of change with time of a limiting reactant or at least one not present in great excess (11).

In general, the reaction rate is a function of the species present in a reaction mixture, i.e.,

$$\text{Reaction Rate} = f(C_1, C_2, \dots, C_n) \quad \dots\dots\dots(1)$$

An assumption often made by the modeler is that the manner in which the rate of a chemical reaction depends on the concentration of each reactant can be represented as a power exponent of that reactant's concentration. The exponent is known as the reaction order with respect to that particular reactant (11).

The kinetic aspects of wood pulping were examined very early in the development of the pulping processes (12), but have not been applied on an industrial scale until rather recently. The very complicated nature of the chemical dissolution of lignin in wood has impeded rational kinetic studies.

Despite the economic importance which the pulp industry has had for about a century, only a few scientific studies on the kinetics of the pulping processes have been reported prior to 1970's (12).

The rate model developed must be able to predict, with a specified degree of confidence, the overall pulping rate, i.e., the time required under certain specified conditions of temperature, liquor concentrations, liquor to wood ratio, to reach a particular degree of delignification, and the quality of the resulting pulp (13).

In the design and analysis of a chemical reactor, it is necessary to establish that the reaction vessel is capable of withstanding the applied pressure or vacuum at the reaction temperature and that it possesses sufficient ancillary equipment to maintain the process operating conditions at their desired values. In the case of batchwise or continuous reaction, it is essential that the chemical reaction is carried at the most suitable combination of temperature, time, and pressure for the maximum conversion of reactants to the required product. A non-optimal selection of processing conditions may lead to either low conversion of reactant, or alternatively to its conversion by side reactions to unwanted products (9).

In designing the pulping reactors, the important



properties of the product are (13):

- a) degree of delignification
- b) total yield
- c) degree of polymerization of cellulose, and
- d) mass fraction of undefibered wood (rejects).

To predict the rate model, one requires a knowledge of how each of the important system variables such as chemical concentrations of the reactants, temperature, time, and chip size affect the pulp quality (13).

Not much work has been reported in rate studies till the late 1960's. The most complete rate model was developed by Gustafson (14), who used literature data to derive the lignin, carbohydrates, alkali kinetic equations, and the alkali diffusivity equations. His mathematical model consisted of a series of differential equations describing the combined diffusion and kinetics within a wood chip during kraft pulping. The theoretical model applies only to kraft processes, but the same basic framework would apply to any chemical pulping process if the rate equations (delignification rate equations, cellulose degradation equations, etc.) were available (14).

On literature survey, very little rate data, and no rate equations have been reported for sulfite pulping process in general, and no existing pulping

models for ASAQ pulping.

Hence on the basis of the above, one needs to

- a). Obtain chemical rate data for ASAQ pulping,
- b). Establish what is the controlling mechanism for ASAQ pulping,
- c). Obtain diffusion data for chemical species involved in ASAQ pulping.

The thrust of the thesis deals with identifying the controlling mechanisms or the resistances that control the rate of reaction. The overall rate of a heterogeneous fluid - solid reaction is made up of a series of physical steps as well as the actual chemical reaction. Of these steps, one is often comparatively slow, and will therefore have an overriding effect on the reaction rate. This slow step is the rate determining step of the reaction sequence or the controlling step (controlling mechanism), which is studied, and leads to the formulation of the kinetic rate. In an extreme case, all the steps would have similar rates and the overall rate equation would depend on each step (9).

The objective of the experimental study is then to

- i) provide observations from which the form of the model can be developed, (i.e. film diffusion controlled, internal diffusion controlled, or chemical reaction controlled), and

ii) to provide the values of the parameters used in the model (i.e. reaction rate orders, rate constants, and activation energies).

## THEORY SECTION

In the introduction section, we discussed the the necessity of doing a study on ASAQ pulping process, why we need a rate data, and why one should determine the controlling resistances or the controlling mechanisms during a certain pulping process.

In the theory section, we will consider the different rate processes in detail and how one designs experiments to distinguish between the various controlling mechanisms.

Delignification processes are chemical processes. They involve the transport of chemical reactants and products as well as competing chemical reactions involving delignification and carbohydrate degradation. Understanding these rate processes is an important first step in designing and optimizing delignification reactors. Designing delignification reactors means more than specifying the hardware; it also includes specification of chip size, the operating range of temperature, the time of pulping, and the liquor concentration profile during pulping.

Delignification reactors are fluid - solid reactors, usually either batch or continuous, and operate over a wide range of temperatures, chemical charges, and chemical concentrations. Three factors control the design of fluid - solid reactors: the reaction kinetics for

single particles, the size distribution of these solids being treated, and the flow patterns of both solids and fluids in the reactor (10).

When wood is delignified by chemical means, the process occurs in steps:

- a) Transport of delignifying agents from the bulk phase surrounding the wood (usually liquid) to the wood surface. When this step controls the rate, we refer to the process as being "film diffusion controlled".
- b) Diffusion of the delignifying agents into the wood. When this mechanism controls, the process is said to be "internal diffusion controlled", or the process is said to be in the dynamic regime.
- c) Reaction of the delignifying agent with lignin or carbohydrates in wood, resulting in the dissolution of lignin or carbohydrates. When this mechanism dominates, the reaction rate is said to be "chemical reaction controlled", or the process is said to be in chemical regime.

The term regime is used to distinguish the rate determining process in a system in which several other processes in series or parallel may be occurring (15). In a given system, the regime depends upon the relative magnitudes of various reaction resistances, and these will vary with the conditions of operation.

- d-f) Transport of the dissolved lignin and carbohydrates out of the wood by the reverse of the processes in

steps (a-c).

In describing delignification processes, the delignification reactions are usually treated as irreversible (14). Hence, steps d-f are neglected when modelling the rate processes.

The rate of a heterogeneous chemical reaction (or any rate process) can be expressed as

$$\text{Rate} = \text{Driving Force} / \text{Resistance} \quad \dots\dots(2)$$

The driving force usually depends on chemical concentrations. The specific functional relationship depends on which step provides the controlling resistance. An important part of designing a delignification reactor is determining the maximum chip dimensions for which diffusion is not a controlling resistance. Using larger chips causes overcooking of the outside and undercooking of the chip center. This results in reduced pulp yield at a given degree of lignin removed and excessive unpulped fiber bundles (screen rejects). A proper knowledge of the rate processes can determine what chip thickness is best for the pulping process.

The other parameters of importance are the maximum temperature and the length of time pulping is carried out.

In the steady state case, the overall rate of the process for convective mass transport from bulk fluid to the solid interface (16) is given by

$$q_C = A_S * (Na)_C = k_L * A_S * (C_{a,b} - C_{a,s})$$

or,

$$q_c = (C_{a,b} - C_{a,s}) / (1/k_L * A_S) \quad \dots\dots\dots(3)$$

In equation (3), the resistance to convective mass transport is  $1/(k_L * A_S)$ .

The rate of an internal diffusion process, or transport by diffusion within the solid phase is given by Fick's Law:

$$\begin{aligned} q_d &= A_S * (N_a)_d = D_a * A_S * (C_{a,s} - C_{a,i}) / L \\ &= (C_{a,s} - C_{a,i}) / (L / D_a * A_S) \quad \dots\dots\dots(4) \end{aligned}$$

In equation (4), the resistance to mass transport by diffusion is  $(L/D_a * A_S)$ .

The chemical reaction rate (disappearance of constituent "a"), is given by the following equation:

$$\begin{aligned} q_r &= A_S * (N_a)_r = (U_a^* * A_S * L) \\ &= C_a / (C^* / U_a^* * A_S * L) \quad \dots\dots\dots(5) \end{aligned}$$

The resistance to disappearance of constituent "a" by chemical reaction is  $C^* / (U_a^* * A_S * L)$  (16)

$C^*$  is related to the mass percent lignin in the solid phase [L] by the following equation

$$C^* = [ 1 / (100 * W) ] * [L] \quad \dots\dots\dots(6)$$

where,  $w = (\text{liquor volume} / \text{dry solids})$  in the reactor.

The first problem in studying heterogeneous reaction is to find out which variables affect each of these above mentioned mechanisms, and to what degree. Only when we determine the magnitude of each resistance, do we have a clear understanding of the impact of these variables on the rate of a reaction. Furthermore, only when we have this information do we have confidence in the ability of

extrapolations of small-scale laboratory kinetic data to predict the performance of large - scale industrial equipment (10).

The empirical method of determining the prevailing regime consists in observing experimentally the effect of certain variables on the overall reaction rate. This method is particularly applicable where both chemical and diffusional resistances are involved. For such a system, the design of a plant and the choice of operating conditions will depend largely on whether a dynamic or a chemical regime prevails (15).

When the convective mass transfer controls, the resistance to convective mass transport ( $1/(k_L * A_S)$ ) will be much greater than the resistance to transport by diffusion ( $L/(D_a * A_S)$ ). Hence,

$$1/(k_L * A_S) \gg L/(D_a * A_S) \quad \dots\dots\dots(7)$$

Therefore,

$$(k_L * L)/D_a \ll 1 \quad \dots\dots\dots(8)$$

The quantity on the left hand side of equation (8) is termed as the Biot Number (Bi), which is the ratio of the resistances of mass transport by diffusion to mass transport by convection. When the Biot number is less than 0.1, the overall rate is controlled by convective transport. When the Biot number is greater than 10, the convective resistance can be ignored.

When we consider the convective transport to be



negligible, the ratio of resistances to chemical reaction to the resistance to transport by diffusion is given by Damkohler Number ( $D_k$ ).

Thus,

$$D_k = (C^*/U_a^* * A_s * l) / (l/D_a * A_s) \quad \dots\dots\dots(9)$$

$$= (C^* * D_a) / (U_a^* * l^2) \quad \dots\dots\dots(10)$$

In equation (10),

$$U_a^* = (1/(100 * W)) * dL/dt \quad \dots\dots\dots(11)$$

where  $dL/dt$  is the overall rate of disappearance (or conversion) of a part of a solid phase.

It is given by the relation,

$$dL/dt = k * (C_i^m, C_j^n, \dots\dots\dots) * [L] \quad \dots\dots\dots(12)$$

Figure (2) shows qualitatively how the steady-state concentration profiles behave when each of the three resistances controls the reaction rate.

The overall rate of the reaction, in terms of transport and chemical kinetic resistances for the three processes, is given by

$$q_c = (C_{a,b} - C_{a,i}) / ((1/k_L * A_s) + (l/D_a * A_s) + (C^*/U_a^* * A_s * l)) \quad \dots\dots(13)$$

This equation ignores the effect on the overall rate of the transport of any reaction products formed from the wood particle. It is valid for irreversible chemical reactions. It also ignores changes in cross-section area with position in direction of transport (i.e. for spheres)

When the transport properties and chemical kinetics are not known well enough to determine the rate controlling mechanism from the dimensionless groups, the

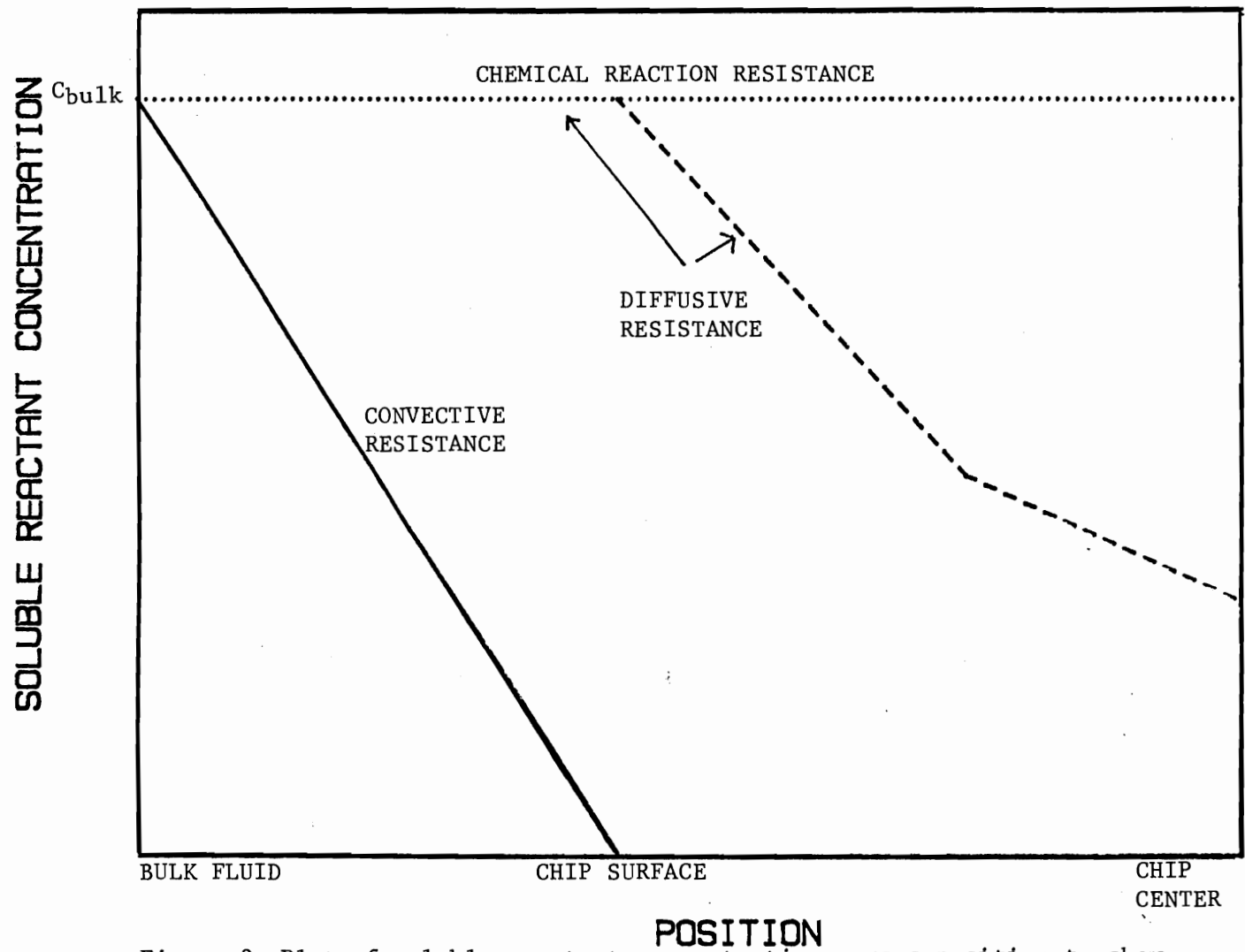


Figure 2. Plot of soluble reactant concentration versus position to show steady state concentration profiles for the different resistances controlling the overall rate of reaction.

problem is to model the various transport and chemical reaction steps in a heterogeneous reaction. Reaction models can be developed using Levenspeil's shrinking - core model (17). This model can be applied to delignification of wood chips, particles, or fibers. It treats the reaction as occurring first at the outer surface of the solid particle. The zone of reaction then moves into the solid, leaving behind completely converted material and inert solid. Thus, at any time during reaction, there exists an unreacted core of material, which shrinks in size during reaction. This implies that lignin is removed completely from the outer fiber wall before any is removed from further in. Observations with wood lend weight to the shrinking core model (10). An analysis of fluid - solid reaction data using the shrinking core model can be carried out to determine the rate processes. The shrinking core model has been used to describe chlorination of wood pulp fibers (17).

Other assumptions of the shrinking core models are:

1. wood chips, particles, or fibers are represented as long, hollow cylinders, or spheres, or slabs,
2. overall dimensions do not change as the reaction proceeds,
3. diffusion occurs only in one direction,
4. diffusion of products from the fibers may be neglected,
5. the diffusivity of the delignifying agent is

independent of position within the fiber and degree of delignification,

6. the lignin density within the fiber is independent of position initially, and
7. the concentration of the delignifying agent in the bulk fluid remains constant during delignification.

In the case of film diffusion controlling, we assume that the rate of chemical reaction equals the rate of transport of delignifying agent from the bulk fluid to the fiber surface.

For cylindrical particles, the equation that relates the time of reaction to the outer radius of the particle,  $R$ , and the radius of the unreacted core,  $r_c$ , (10) is given by

$$t = (\rho L^2 R^2 / 2w^2 k_B C_{P,B}) * ((1 - (r_c/R)^2)) \dots (14)$$

Defining a reference time,  $t_a$  at which the core shrinks to radius  $r_a$ , we get

$$t_a = [(\rho L^2 R^2) / (2w^2 k_B C_{P,B})] * [1 - (r_a/R)^2] \dots (15)$$

Dividing equation (14) by (15),

$$t/t_a = [1 - (r_c/R)^2] / [1 - (r_a/R)^2] \dots (16)$$

Since the fractional conversion is expressed as the

$$\text{Volume of unreacted core} / \text{total fiber volume} = 1 - X_c \dots (17)$$

thus,

$$(1 - X_c) = (\pi r_c^2 L) / (\pi R^2 L) = (r_c/R)^2 \dots (18)$$

and the final expression is,

$$(t/t_a) = (X_c/X_a) \dots (19)$$

For the internal diffusion case, the flux

relationships for a partially reacted particle or fiber core are developed, and then integrated over the particle fiber diameter. Aside from the set of limiting assumptions stated earlier, the following additional assumptions apply:

- a) the rate of movement of the delignifying agent towards the unreacted core is considerably faster than the rate of shrinkage of the unreacted core. This implies that the concentration gradient of the delignifying agent can be assumed to be a steady state gradient at any time, although it will change as the core shrinks.
- b) The rate of reaction of the delignifying agent at any instant equals the rate of diffusion through the delignified fiber.

Equations have been derived for the internal diffusion case for the time that the reaction is carried out (10). Selecting a reference time  $t_a$ , and relating it to the fractional conversion, the equation governing the time ratio ( $t/t_a$ ) and the fractional conversion for a long cylinder, is given by

$$\frac{t}{t_a} = \frac{[X_c + (2(1-X_c)) \ln((1-X_c)^{1/2})]}{[X_a + (2(1-X_a)) \ln((1-X_a)^{1/2})]} \dots (20)$$

In the case of chemical reaction resistance controlling the rate of reaction, the reaction progresses independently of the location of the lignin, and the quantity of lignin reacted is proportional to the surface

of the unreacted core.

The equation that governs the time ratio and the degree of fractional conversion for a long cylinder when chemical reaction is controlling the rate of reaction is given by

$$\frac{t}{t_a} = \frac{[1 - (1 - X_c)^{1/2}]}{[1 - (1 - X_a)^{1/2}]} \quad \dots\dots(21)$$

Equations can be similiarly derived for film diffusion, internal diffusion, and chemical reaction controlling cases for other geometries like sphere and slabs.

Equations 19 to 21 can be used to interpret the delignification rate data for alkaline sulfite pulping. Residual lignin versus time data must be obtained for pulping at constant temperature and constant concentration of the delignifying agents. The residual lignin concentrations are expressed on a basis of the original wood weight. Calculations are then carried out to find the values of time ratios ( $t/t_a$ ) and the function of fractional conversions expressed by equations for different geometries and different mechanisms.

As the equations governing these mechanisms are straight line equations, of the form

$$y = m * x \quad \dots\dots(22)$$

hence, plots are constructed with time ratio ( $t/t_a$ ) on the y - axis and the function of fractional conversion on the x - axis. A linear plot means that the assumed

mechanism is correct. Nonlinear plots mean that either the assumed mechanism is not correct or the model is not appropriate. If the plots for different mechanisms are nonlinear, the rate is either controlled by more than one mechanism or one or more of the assumptions on which the the models are based are incorrect.

An alternate model for chemically controlled delignification is based on the assumption that the reacting particle is permeable to the fluid phase and that the reactant concentration is uniform throughout the particle (uniform concentration model). According to this model, lignin remains uniformly distributed throughout the fiber. The lignin content decreases uniformly with time and the concentration of the delignifying agent remains constant. Hence, it implies that the rate of delignification is proportional to the remaining lignin content.

In the uniform concentration model, the rate of disappearance of lignin is equal to the rate at which lignin concentration is decreasing.

Thus,

$$dN_L/dt = -dL/dt = k_S' * C_{P,B} * [L] \quad \dots\dots(23)$$

Rearranging the above equation

$$- dL/[L] = k_S' * C_{P,B} * dt \quad \dots\dots(24)$$

Integrating equation (24) in the limits of the initial lignin content  $[L]_0$ , and the residual lignin content  $[L]$ , that the wood chips have after time,  $t$ . Hence,

the limits of integration for time are from time = 0  
to time = t.

$$\text{Thus, } - \int_{L_0}^L dL/L = k_S' * C_{P,B} * \int_0^t dt \quad \dots\dots(25)$$

$$\text{or, } \ln[L/L_0] = - k_S' * C_{P,B} * t \quad \dots\dots(26)$$

If the refernce time is  $t_a$ , then

$$\ln[L_a/L_0] = - k_S' * C_{P,B} * t_a \quad \dots\dots(27)$$

Dividing equation (26) by (27),

$$t/t_a = \ln[L/L_0]/\ln[L_a/L_0] \quad \dots\dots(28)$$

Writing this equation in terms of the fractional  
conversion, we get

$$\frac{t}{t_a} = \frac{\ln(1-X_C)}{\ln(1-X_a)} \quad \dots\dots(29)$$

$$\text{where, } X_C = (L_0 - L)/L_0$$

Hence, a plot of  $[\ln(1-X_C)]/[\ln(1-X_a)]$  versus  $t/t_a$  will give a straight line if the rate is chemically controlled and this alternate model is appropriate. It should be noted that equation (29) applies for any particle shape or geometry. This model is more appropriate for a porous material such as wood and is used in this study along with the shrinking core model for chemical reaction controlled.

Table 1 shows the equations for  $f(X_C, X_a)$  for the different geometries.

In general, a mixed regime i.e., diffusion and chemical reaction controlled regime exists when there are



two or more reaction resistances which significantly influence the reaction rate. This type of problem is often encountered. A mixed regime marks a danger point in any new process since it is not always possible to find a reliable basis for predicting large scale results from small-scale experiments. It is sometimes feasible to move a reaction out of the region of mixed regime by changing the operating conditions so that one or the other resistance becomes negligible. Since chemical reactions have higher temperature coefficients than diffusional phenomenon, increasing the temperature tends to convert a chemical regime first into a mixed, and finally into a viscosity controlled dynamic region. Similarly, where there is a heterogeneous chemical regime, reducing the degree of agitation increases the diffusion resistance so that the regime tends to become first mixed, and then wholly dynamic. In each case, a change of temperature or agitation, respectively, in either direction, if great enough, would take the reaction out of the region of mixed regime (15).

Where there is a chemical regime in either a heterogeneous or a homogeneous system, the reaction rate does not depend on the rate of mass transfer, and is therefore independent of the fluid velocity. Evidently, as mass transfer coefficients and (in the case of free interface heterogeneous systems) interfacial area decreases, a point will be reached at which the regime

Table 1. "Shrinking Core" Heterogeneous Reaction

Models for various geometries,  $f(X_c, X_a)$  (10).

Geometry	Film Diffusion	Internal Diffusion
2 Dim Slab	$X_c/X_a$ *	$(X_c/X_a)^2$
Long Cyl.	$X_c/X_a$	$\frac{X_c + (2*(1-X_c))*\ln(1-X_c)^{1/2}}{X_a + (2*(1-X_a))*\ln(1-X_a)^{1/2}}$
Sphere	$X_c/X_a$	$\frac{1 - (3*(1-X_c)^{2/3}) + 2*(1-X_c)}{1 - (3*(1-X_a)^{2/3}) + 2*(1-X_a)}$
Geometry	Chemical Reaction	Uniform Conc. Model
2 Dim.Slab	$X_c/X_a$ *	$\frac{\ln(1-X_c)}{\ln(1-X_a)}$
Long Cyl.	$\frac{(1-(1-X_c)^{1/2})}{(1-(1-X_a)^{1/2})}$	$\frac{\ln(1-X_c)}{\ln(1-X_a)}$
Sphere	$\frac{(1-(1-X_c)^{1/3})}{(1-(1-X_a)^{1/3})}$	$\frac{\ln(1-X_c)}{\ln(1-X_a)}$

\* It is impossible to distinguish between film diffusion and chemical reaction reaction resistance controlling for a two dimensional slab by this method.

changes from chemical to dynamic regime and the reaction rate then becomes dependent on the rate of agitation (15). The general effect of agitation is to increase the degree of turbulence in a fluid medium, reduce the thickness of streamline boundary films, and so diminish the resistance to process of mass transfer by convection (15).

Physical reactions such as a mass transfer reaction tend to be accelerated by a rise in temperature, especially when they take place in the liquid phase. The principal factor is the reduction in viscosity with the rise in temperature, and there is also an increase in diffusivity or diffusion coefficient (15).

The effect of temperature is to increase the rate of both chemical and physical reactions by diminishing the resistances in the generalized rate equation (equation 2). In the case of balanced chemical reactions, a temperature rise may also shift the equilibrium point in a direction which reduces the driving force of the reaction, i.e. difference between the actual and equilibrium concentration. The effect of a small temperature rise on the driving force of a chemical reaction is usually negligible as compared with its effect on the reaction resistance, or its reciprocal, the velocity constant (15).

In general, the rate of a particular reaction (or a combination of reactions) can be expressed as a function of the concentration (or activity) of the reactants, as

well as the temperature at which the reaction is being carried out.

If delignification is considered as being represented by one reaction, the rate of delignification at any time would be related to the lignin content of the wood at that particular time as well as the concentration of the delignifying agents and the temperature of the system (13). Hence,

$$\text{Rate} = f(L, C, T) \quad \dots\dots(30)$$

The usual approach to relating delignification rate to the lignin content has been to assume that all of the lignin is available for the reaction and to consider the rate to be directly proportional to the amount of lignin present.

The empirical concept of the reaction order can be used to write a general rate expression, and the constants in the expression can be determined directly from the experimental data (13).

In applying such a procedure, it is assumed that the rate of any particular reaction (or class of reactions) can be represented as being directly proportional to the product of the important reactant concentrations, each raised to a power.

Thus, for delignification,

$$-r_L = -dL/dt = k * C_{i,x} * C_{j,y} * [L]^n \quad \dots\dots(31)$$

It should be emphasized that the writing of such a rate expression implies nothing about the mechanism of the

reaction.

The delignification rate constant  $k$  is often found to be related to the absolute temperature  $T$  by the Arrhenius' equation, which is as shown below:

$$k = A \exp (-E_a/RT) \quad \dots\dots(32)$$

It will be noted from the above equations, that in order to employ the design equations, it will be necessary to know the variations in wood lignin content, liquor concentrations, and temperature during the course of the cook in order that time may be calculated from the design equations. In a typical batch digestion process, all three of these variables are changing with time, and possibly from point to point within the digester. The answer is that these variables must be studied separately by varying one and keeping others either constant or varying in some known fashion (13).

Wood is a material where the pore structure differs greatly in the three directions, namely longitudinal, radial, and tangential directions, and as such, effective diffusivity will also differ (18). For diffusion through porous materials the concept of effective diffusivity can be employed (16).

$$\text{Effective diffusivity} = D/D_o \quad \dots\dots(33)$$

McKibbins (18) dealt with diffusion in wood which had been modified from its natural state by means of a conventional pulping process. He concluded that, despite the complex character of wood, the overall rate controlling

mechanism appears to be that of diffusion. The longitudinal diffusion coefficients were found to be two or three times as large as the transverse diffusion coefficients.

According to McKibbins, the activation energy for diffusion in the longitudinal direction was higher than that in the transverse direction. The reason for that is probably related to the structure of wood itself. In wood, the longitudinal diffusion is essentially through long capillaries, while the transverse diffusion is between tracheid tubes. Christensen (19) has pointed out that in capillary diffusion, the activation energy is in an inverse proportion to the capillary diameter. As would be expected, the rate of movement in the transverse direction has been somewhat lower due to the hindrance effect offered by the tracheid walls.

Most polymeric materials swell different amounts depending on the liquid in contact with them. Hartler (20) has shown that wood swells more in the radial and tangential direction. It does not swell appreciably in the longitudinal direction (which is usually the largest chip dimension). He shows that, under alkaline conditions, the rate of diffusion is determined by the smallest chip dimension.

Gustafson (14) has presented an empirical model which describes a relationship between the diffusivity of NaOH in wood chips and temperature, alkali concentration, and degree of delignification. The relationship, in which

McKibbins' data was used to determine the constants, is given by the following equation:

$$D = 5.7 \cdot 10^{-2} \cdot (T)^{1/2} \exp(-4870/(R \cdot T)) \quad [-.02 \cdot [L] + .13 \cdot [OH] \cdot 55 + .58] \quad \dots\dots (34)$$

The above relation assumes that the effects of degree of delignification and alkali concentration on diffusivity are linearly additive and independent of temperature.

Equation (35) shows that the diffusivity of hydroxyl ions in the same liquor in the absence of a porous solid,  $D_0$  is a function of Temperature.

$$D_0 = 5.7 \cdot 10^{-2} \cdot (T)^{1/2} \cdot \exp((-4870/(R \cdot T)) \quad \dots\dots (35)$$

#### Accounting for Apparent Time Varying Diffusivity:

When internal diffusion ( or intraparticle diffusion) resistance controls the rate of reaction, shrinking core models (10) show that the time required to achieve a certain degree of delignification ( $t$ ) is related to the fractional conversion ( $X_C$ ) for a spherical geometry, by the relation

$$t = \rho_B \cdot (R)^2 \cdot [1 - (3 \cdot (1 - X_C)^{2/3}) + (2 \cdot (1 - X_C))] / (6 \cdot b \cdot D \cdot C_{A,g}) \quad \dots\dots\dots (36)$$

$$\text{Let } [1 - (3 \cdot (1 - X_C)^{2/3}) + (2 \cdot (1 - X_C))] = f(X_C) \quad \dots\dots (37)$$

Rearranging the above equation, we get

$$f(X_C) = \frac{6 \cdot b \cdot D \cdot C_{A,g}}{\rho_B} \cdot \frac{t}{R^2} \quad \dots\dots (38)$$

Equation (38) is the equation of a straight line of the form,

$$y = m * x \quad \dots\dots\dots (39)$$

A straight line obtained by plotting  $f(X_c)$  versus  $t/(R^2)$  is evidence that the effective diffusivity of the chemical species in the wood chips is constant throughout the pulping process. If a straight line is not obtained, the apparent diffusivity is not constant. Rearranging equation (38) so that the coefficients of  $t/R^2$  is the product of constant terms, we find that

$$\frac{f(X_c)}{D} = [(6*b*C_{A,g})/9B]*(t/R^2) \quad (40)$$

Equation 40 plots as a straight line if the time time dependence of  $D$  is known and included in the  $f(X_c)/D$  term. One should expect a straight line if the correct functional dependence for  $D$  is assumed. If the functional relationship for  $D$  is correct but the technique fails, it means that  $D$  alone is not varying but something else is varying too.

Dividing equation (34) by (35), we get

$$D/Do = [(-.02*L) + (.13*(OH)^{.55}) + (.58)] \quad (41)$$

Thus, from equation 41,

$$(D/Do) = f(L) \quad (42)$$

From the equation 42, it is evident that we would expect the effective diffusivity to change during the cook since the residual lignin content ( % on wood ) will change as the cook proceeds.

Figure 3 is a plot of effective diffusivity ( $D/Do$ )



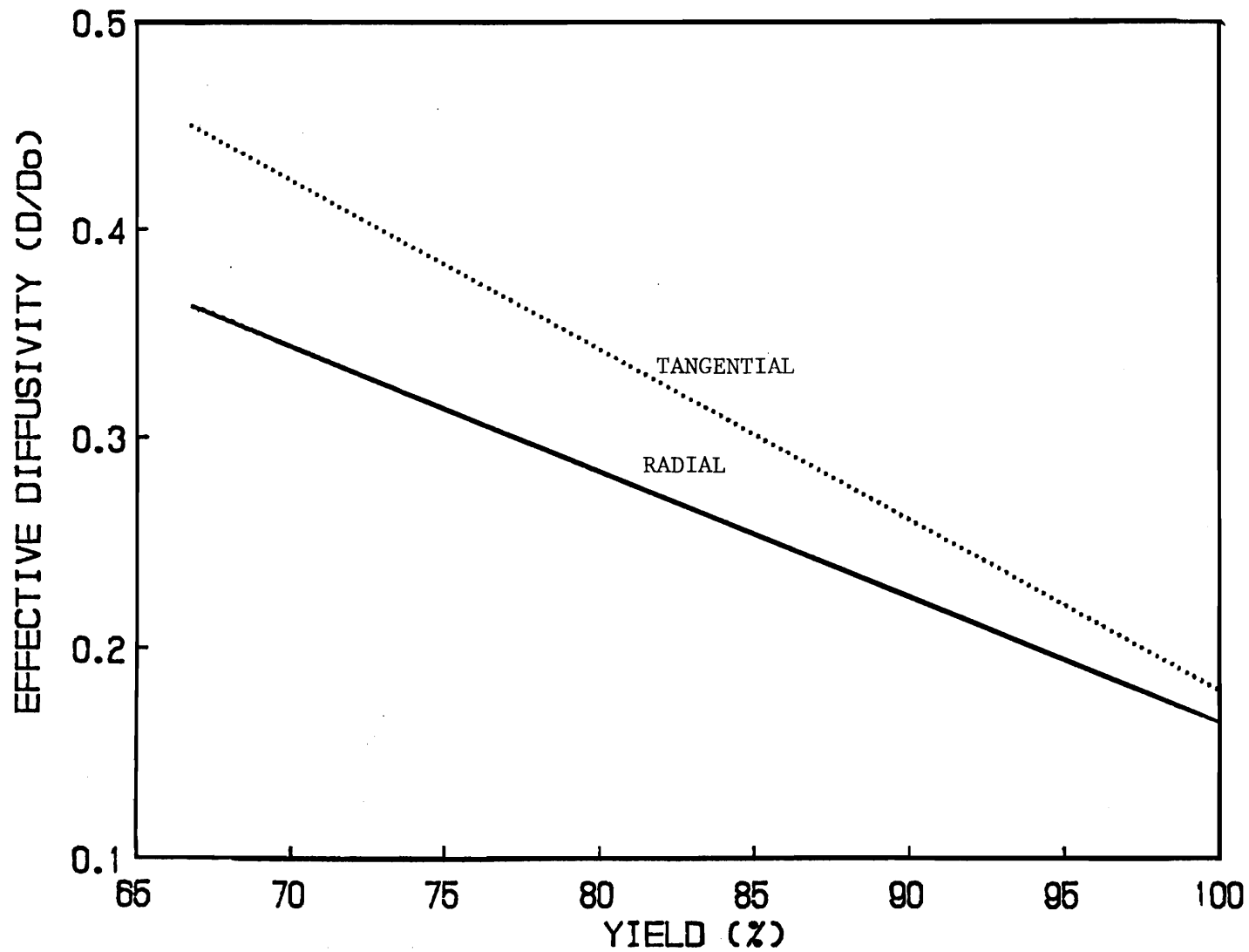


Figure 3. Plot of effective diffusivity ( $D/D_0$ ) versus yield for pulped wood at pH 13.2.

for pulped wood versus yield at pH 13.2 (20), to show how effective diffusivity changes with the residual lignin content of wood. An expression analogous to equation 40 is obtained by dividing equation 38 by the effective diffusivity ( $D/D_0$ ).

Hence,

$$f(X)/(D/D_0) = (6 \cdot b \cdot C_{A,g} / \rho_B) * (t/R^2) \quad \dots\dots\dots (43)$$

By plotting  $f(X)/(D/D_0)$  versus  $t/R^2$

and by observing the nature of the plots, one can draw conclusions about the time variable diffusivity.

While doing such a study, one needs to treat transport in each direction, because for each chip dimension of particular interest, transport is important in all three directions except at a very high pH ( $\text{pH} > 12.5$ ). The procedure for carrying out such an analysis ( to calculate the effective diffusivity ) is as follows:

From the continuity equation, assuming unidirectional mass transport by diffusion in a stationary flat slab (16), we get

$$dC_A/dt = D * d^2C/dx^2 \quad \dots\dots\dots(44)$$

If the initial concentration of solute "a" is uniform throughout the phase and its boundaries are subjected to a step change in concentration at time zero, then the solution to equation (45) is given by (16)

$$E_{a,x} = \frac{8}{\pi^2} * \frac{1 * \exp(-((2*n)-1)^2 * D*t / (l^2))}{((2*n)-1)^2} \dots\dots\dots (45)$$

One needs to keep in mind while doing the calculations, that the diffusion path length (l) is taken to be the thickness.

For diffusion into a rectangular block from all six faces,

$$E_a = E_{ax} * E_{ay} * E_{az} \dots\dots\dots (46)$$

where  $E_{ax}$ ,  $E_{ay}$ , and  $E_{az}$  are determined independently from the geometry of the block and the diffusivities (16).

To plot  $f(x)/(D/Do)$  versus  $t/(R^2)$  for a spherical geometry (as all the wood chips are approximated as spheres), the following steps are carried out.

1. Calculate D by using equation (35) for the diffusivities in the radial and tangential directions from the residual lignin (% on wood) and time values at a certain temperature,
2. Calculate  $D_o$  for the diffusivity in the longitudinal direction by using equation (35).
3. Multiply  $D_o$  by  $D/D_o$  value for species of wood used, from Table 2.
4. Calculate  $(D*t)/(l^2)$  for longitudinal, radial, and tangential directions where l is the chip dimension, i.e. length, width, and thickness respectively.

Table 2. Effective diffusivity ( $D/D_0$ ) values in the longitudinal, radial, and tangential directions for various wood species (Gustafson et, al., 1982, p.47(14)).

-----					
( $D/D_0$ )					
Species	Sp.gr.	Solute	longitudinal	radial	tangential
Balsa	0.31	KCl	0.56		
Spruce	0.45	KCl	0.51	0.028	0.034
W.Pine	0.35	KCl	0.54	0.032	0.031
D.Fir	0.48	KCl	0.42	0.02	0.022
Hemlock	0.42	KCl	0.47	0.029	0.024
S.Spruce	0.34	NaCl	0.59		0.015
D.Fir	0.45	NaCl	0.47		0.011
D.Fir	0.50	NaCl	0.43		0.012
W.Cedar	0.34	Naphthalene	0.55		0.006
		in benzene			
W.Cedar	0.28	NaCl	0.64		0.016
-----					

5. Use Figure 4 drawn on basis of the solution to unsteady state diffusion equation for a slab to read  $E_{ax}$ ,  $E_{ay}$ , and  $E_{az}$  values corresponding to tangential, longitudinal, and radial directions.
6. Calculate  $E_a$  by use of equation (46).
7. Calculate  $R$ , which is the radius of sphere, as the inverse of Specific Area / Volume for a particular chip size.
8. Refer to figure 4 for a sphere, and read the value of  $(D*t)/a^2$  for a certain value of  $E_a$ .
9. Calculate  $a$  = radius of sphere, ( in figure 4 )  

$$= [ 3 * (\text{Volume}) ] / (\text{Specific Area})$$
10. Use the read value of  $(D*t)/a^2$ , and the calculated value of  $a$  to calculate  $D$ .
11. Calculate  $D/D_o$ , by dividing the value of  $D$  calculated in step 10 by value of  $D_o$  calculated in step 2.
12. Divide  $f(X_c)$  by  $D/D_o$ .

These values of  $f(X_c)/(D/D_o)$  are then used to plot against  $t/(R^2)$  to prove whether internal diffusion resistance controls the rate of reaction.

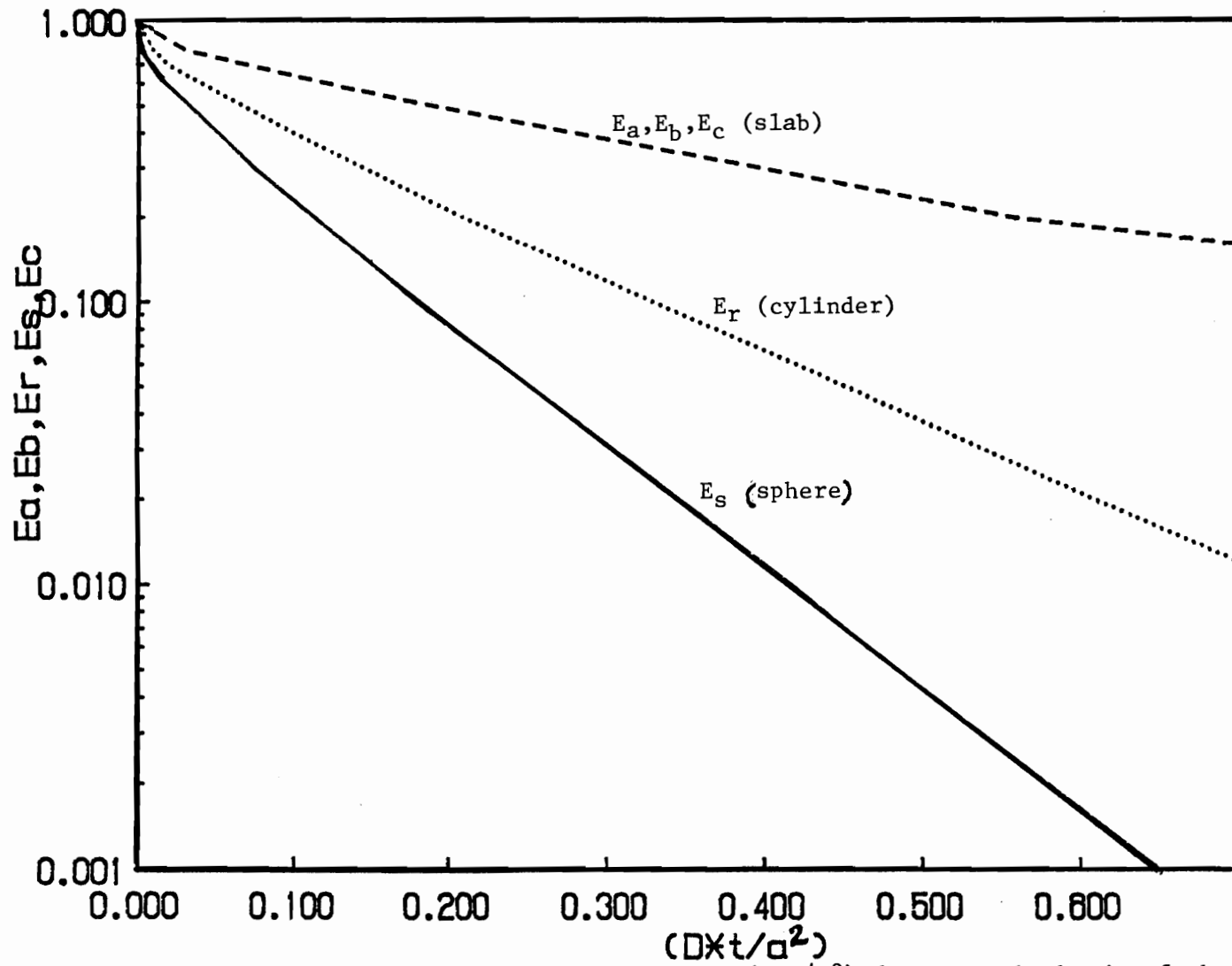


Figure 4. Plot of  $E_{ax}$ ,  $E_{ay}$ , and  $E_{az}$  versus  $(D \times t / a^2)$  drawn on the basis of the solution of unsteady state diffusion equation for a slab, cylinder, and spherical geometries.

Analysis of the rate data using the Activation  
Energy data:  
-----

Another way that can be used to differentiate between whether diffusion or chemical reaction resistance is controlling the rate of reaction is by determining the Arrhenius activation energies. The higher the activation energy, the more temperature sensitive is the process, and vice versa. The literature reported values (15) of activation energies for internal diffusion resistance are of the order of 5 Kcals/gm mole, and for chemical reaction resistance are typically between 20 - 35 Kcals/gm mole.

**Activation Energy Calculations:**

Since mass transfer by diffusion is a rate phenomenon, Glasstone, Laidler, and Eyring (21) point out that there will be an associated activation energy,  $E_a$  which is required to elevate the diffusing molecules to that energy level sufficient to initiate molecular transport.

Substituting equation (32) into equation (31),

$$-r_L = -dL/dt = A * \exp (-E_a/(R*T)) C_i^X * C_j^Y * L^n \quad \dots(47)$$

Equation (47) applies regardless of the mechanism controlling the reaction as long as that mechanism does not change during the process.

Equation (47) can be further simplified and written in the following manner,

$$-r_L = - dL/dt = A * \exp (-E_a/(R*T)) * f(C_i) \quad \dots(48)$$

where,  $f(C_i)$  is a function of the concentration of the chemicals used for delignification processes.

On rearranging equation (48), we get

$$-dL/f(C_i) = A \cdot \exp(-E_a/(R \cdot T)) \cdot dt \quad \dots \quad (49)$$

As the temperature (T) is independent of time (t), we integrate equation (49) at constant temperature to get

$$- \int \frac{dL}{f(C_i)} = A \cdot \exp(-E_a/(R \cdot T)) \cdot \int dt \quad \dots \quad (50)$$

$$\text{or } - \int \frac{dL}{f(C_i)} = A \cdot \exp(-E_a/(R \cdot T)) \cdot t \quad \dots \quad (51)$$

Taking logs of both sides of equation (51)

$$\ln \left[ - \int \frac{dL}{f(C_i)} \right] = \ln(A) - (E_a/R \cdot T) + \ln(t) \quad \dots \quad (52)$$

The left hand side of the above equation is constant if the initial reactant mixture is the same at all temperatures and the limits of integration are the same, which means that the integral is evaluated over the same range of lignin contents in all cases.

On rearranging equation (52), we get

$$\text{Constant} - \ln(t) = \ln(A) - (E_a/(R \cdot T)) \quad \dots \quad (53)$$

or

$$\text{Constant} + \ln(1/t) = \ln(A) - (E_a/(R \cdot T)) \quad \dots \quad (54)$$

Hence, by constructing a plot between  $\ln(1/t)$  on the y - axis, and  $(1/T)$  on the x - axis, the slope of the straight line drawn should be equal to  $(-E_a/R)$ .

$$\text{Slope} = (-E_a/R) \quad \dots \quad (55)$$

or,



$$E_a = - R * (\text{Slope of the plot}) \dots\dots(56)$$

To plot  $\ln(1/t)$ , versus the reciprocal of the absolute temperature, one must use time values that correspond to the same lignin content for different temperatures. These are obtained by interpolating with lignin content versus time plots at different temperatures.

To summarize the entire theory section, we have three powerful tools to analyze the delignification rate data, and to predict the controlling resistances during ASAQ pulping process. They are as follows:

1. Prediction of the controlling resistances by using dimensionless groups like Biot Number ( $B_i$ ) and Damkohler Number ( $D_k$ ).
2. Use of shrinking - core reaction rate models and an alternate model for chemically controlled delignification to predict the controlling resistances that control the rate of reaction.
3. Calculation of activation energy to predict the regime we are going to be in during this pulping process.

In addition, time - varying apparent diffusivity can be included in the shrinking core models if the functional dependence of diffusivity on measurable variables is known.

Experimental design for pulping studies to determine the controlling resistance(s) can be based on one or

more of the above methods. This is discussed in the next section.

## EXPERIMENTAL DESIGN SECTION

The last section (Theory) discussed different methods involved in determining the controlling resistances during the process of chemical delignification of wood. This section deals with how different concepts are applied to the design of experiments that need to be carried out to determine controlling resistances by different methods during ASAQ delignification of wood.

### a) Controlling Regime from Dimensional Analysis: -----

To use the Biot number estimation method to distinguish between convective and diffusive mass transfer, one needs to know parameters like particle dimension ( $l$ ), mass transfer coefficient ( $k_L$ ), and the diffusivity of  $[\text{OH}]^-$  in wood chips ( $D$ ). The equations used to measure these parameters have been discussed in the theory section. To use the Damkohler number estimations to distinguish between diffusive mass transfer and chemical reaction resistance controlling the rate of reaction, one needs to know rate at which the delignification takes place ( $-dL/dt$ ), diffusivity of  $[\text{OH}]^-$  in wood chips ( $D$ ), and the residual lignin content in the wood chips after a certain time that pulping is carried out. The equation supporting the Damkohler number estimation method was shown in the theory section.

For designing experiments on the basis of

requirements of Biot number and Damkohler number estimations, one needs to measure the delignification rate. This requires that lignin content be measured as a function of time at several temperature levels.

To interpret the results, the Biot numbers are first calculated. If it is in the range for convective transport (film diffusion), then film diffusion controls the rate of reaction. If the Biot numbers indicate that convective transport does not control the rate of reaction, then one needs to estimate Damkohler numbers for the process to determine whether internal diffusion or chemical reaction resistance controls the rate of reaction.

If chemically controlled rate data is obtained over the range of temperatures and chemical concentrations selected, then the  $B_i$  and  $D_k$  can be used for any range of particle sizes, liquor circulation rate, etc. to determine which mechanism is controlling.

The limitation of using this method is that it differentiates clearly between controlling regimes only if the numbers are either very much less than 0.1 or if they are very much higher than 10.0. When the numbers approach 0.1 (on the lower limit) and 10.0 (on the higher limit), errors in the parameters that have been used to calculate these numbers may affect the interpretation.

b). Controlling Regime from Shrinking Core Models:  
-----

To use this method, one must have lignin concentration versus time data with all the other variables (temperature, chemical concentration, particle sizes) kept constant. Hence, the reaction must be carried out with either a constant particle size (or a narrow range of particle sizes), at a constant temperature, and with sufficient excess of pulping chemicals so that concentrations do not change during the cook. If the aim is to determine whether internal diffusion or chemical reaction resistance controls the rate of reaction, then, the liquor circulation rate should be large enough so that film diffusion is not important.

In interpreting the data, one needs to plot the appropriate functions of lignin concentrations ( as shown in Table 1 in the Appendix ) versus  $t/t_a$ . The equation which represents the controlling mechanism is the one for which  $f(X_c, X_a)$  versus  $t/t_a$  plot gives a straight line.

The limitations in using this technique to determine the controlling resistances are the assumptions on which this technique is based on. These assumptions were discussed in the theory section. However, there are two assumptions, in particular, that need to be mentioned as these may not be valid here:

1. There should be no change in mechanism during

delignification. It has been shown that there is no change in mechanism during kraft pulping over most of the range of delignification (13) and probably in sulfite pulping (12). If this assumption is not valid for alkaline sulfite pulping, we would not obtain straight lines from plots of shrinking core model equations, and

2. No change in time varying apparent diffusivity. It is known that effective diffusivity ( $D/D_0$ ) changes with the degree of delignification (14). Hence, the effect of apparent diffusivity can be incorporated into the shrinking core internal diffusion Models for various geometries, as indicated in the theory section.

c). Controlling Regime from Activation Energy :

As discussed in the theory section, the controlling regime during this pulping process is inferred from the magnitude of the activation energy values. The typical values of activation energies for diffusion controlled and the chemical reaction controlled mechanisms were indicated in the theory section.

As a basis for comparison, one can use published data for kraft pulping, where the data can also be checked using dimensionless numbers analysis and shrinking core models to determine what magnitude of activation energy

values correspond to internal diffusion control and the kinetic control.

For the experimental data required, one needs sufficient lignin (% on wood) versus time at several temperatures, but all at same chemical charge and the chemical concentrations of liquor constant during the cook. One must also maintain constant temperature during each cook. The particle sizes should be nearly mono-disperse. One must also have enough of lignin content versus time data so that one can interpolate to the same lignin content in all cases for comparison. To calculate activation energies, one needs to plot  $\ln(1/t_n)$ , where  $t_n$  is the time corresponding to a certain degree of delignification, versus  $1/T$  ( $K^{-1}$ ).

The limitations of interpreting the rate data by this method is that the plot of  $\ln(1/t_n)$  versus  $1/T$  must be a straight line, if a single mechanism controls over the entire temperature range. One may not get a straight line if the mechanism is changing from reaction to diffusion controlled as temperature increases.

On the basis of the above mentioned experimental needs, one must have a delignification rate data (lignin versus time data) and the particle size data for wood particles.

One must also choose conditions for rate data based on the most stringent requirements stated above (high chemical concentration of liquor, constant temperature, a

narrow range of wood particle size data, pulping data at various times of pulping)

The experimental requirements for obtaining delignification rate data that meets these requirements are:

- a) a number of particle sizes,
- b) a number of temperatures at which pulping is carried out,
- c) one chemical concentration which remains constant during delignification,
- d) target range of residual lignin (% on wood).

All the experiments need to run at a constant temperature with a high chemical charge and liquor to wood ratio, so that the chemical concentration remains constant during the cook.



## EXPERIMENTAL PROCEDURES SECTION.

This section deals with the various procedures, used in conducting various experiments. It is divided into three major parts:

1. Wood Supply.
2. Pulping Experiments.
3. Pulp Analysis.

WOOD SUPPLY:  
-----

The wood chips used in this study were a commercial chip mix, supplied by Arbokem, Inc. The mixture contained 70 % by weight of balsam, 20 % by weight of spruce, and 10 % by weight of northern pine. The chips were received wet. They were air dried and stored at 72<sup>0</sup>F and 50 % R.H., to minimize decay until needed for pulping. The moisture content of chips was measured before each pulping experiments were conducted.

The air dried samples were separated using a Stalvet chip classifier to collect the

- a. ( -5/8", + 3/8"), (the chip fraction that passed through 5/8" and was collected in the 3/8", and
- b. (-3/8", + 3/16"), (the chip fraction that passed through 3/8" and was collected in the 3/16" fractions.

The smaller fractions than (-5/8", + 3/8") and (-3/8",

+3/16") were obtained by hammermilling the original lot of chips, and classifying the product from the hammermill, to obtain (-3/8", +3/16"), (-3/16", +1/16"), and -1/16" fractions. The -1/16" fraction is the one that passes through all the screens, and is collected in the pan (fines).

The dimensions of chips for each lot were obtained by measuring the length, width, and thickness of fifty samples of each chip size. The average chip dimensions, their standard deviations, and the average surface area / volume ratio were calculated for each chip size. The surface area / volume ratio was calculated assuming that the chips were rectangular in cross section. Table 3 contains the results of these measurements and calculations.

The lignin content of each chip size was measured on an extractive - free basis for each chip size using TAPPI standards T 12 m and T 13 m. The moisture contents were determined by oven drying. The results are shown in Tables 4 and 5.

#### PULPING EXPERIMENTS:

The digester used for the delignification rate studies was type 316 stainless steel cylindrical digester, 17.5" in height and 6.25" in diameter. Steel mesh bags were used for containment of chips, so as to separate each of the five chip sizes during pulping. Five bags carrying the five different sizes were pulped at the same time in the

Table 3. Average values of the size measurements of  
five chip sizes used in the experiments.

Sample	length	width	thickness	Average
Number	(cms.)	(cms.)	(cms.)	Surface Area/Volume, $\text{cm}^{-1}$
1	2.63±0.19	1.06±.06	0.35±.03	8.3
2	2.18±.11	0.55±.02	0.21±.03	14.0
3	1.76±.09	0.29±.02	0.15±.06	21.0
4	1.42±.13	0.22±.02	0.11±.05	30.0
5	1.00±.10	0.16±.03	0.05±.02	53.0

Note: dimensions are reported as the average ± one  
standard deviation.

Table 4. Lignin contents of the five chip sizes used  
in this study.

---

Sample Number	Lignin Content, %
1.	27.23
2.	26.83
3.	27.80
4.	26.14
5.	26.10

---

Table 5. Typical moisture content data for chips  
stored at 50 % R.H., and 72°F.

---

Sample Number	Moisture Content, (% , wet basis)
1	6.65
2	7.53
3	6.91
4	6.76
5	7.54

---

digester. Fifty grams of dry chips of each chip size were used. A high liquor/wood ratio (35:1) was used to maintain constant chemical composition during each cook. The pulping liquor, was composed of 43.60 g/liter of sodium sulfite, 12.22 g/liter of sodium carbonate, and 0.428 g/liter of anthraquinone in water. The liquor volume used, and the details of the liquor preparation calculations are given in the Appendix, section 2.

Two different methods of pulping were carried out.

1. Finite Heat-Up Method:

In this method, the chips and liquor were added to the digester. The lid was shut. The digester was then heated at a constant rate of temperature increase ( $1^{\circ}\text{C}/\text{min}$ ) until the desired final temperature ( $165^{\circ}\text{C}$ ) was reached. The digester temperature was then held constant for the desired pulping time. The different times of pulping at constant temperature were 0, 20, 60, and 180 minutes.

2. Isothermal Method:

In this method, we used two vessels. The basis for using the isothermal method of pulping is that before the chips would be introduced into the digester, the digester walls should have already achieved the temperature to be used for pulping. In order to do that, one digester is filled with the necessary volume of liquor. The lid is shut and this digester is heated up to a temperature, which is higher than the temperature which is desired for pulping. The other digester (where pulping is

to take place) is filled with water, the lid is shut and the digester is heated up to the temperature that is desired for pulping. As soon as this digester has reached the necessary temperature, it is drained, opened, and the chips are put in. The digester lid is again shut. The liquor is then recirculated, between the two digesters for the desired time of pulping.

A rate of liquor recirculation of 20 liters/min, corresponding to a superficial velocity of 0.055 ft/sec is maintained in both methods to minimize any resistance to mass transfer that might have been offered due to film resistance.

The isothermal method of pulping was carried out at three different temperatures, i.e. at 435°K, 444°K, and 453°K, and at different times at each of these temperatures. The time at constant temperature, were 10, 20, 30, and 60 minutes, and at 453°K, the cook was carried out at 75 minutes instead of 60 minutes. The delignification data obtained from pulping experiments is given in Table A-1 to Table A-16 in the Appendix.

#### PULP ANALYSIS:

-----

After the pulping experiments were completed, the yield of the pulp produced was calculated. If the yield was higher than 80 % , then, lignin measurements were carried out using Tappi Standard Method T-54m. Those pulps with a yield of less than 80 % were analyzed for kappa

number, and the lignin content was determined from the calibration curve shown in Figure 5. The calibration curve was prepared by measuring the lignin content and Kappa Numbers of six samples in the Kappa Number range of 55-150 and a yield range of 55-75. The data for the calibration plot is shown in Table A-17 of the appendix section.

Lignin content and, where replicate measurements were made, their standard deviations for each of the pulping experiments are included in Tables A-1 through A-16.



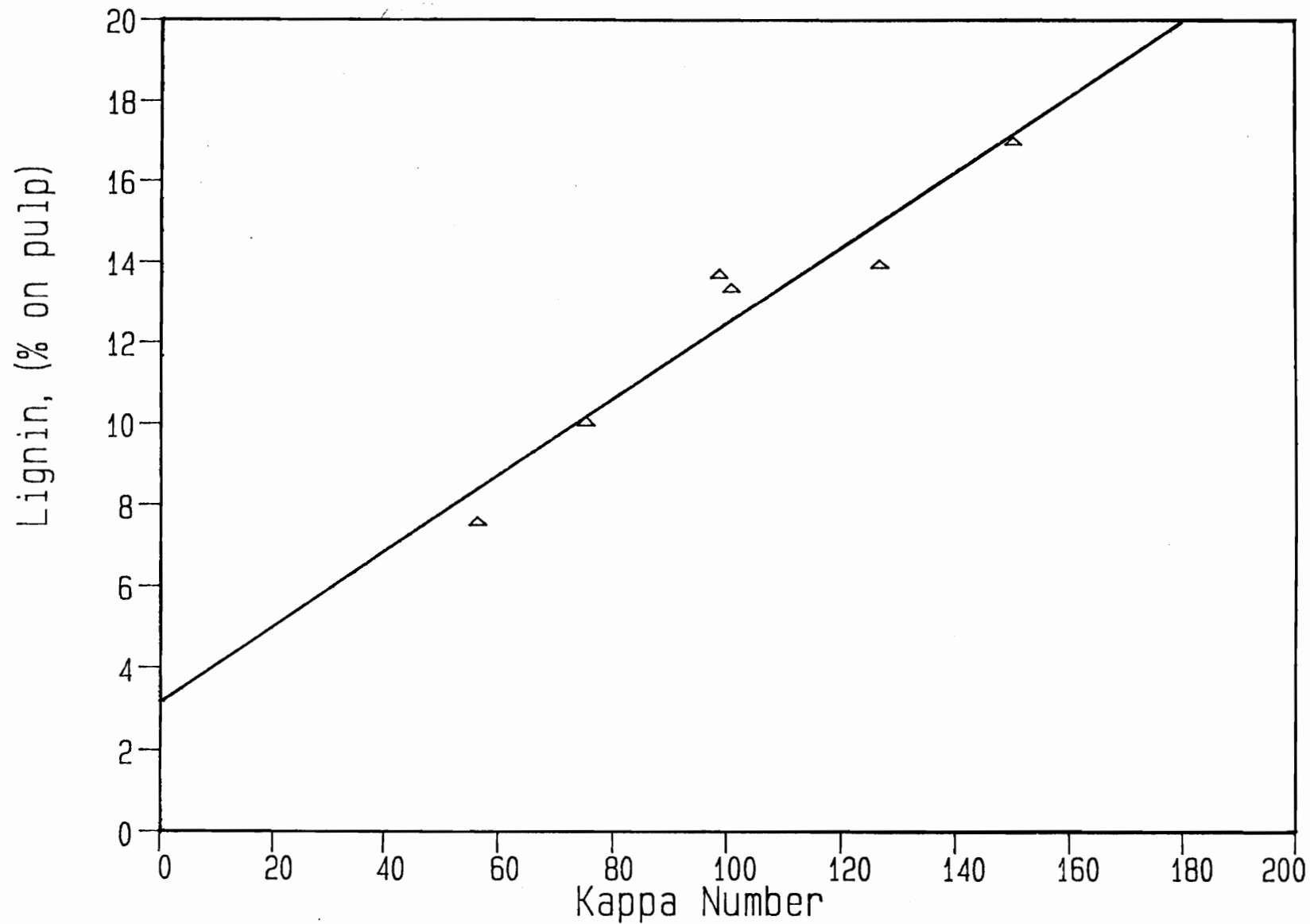


Figure 5. Calibration curve between kappa number and lignin (% on pulp) of pulps.

## RESULTS SECTION

In this section, we discuss the results of the analysis of the rate data for the ASAQ delignification process, which were obtained using the experimental design and procedures indicated in the previous two sections. This section is divided into four major parts:

1. Analysis of the rate data using dimensionless numbers  $B_i$  and  $D_k$ .
2. Analysis of the rate data using shrinking core models.
3. Analysis of the rate data using the concept of time varying apparent diffusivity.
4. Analysis of the rate data based on activation energies.

Results from the analysis of rate data using the  
-----  
dimensionless number analysis:  
-----

- a. Results from the estimation of Biot numbers:  
-----

Table 6 contains the Biot Numbers calculated at the beginning and end of cooks made by the isothermal pulping data at each temperature and for each chip size. A sample calculation of the Biot numbers is included in the Appendix (section 1, Sample Calculations). In Table 6, the Biot number values range from 41 for the smallest chip size ( $d_e=0.11$  cms.) to 249 for the largest chip size ( $d_e=0.72$  cms.). As all Biot numbers are greater than 10, we can conclude that for the conditions used in this study,

Table 6. Estimated Biot Numbers at the beginning  
and at the end of the cooks. Isothermal  
method of pulping.

de, cms	0.72		0.43		0.28		0.20		0.11	
Temperature, I*	F*	I	F	I	F	I	F	I	F	
<sup>o</sup> K										
435	306	143	215	108	197	83	126	67	89	47
444	290	141	207	103	190	79	120	65	85	45
453	290	128	199	93	184	72	117	59	82	41

\* I = Initial ; F = Final

film diffusion resistance does not control the rate of delignification in ASAQ pulping. The Biot numbers decrease with decreasing chip size which indicates that internal diffusion resistance becomes less important as chip size decreases. The Biot number is always smaller at the end of the cook than at the beginning, which is consistent with a decreasing internal diffusion resistance as lignin is removed.

b. Results from the estimation of Damkohler numbers:  
-----

Damkohler numbers were calculated corresponding to the initial and final conditions for cooks done at each temperature and chip size. The results are included in Table 7 . A sample calculation for the estimation of Damkohler Numbers is included in the Appendix (section 1 Sample Calculations).

Table 7 indicates that for the largest chip size ( $d_e=0.72$  cms), as the Damkohler numbers are less than 0.1 during the initial delignification period, hence, internal diffusion resistance controls the rate of reaction for this chip size. However, during the final delignification period, as  $D_k$  are between 0.1 and 10, so the process tends to be in mixed regime with both internal diffusion resistance and chemical reaction resistance controlling the rate of reaction.

For the middle three sizes, ( $d_e=0.43$  cms,  $d_e=0.28$  cms, and  $d_e=0.20$  cms) the  $D_k$  for both the initial and

Table 7. Table of Damkohler Numbers at the beginning and at the end of cooks. Isothermal method of pulping.

de, cms	0.72		0.43		0.28		0.20		0.11		
	I*	F*	I	F	I	F	I	F	I	F	
Temperature (°K)											
435	.066	.15	.23	1.1	.27	1.98	1.6	3.5	2.3	13.6	
444	.07	.19	.13	.33	.35	3.71	.37	5.0	1.2	37.9	
453	.03	.33	.07	.79	.16	2.3	.37	3.5	1.1	12.5	

\* I = Initial ; F = Final.

final delignification period are between 0.1 and 10 showing that for these chip sizes, throughout the process, internal diffusion and chemical reaction resistance control the rate of reaction.

For the smallest chip size under study ( $d_e=0.11$  cms), during the initial delignification period, the process tends to be in mixed regime. However, as  $D_k$  for the final delignification period are greater than 10, hence chemical reaction resistance is controlling the rate of reaction during this period.

In mixed regimes, an increase in temperature moves the process more toward diffusion control. The initial delignification data in Table 7 are generally consistent with this, as the Damkohler numbers usually decrease with increasing temperature. The Damkohler numbers do not show a consistent trend with temperature at the end of the cooks, however. This is probably because the lignin content of chips of different sizes, pulped at different temperatures, vary between 4 and 11 % based on initial wood (see tables A-8, A-12, A-16). The diffusion resistance, and therefore the Damkohler number depends on the lignin content of the chip.

Results from the analysis of rate data using  
-----  
shrinking core models:  
-----

In determining the controlling resistances by this method, plots were constructed between the functions of conversion  $f(X_c, X_a)$  (Table 1) and  $t/t_a$ . Figure 6 is such

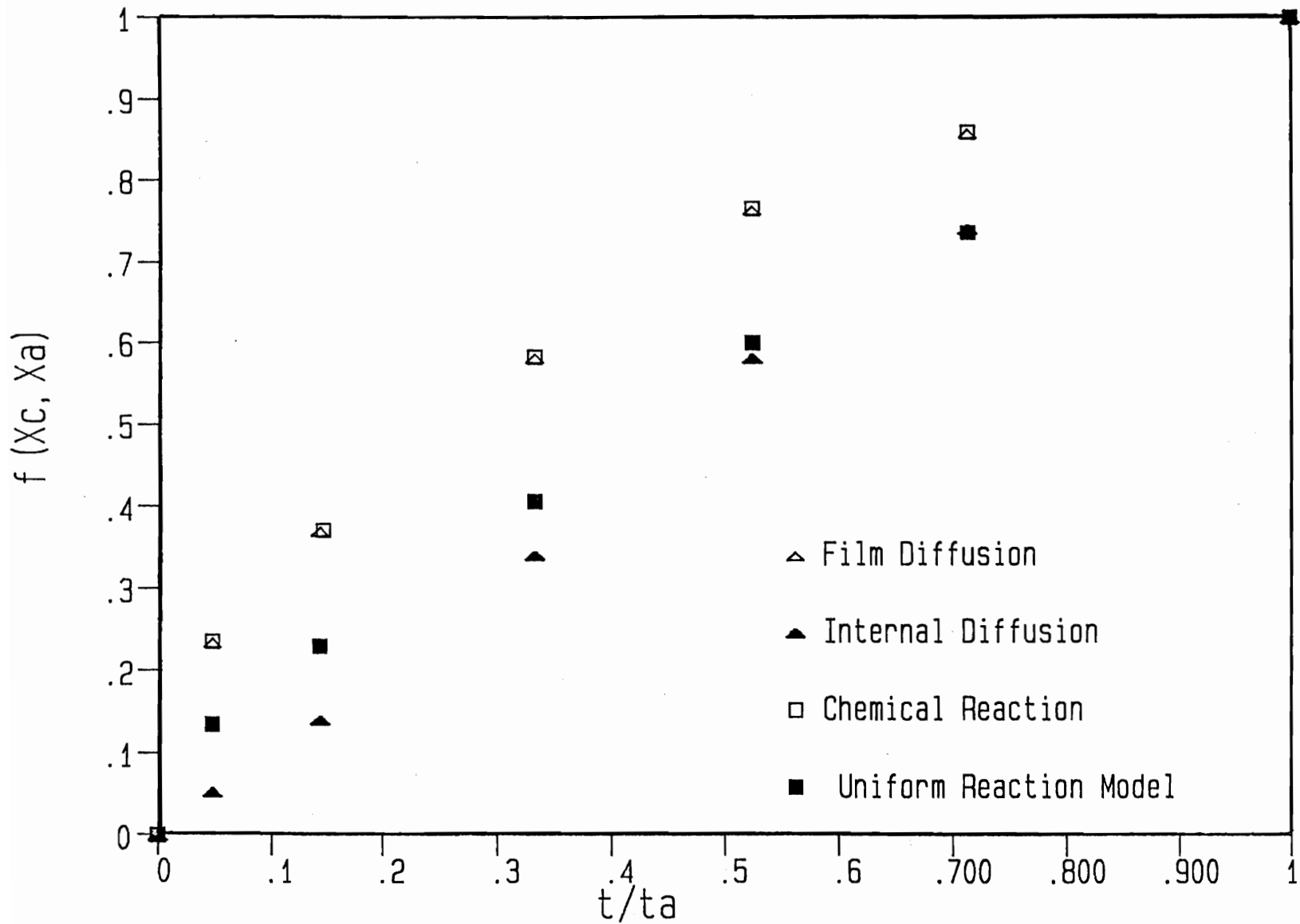


Figure 6. Plot of  $f(X_c, X_a)$  versus  $t/t_a$  of Wilder & Daleski's delignification rate data.

a plot for Wilder and Daleski's kraft pulping data (13). The data supporting this plot is shown in Table A-18 of the Appendix. This data shows that the technique of using shrinking core models works well in determining a particular resistance that controls the rate of reaction of any pulping process. From Figure 6, it is seen that the plot of  $f(X_c, X_a)$  versus  $t/t_a$  for the internal diffusion resistance is a straight 45 degree line, which means that for this delignification rate data, internal diffusion resistance controls the rate of reaction. This is consistent with the chip size (6 mm of Loblolly pine wafers) used by Wilder and Daleski. Similar results were obtained when plotting Olm and Tistad's delignification rate data for Kraft pulping. The results, shown in Figure 7, are that the internal diffusion controlled models fit much better than do either the film resistance or chemical reaction models. Olm and Tistad's data was obtained using 6 mm pine chips. The data supporting Figure 7 is shown in Table A-19 of the Appendix.

As this technique works only for the constant temperature part of the pulping, hence, for our study, the plots of  $f(X_c, X_a)$  versus  $t/t_a$  were constructed only for the constant temperature part of the cook. The plots were constructed for different chip sizes and different temperatures used in this study. For some sizes, no particular geometry was selected and plots were constructed for all three geometries ( 2-Dim. Slab, Cylindrical, and



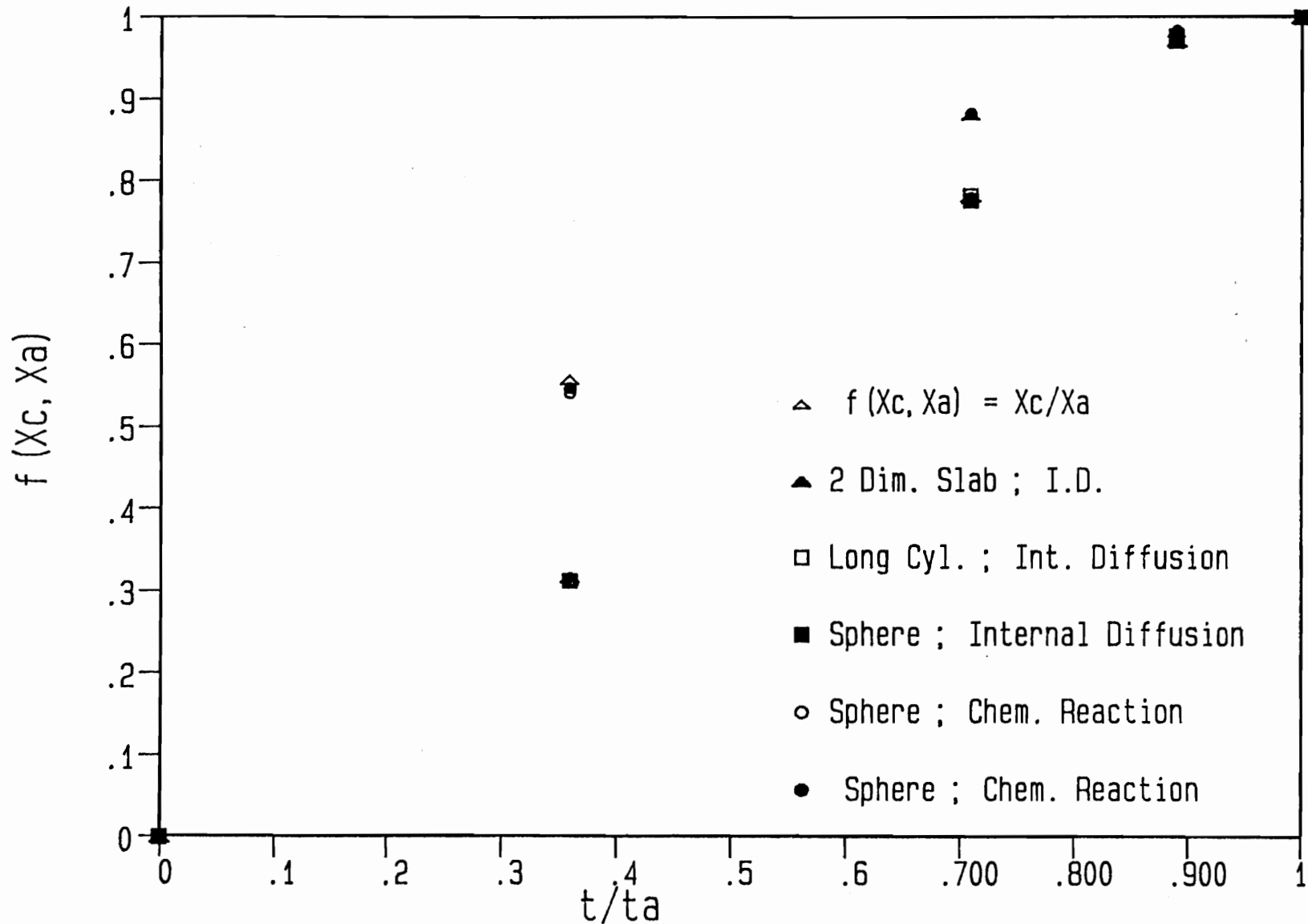


Figure 7. Plot of  $f(X_c, X_a)$  versus  $t/t_a$  ; Olm and Tistad's delignification rate data ; temperature = 313°K.

Spherical). On the other hand, for the smallest chip size ( $d_e=0.11$  cms), a spherical geometry was a reasonable assumption on the basis of the chip dimensions (see Table 4).

While constructing these plots one can select any value of lignin as the initial lignin content  $[L]_0$  so that the non isothermal part of the pulping data obtained by both the pulping methods could be left out.

Figures 8 to 11 are plots of  $f(X_c, X_a)$  versus  $t/t_a$  for the delignification rate data obtained in this study for the various chip sizes and at different temperatures. Figures 8 and 9 are plots constructed for the finite heat up method of pulping. The data supporting these plots are in Tables A-20 and A-21 of the Appendix. Figure 8 is a plot of  $f(X_c, X_a)$  versus  $t/t_a$  for the largest chip size ( $d_e=0.72$  cms). The plot was constructed for different geometries. None of the sets of points fall exactly on the 45-degree straight line, but the plots for internal diffusion for the spherical and the long cylinder geometries are closest to the 45-degree line, while the plot for film diffusion resistance is farthest from the straight line. The departure of the internal diffusion controlled data from the 45-degree line may result from another resistance (chemical kinetic resistance) contributing to the overall resistance or it may result from the changing apparent diffusivity as lignin is removed from the wood particles.

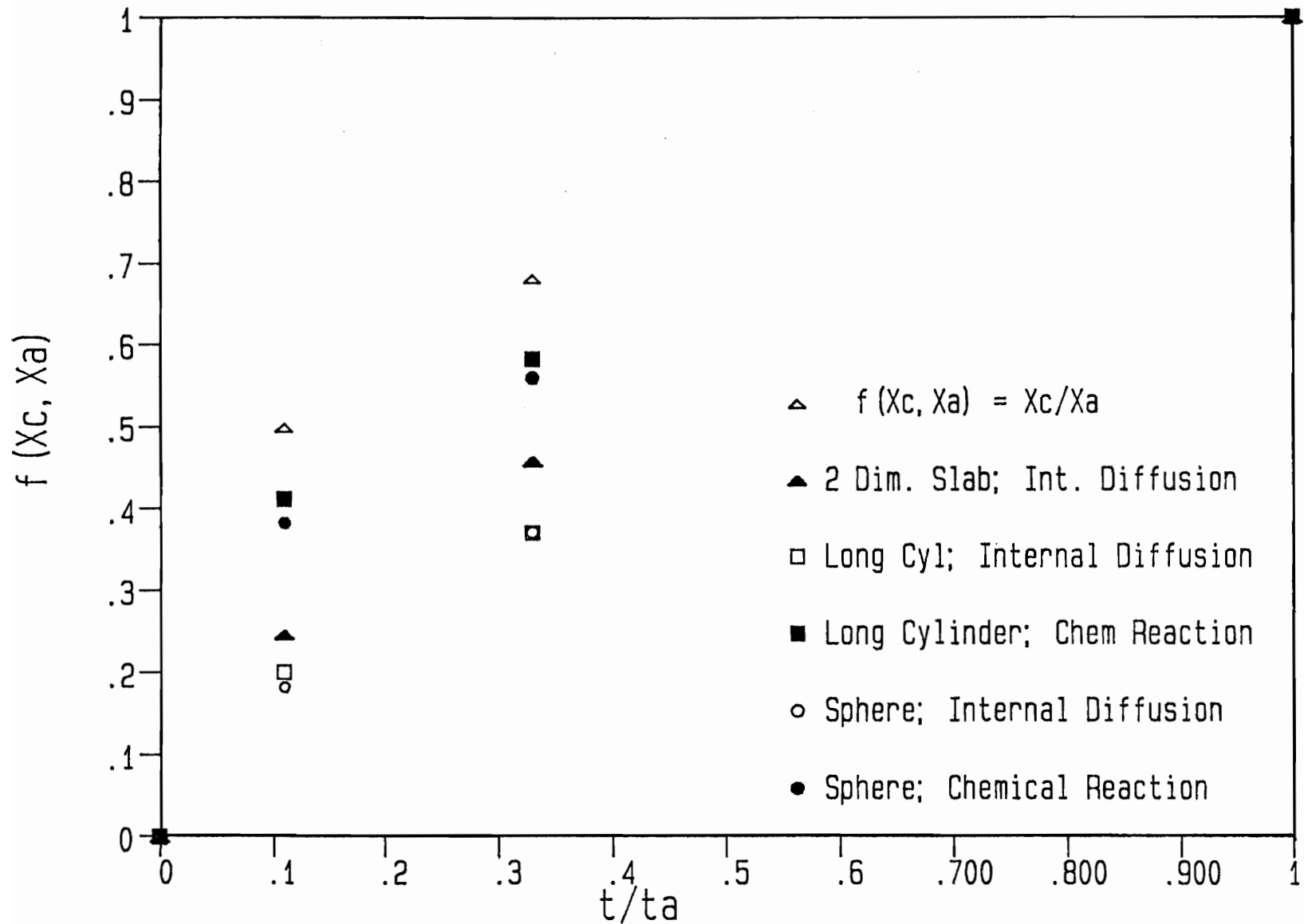


Figure 8. Plot of  $f(X_c, X_a)$  versus  $t/t_a$ ;  $d_e = 0.72$  cms; all geometries; finite heat-up method of pulping.

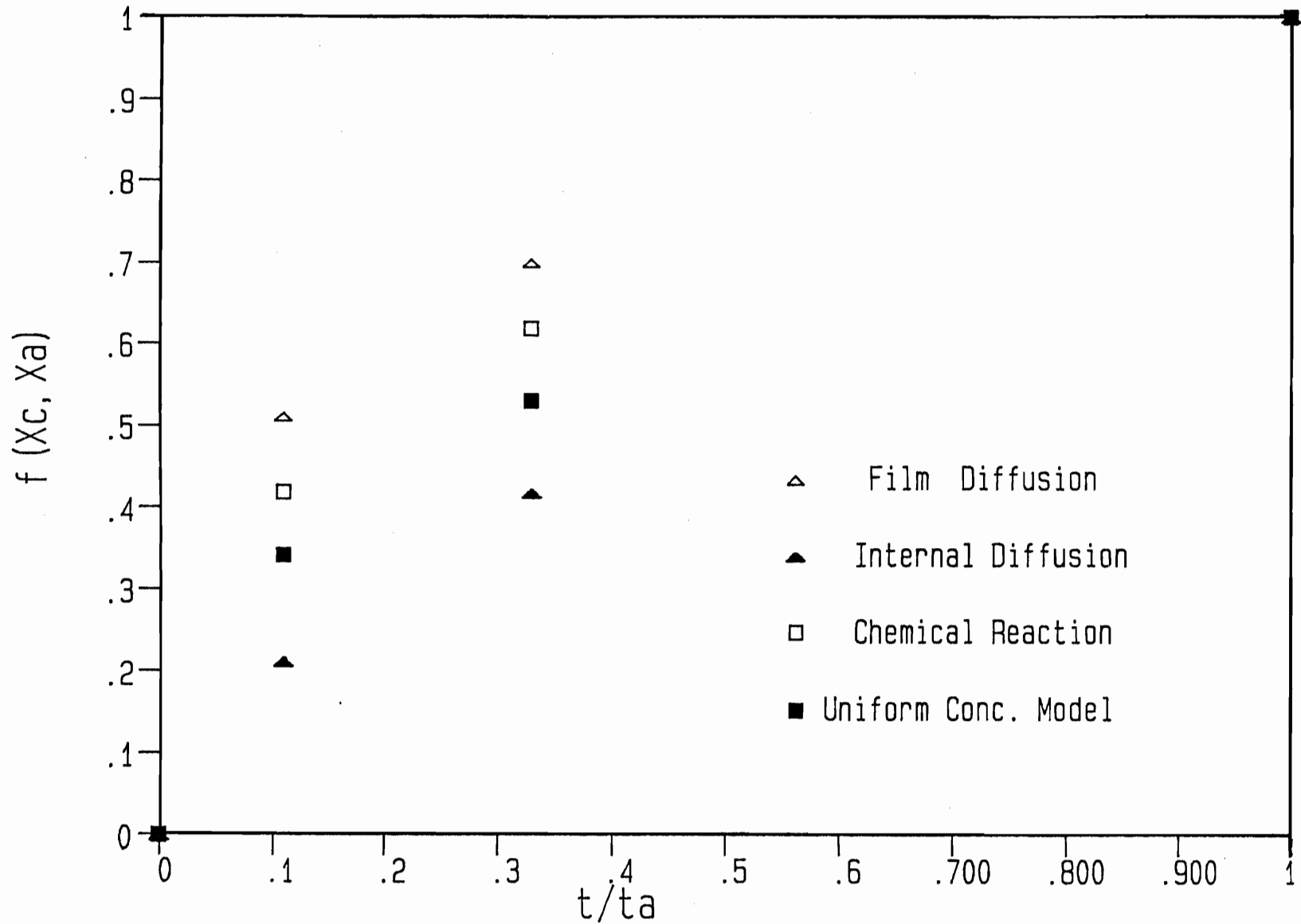


Figure 9. Plot of  $f(X_c, X_a)$  versus  $t/t_a$  ;  $d_e = 0.28$  cms; long cylinder geometry; finite heat-up method of pulping.

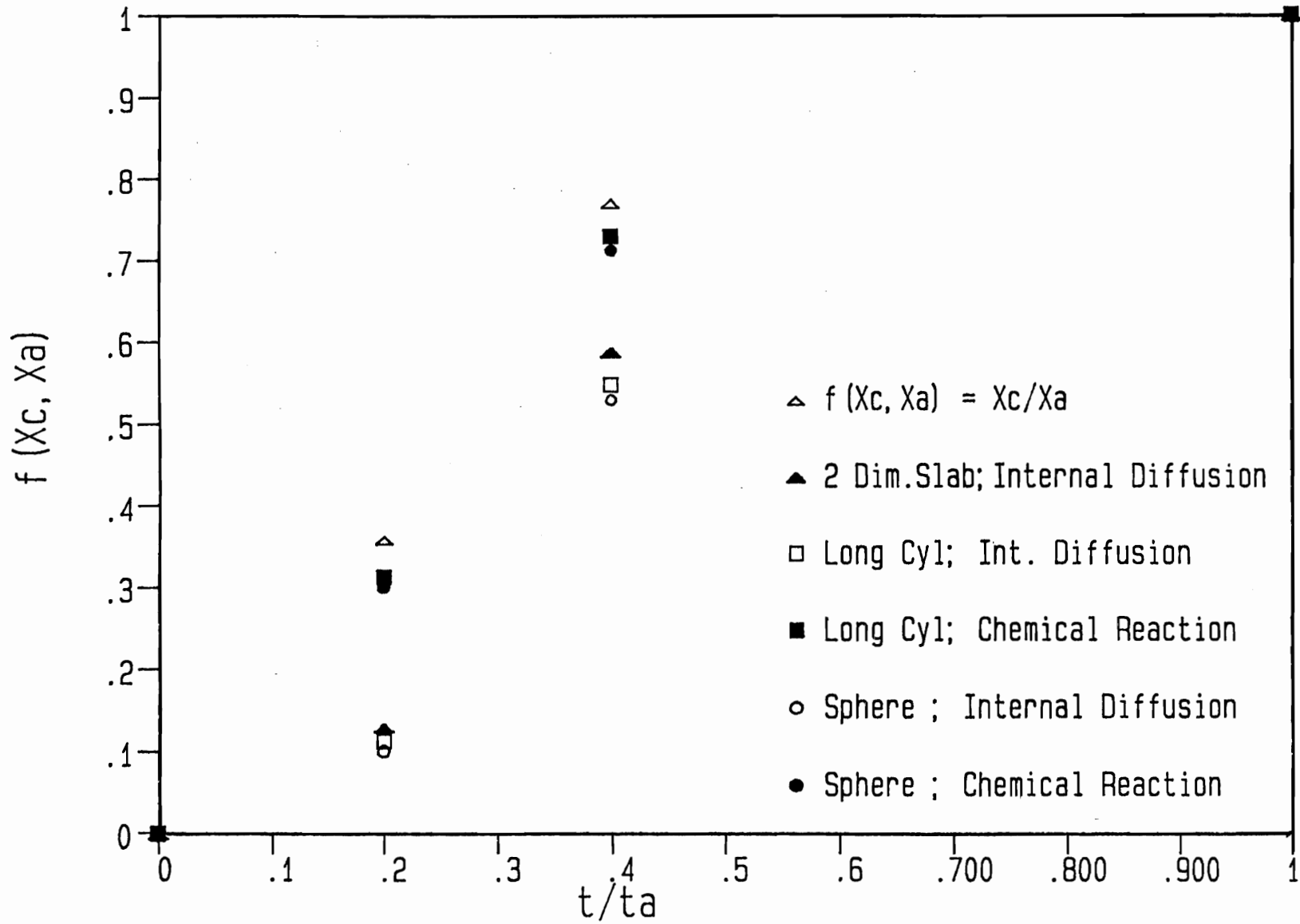


Figure 10. Plot of  $f(X_c, X_a)$  versus  $t/t_a$ ;  $d_e = 0.72$  cms; all geometries; isothermal method of pulping.

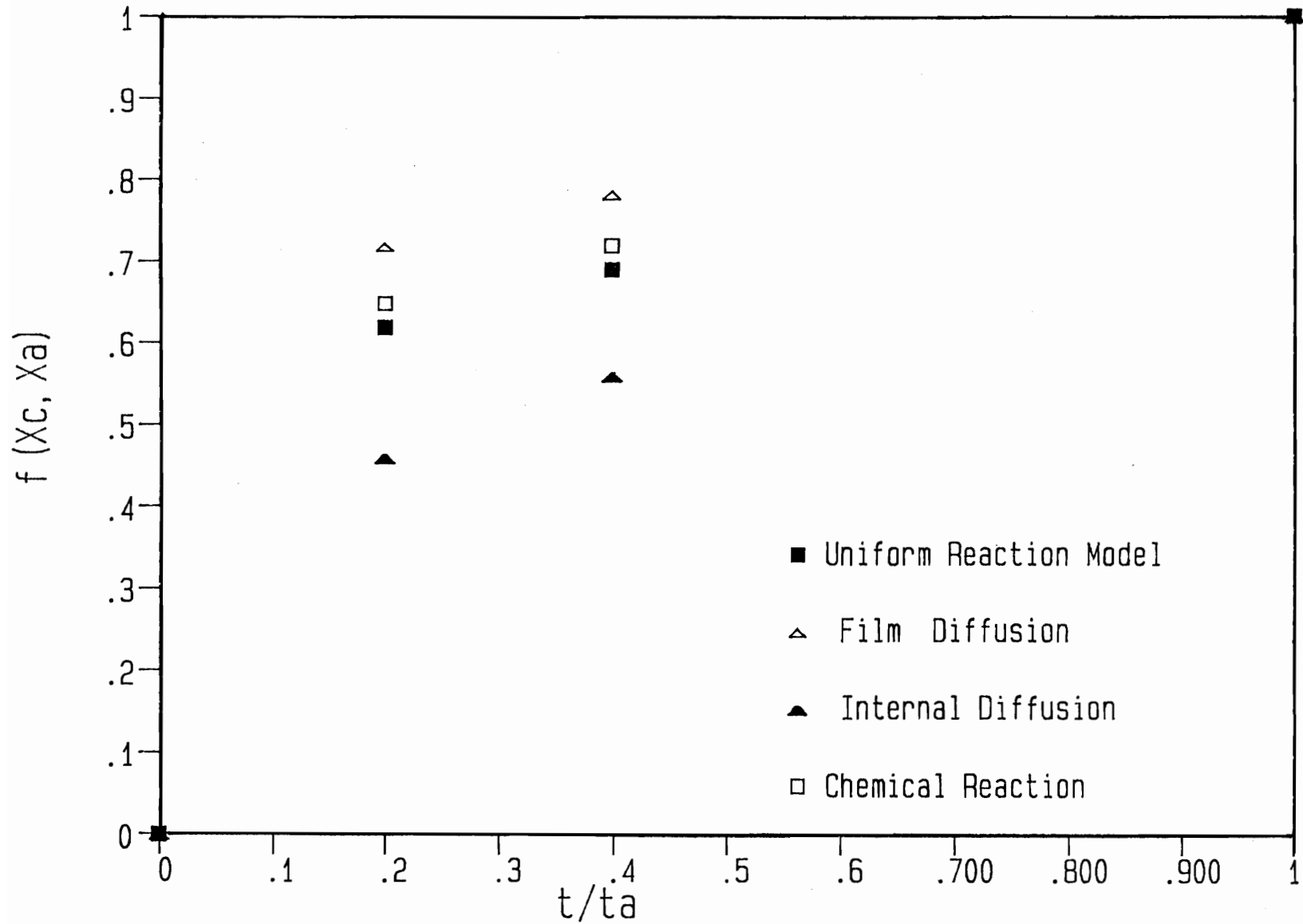


Figure 11. Plot of  $f(X_c, X_a)$  versus  $t/t_a$  ;  $d_e = 0.11$  cms ; operating temperature =  $435^\circ\text{K}$  ; isothermal method of pulping ; spherical geometry.

Figure 9 is a plot for an intermediate chip size used in this study ( $d_e=0.28$  cms). To construct this plot, we assumed a long cylinder geometry on the basis of the chip dimensions. In this plot too, we noticed that the plot for internal diffusion resistance is closest to the  $45^\circ$  line. Hence, for this chip size, the internal diffusion resistance probably controls the rate of reaction. Figures 8 to 11 also includes data plotted as uniform concentration (reaction controlled) model. This model did not fit the data as well as the internal diffusion model did.

Figures 10 and 11 are plots of  $f(X_c, X_a)$  versus  $t/t_a$  for the rate data obtained by the isothermal method of pulping. The data supporting Figures 10 and 11 are shown in Tables A-22 and A-23 respectively in the Appendix.

Figure 10 is a plot for the biggest chip size used in this study ( $d_e=0.72$  cms). Our first observation was that we obtain different shaped data plots than what we obtained with the non-isothermal (finite heat-up method). However, our observation is that the internal diffusion resistance model places the data closest to the 45-degree line. Figure 11 is a plot of  $f(X_c, X_a)$  versus  $t/t_a$  for the smallest chip size used in this study. The data was plotted using the spherical geometry. Our observation is that internal diffusion resistance model places the data closest to the 45-degree line. The observations were the same when the data was plotted using the cylindrical geometry.

On the basis of these results, one can conclude that this method of analysis indicates that internal diffusion resistance is the dominant resistance for the range of chip sizes studied. However, none of the models fit the data perfectly. Several possible explanations should be considered. One is that the apparent diffusivity changes during the cooks. A second is that the chemical reaction mechanism changes during the cooks. A third is that either a combination of resistances or other resistance not considered here (i.e., diffusion of soluble lignin from the particles) controls the rate of reaction.

We will explore the effect of changing apparent diffusivity in the next part of the results section. It is not possible to answer the question regarding a possible changing chemical mechanism during the cook with the data obtained in this study.

Results From The Analysis of Rate Data Using Time  
 -----  
 Variable Apparent Diffusivity concept:  
 -----

In the theory section, we showed that plotting  $f(X)/[D/D_0]$  versus  $t/R^2$ , where  $R$  is the radius of the chip which is approximated as a sphere, would account for a changing apparent diffusivity of  $[OH]^-$  in wood during pulping. Thus, modification of the shrinking core model equation for the internal diffusion resistance controlling case may be necessary to obtain straight lines with internal diffusion controlled rate data when the apparent



diffusivity ratio changes with time during pulping.

We first plotted lignin versus time data in the form of  $f(X)$  versus  $t/R^2$ . We then plotted  $f(X)/[D/Do]$  versus  $t/R^2$  for different chip sizes and at different temperatures.

Figure 12 is a plot of  $f(X)$  versus  $t/R^2$  for the biggest chip size ( $d_e=0.72$  cms) for different temperatures. The data supporting this figure is on Table A-24 in the Appendix. It is observed that the data did not fall on straight lines through the origin. Plots of  $f(x)/[D/Do]$  versus  $t/R^2$  for all chip sizes used in this study are shown in Figures 13-17. The corresponding data for these plots are shown on Tables A-25 to A-29 in the Appendix. The different  $r^2$  values for the data, when fit to a linear regression line are shown in Table 8.

On comparison of  $f(X)$  versus  $t/R^2$  (minutes/cm<sup>2</sup>) plot with  $f(X)/[D/Do]$  versus  $t/R^2$  plot for the largest chip size ( $d_e=0.72$  cms), we find that there is no improvement in the fit to a straight line by including the  $[D/Do]$  term.

From Table 8 of the various  $r^2$  values, one can observe that both increasing the chip size and decreasing the temperature make the data fall closer to a straight line. This is also what we would expect if internal diffusion resistance is the prominent resistance that controls the rate of reaction for the biggest chip size ( $d_e=0.72$ cms), and if both internal diffusion and chemical reaction resistances control the rate of reaction for the

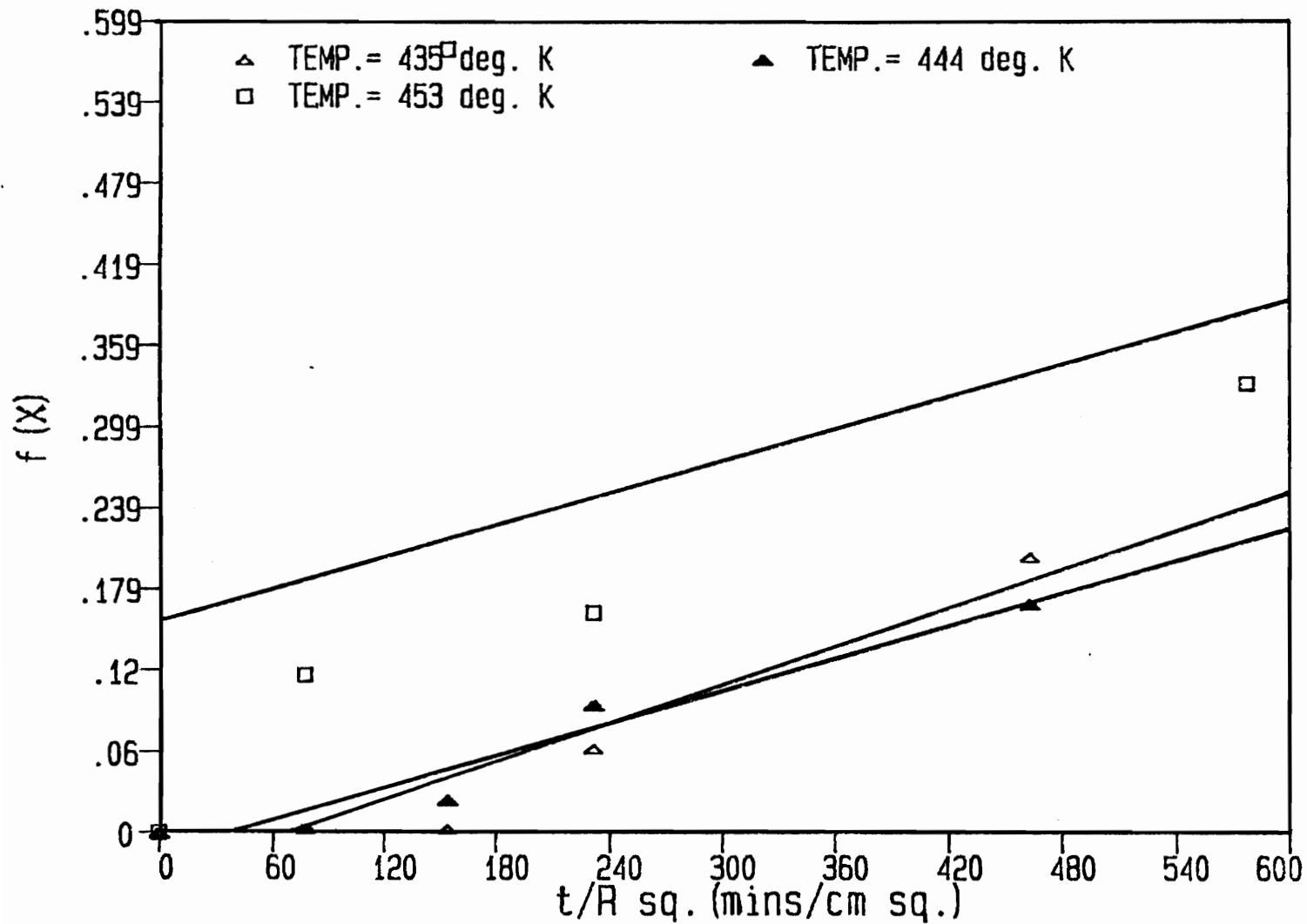


Figure 12. Plot of  $f(X)$  versus  $t/R^2$ ;  $d_e = 0.72$  cms.

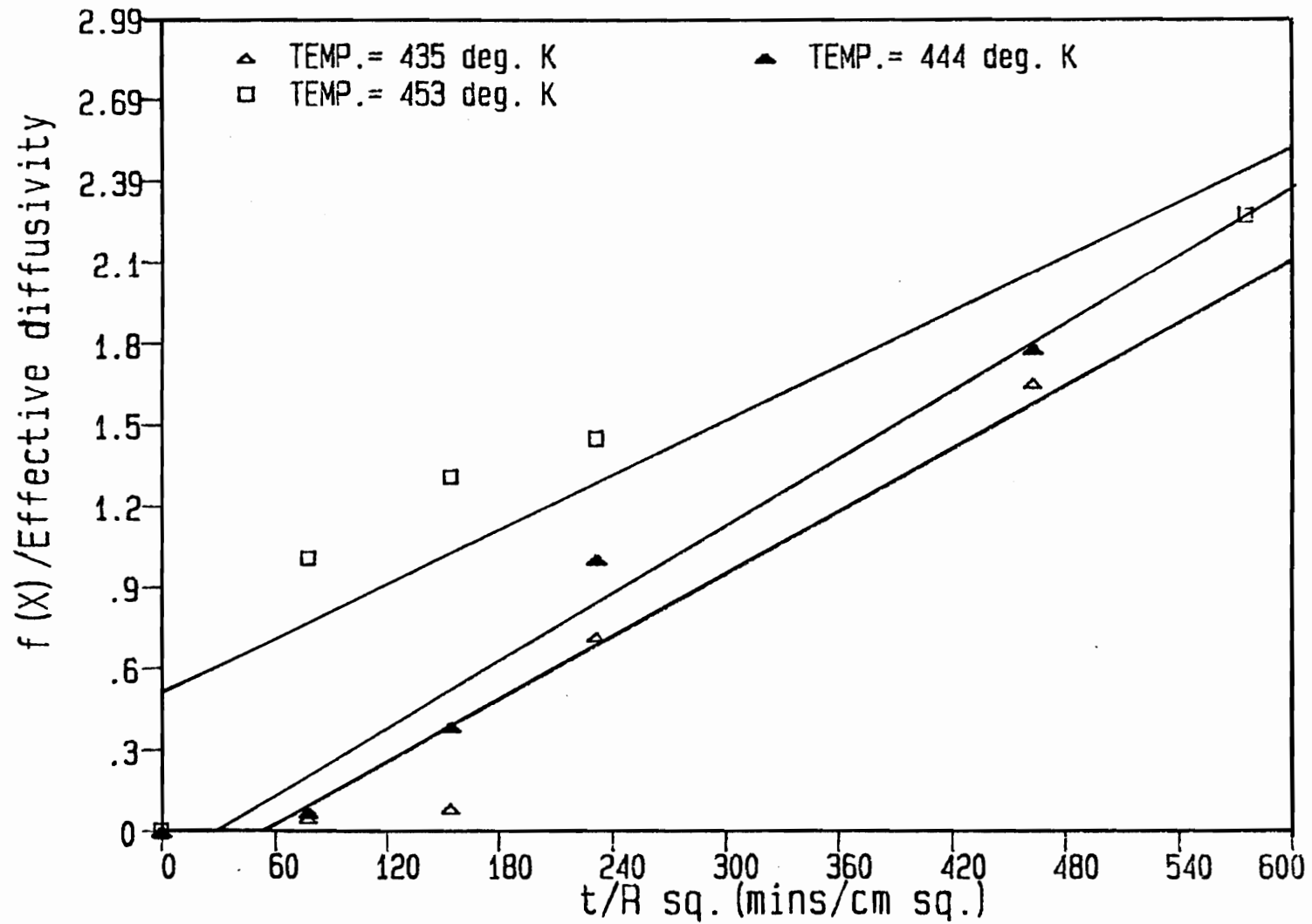


Figure 13. Plot of  $f(X)/\text{Effective Diffusivity}$  versus  $t/R^2$  ;  $d_e = 0.72$  cms.

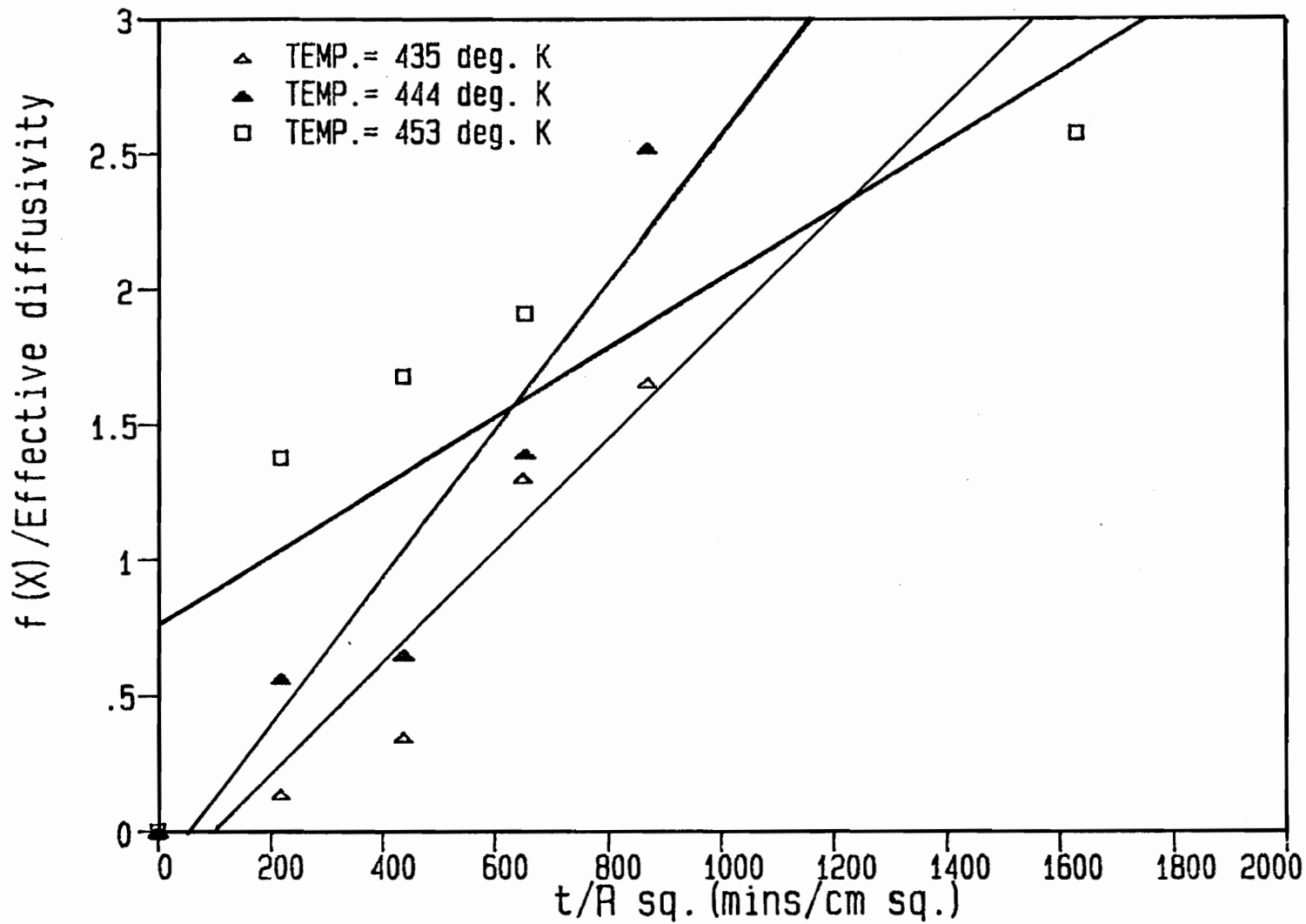


Figure 14. Plot of  $f(X)/\text{Effective Diffusivity}$  versus  $t/R^2$ ;  $d_e = 0.43$  cms.

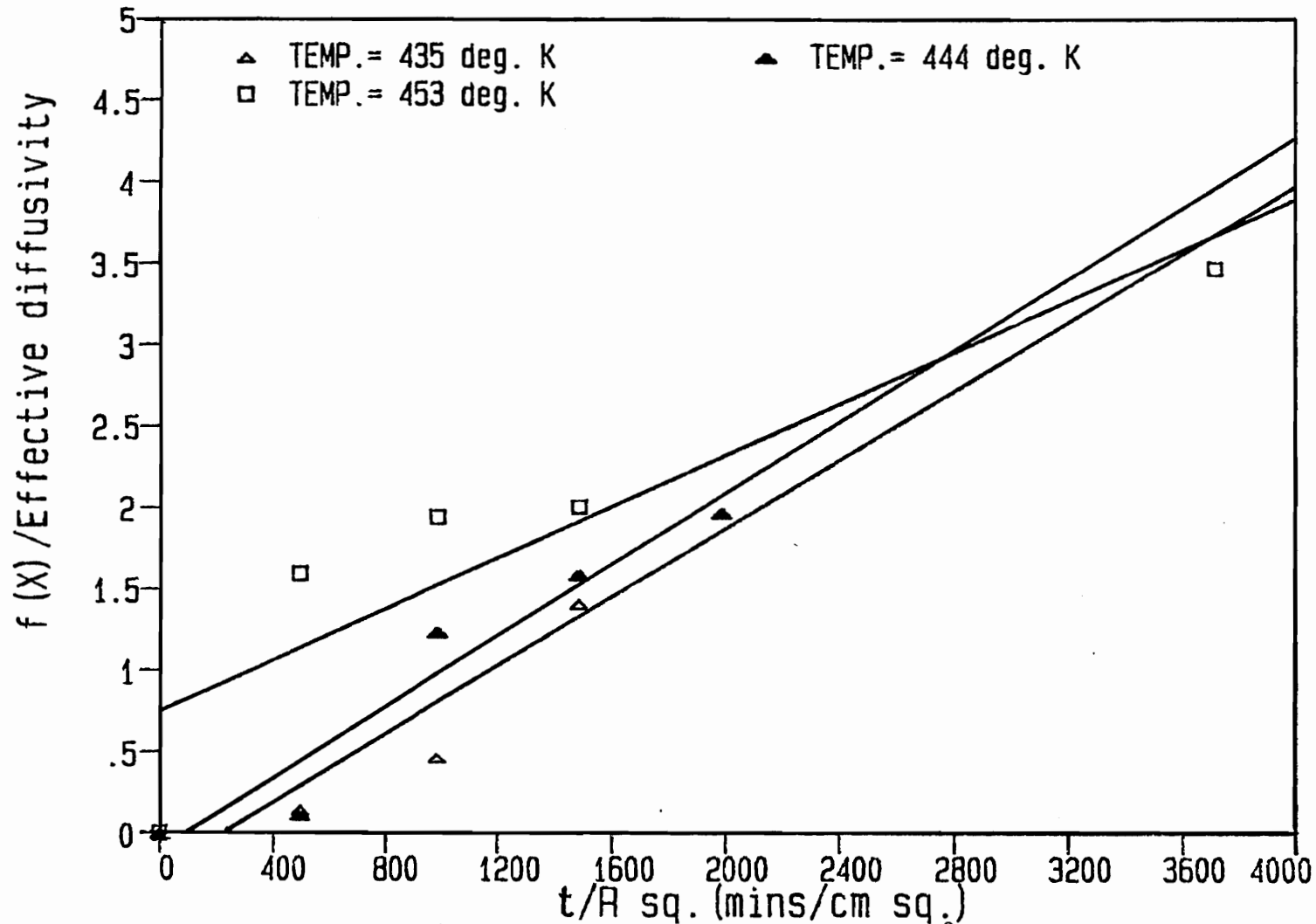


Figure 15. Plot of  $f(X)/\text{Effective Diffusivity}$  versus  $t/R^2$ ;  $d_e = 0.28$  cms.

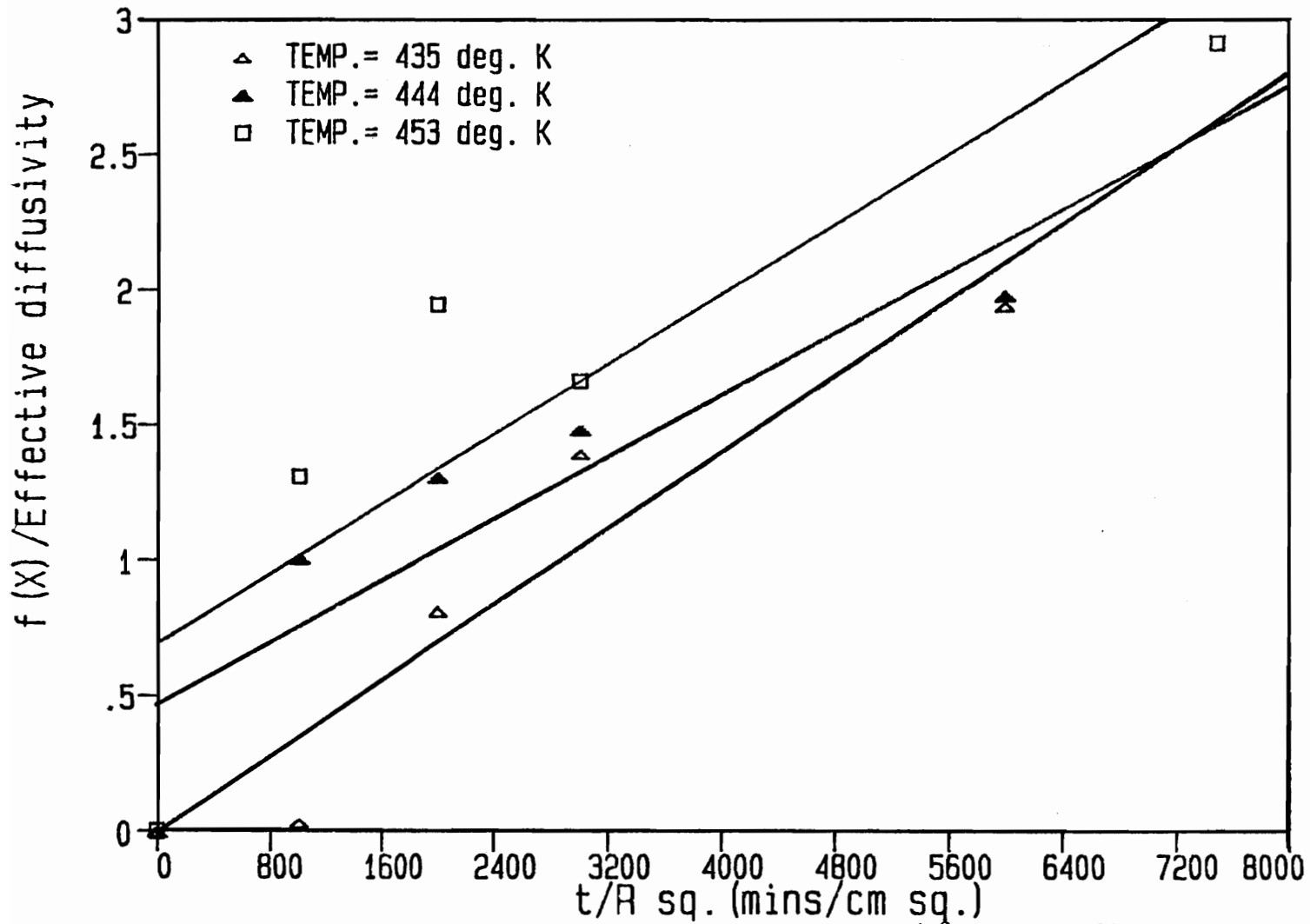


Figure 16. Plot of  $f(X)/\text{Effective Diffusivity}$  versus  $t/R^2$ ;  $d_e = 0.20$  cms.

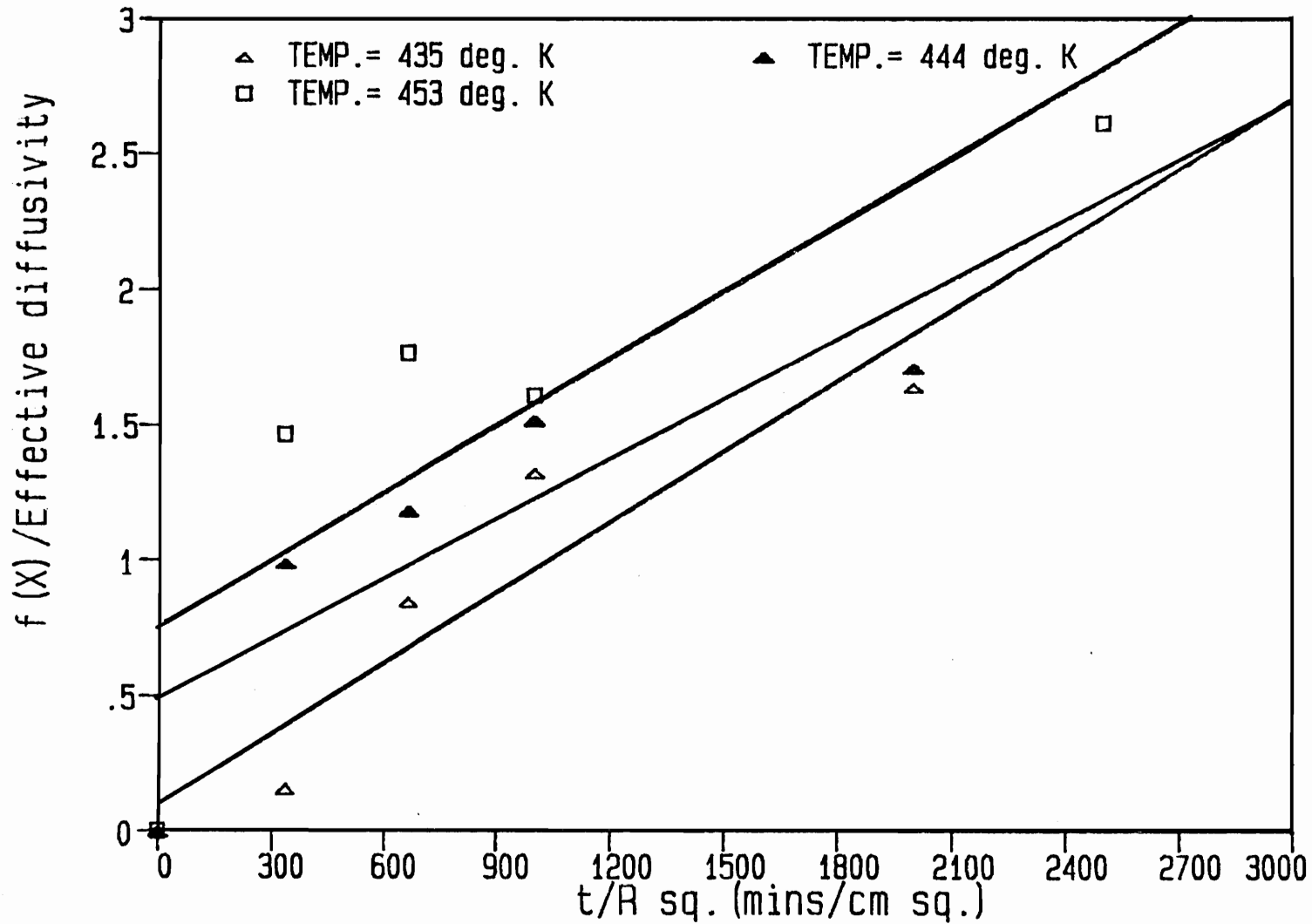


Figure 17. Plot of  $f(X)/\text{Effective Diffusivity}$  versus  $t/R^2$ ;  $d_e = 0.11$  cms.

Table 8. Table of mean square regression ( $r^2$ ) values  
for  $f(X)/(D/Do)$  versus  $t/R^2$  in figures 12-17.

Chip size, (de, cms)	0.72	0.43	0.28	0.20	0.11
Temp( $^{\circ}$ K)					
435	0.93 0.90*	0.88	0.92	0.90	0.87
444	0.97 0.94*	0.90	0.81	0.76	0.84
453	0.87 0.91*	0.74	0.84	0.78	0.72

\* " $r^2$ " values of the plot of  $f(x)$  versus  $t/R^2$  (figure 12).



other chip sizes used in this study.

Results from the analysis of the rate data  
 -----  
 using activation energy data:  
 -----

Table A-30 in the Appendix contains Olm and Tistad's kraft delignification rate data for three temperatures (23). Calculation of  $t_n$ , where  $t_n$  is the time of pulping that it took to reach a residual lignin (% on wood) value of 25.7 % is done at different temperatures used in this study. The details are as shown on Table A-30. Figure 18 is a plot of  $\ln(1/t_n)$ , where  $t_n$  is the time corresponding to 13.6 % delignification versus  $1/T$  for this data. From the slope of this plot, the value of activation energy was calculated to be equal to 6.4 Kcal/g mole.

The magnitude of the activation energy indicates that internal diffusion resistance is controlling the rate of reaction. This is consistent with the interpretation of the shrinking core models plot (Figure 7) for Olm and Tistad's data.

In a similar way, activation energy plots were made for the delignification rate data obtained in this study. Figure 19 is one such plot for one of the chip sizes used in this study ( $d_e=0.28$  cms). The data supporting this plot is shown in Table A-31 of the Appendix. The reciprocal times at each temperature correspond to three different residual lignin values of 12% , 17%, and 21% on wood. Similiar plots were made for all the five

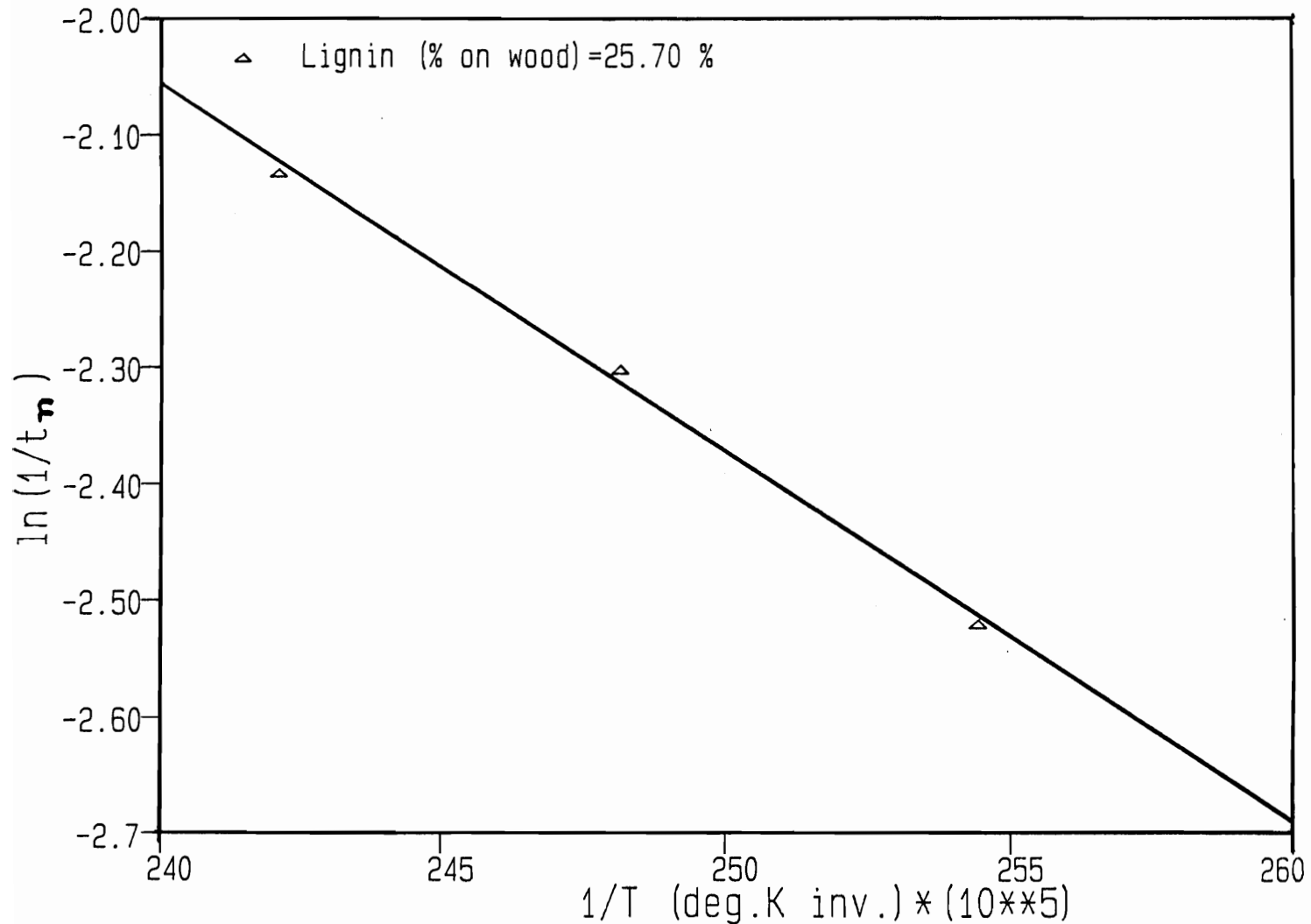


Figure 18. Plot of  $\ln(1/t_n)$ , where  $n = 13.50\%$  versus  $1/T$  for calculation of activation energy of Olm and Tistad's delignification rate data.

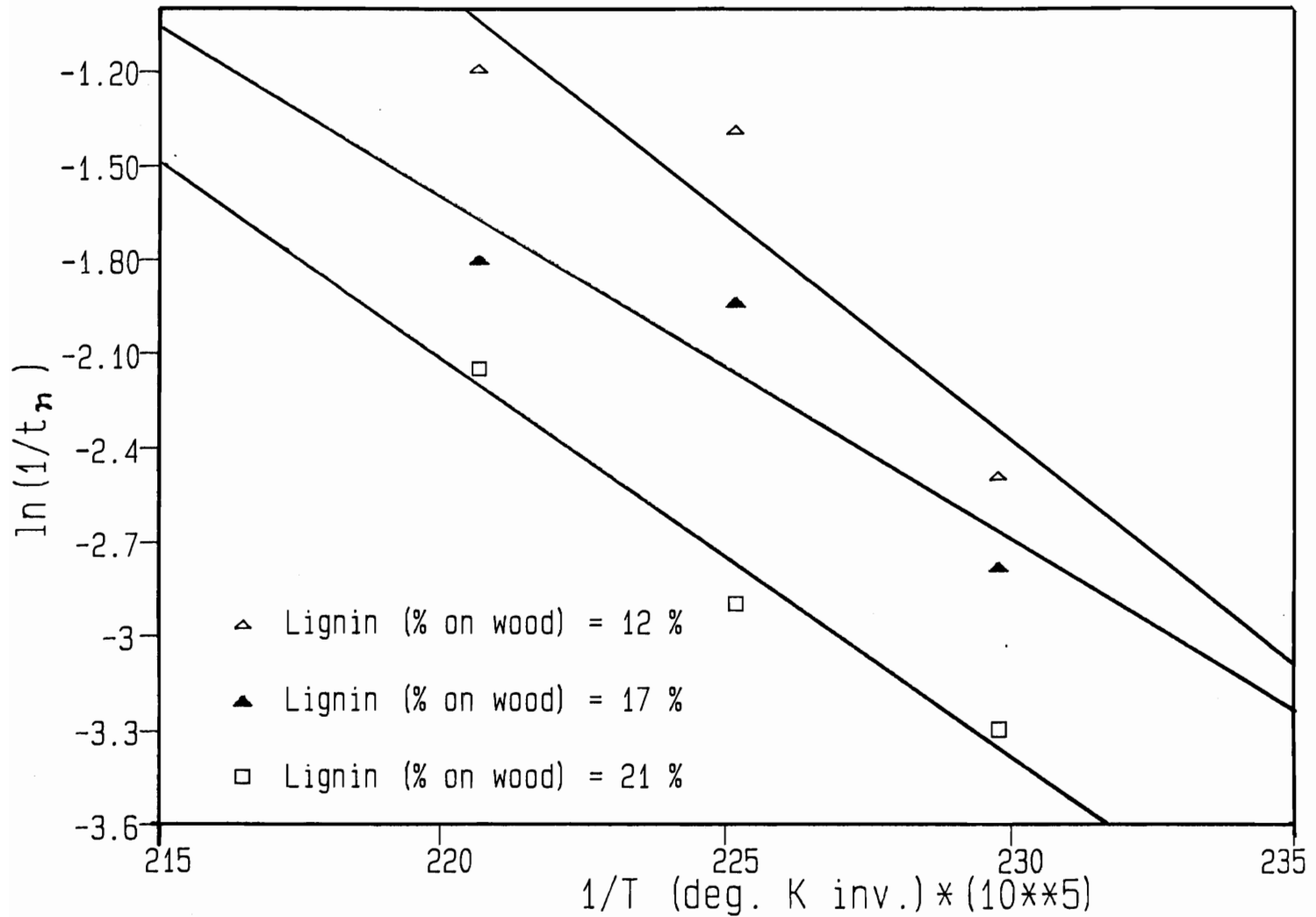


Figure 19. Plot of  $\ln(1/t_n)$ , where ( $n = 56.8\%$ ,  $38.8\%$ , and  $24.4\%$ ) versus  $1/T$  for calculation of activation energy. Isothermal method of Pulping data;  $d_e = 0.28$  cms.

chip sizes in the experimental study.

Table 9 shows the activation energy results for our rate data, with their standard deviations. Table 9 reveals that the activation energies of this process were between 17 and 35 Kcals/gm mole. Since all but one of the activation energies are greater than 20 Kcal/g mole, the analysis indicates that reaction kinetics control the rate of reaction. The mean square regression values ( $r^2$  values) for each plots are shown along with each activation energy value in the Table 9. From the  $r^2$  values one notices that the plots do not turn out to be good straight lines. The curvature of the plots of  $\ln(1/t)$  versus  $1/T$  indicates that the mechanism is changing with the temperature. Hence, one must treat activation energy data with skepticism, giving it less weight than the other analysis ( dimensionless groups, shrinking core models, and time variable apparent diffusivity ).

Though we observe that for Olm and Tistad's delignification rate data, the shrinking core models analysis and the activation energy determination analysis leads us to the same conclusions, we find out that for our rate data, the conclusions that are drawn by various methods of analysis used in this study are not very consistent. We notice that though dimensional analysis and shrinking core models show that internal diffusion resistance controls the rate of reaction for all chip sizes, except for the smallest chip size ( $d_e=0.11$  cms),

Table 9. Table of activation energy values (k cal) of various chip sizes and at various lignin, L (% on wood).

Chip size (de, cms)	0.72	0.43	0.28	0.20	0.11
Lignin, L (% on wood)					
12 (r <sup>2</sup> )	18±8.7 0.88	35± 8.6 0.90	28± 8.1 0.91	24±5.6 0.85	30±4.6 0.86
17 (r <sup>2</sup> )	31±5.4 0.91	39±16.9 0.92	28± 9.5 0.91	24±7.2 0.89	22±2.8 0.90
21 (r <sup>2</sup> )	34±15.5 0.87	35±9.5 0.88	31± 4.0 0.87	31±3.7 0.86	26±6.5 0.89

\* All numbers are expressed as Activation Energy values + Standard deviations of these numbers.

the activation energy analysis predicts that chemical reaction resistance controls the rate of reaction. For the smallest chip size ( $d_e=0.11$  cms) , however, the Damkohler number estimations and the activation energy analysis leads us to the same conclusions.

In view of the above mentioned analysis, and the assumptions required to use these analysis, I have more confidence in using the dimensional analysis as an important method to analyze the delignification rate data for predicting the controlling resistance during this pulping process, as this method is not based on any assumptions. Hence, this method of analysis is recommended for such studies. With proper assumptions and the formulation of the correct rate model, one can rely on shrinking core model technique too for analysis of the rate data.

The ideal chip size used for the commercial pulping process (1) usually ranges from 1-3 cms. in length, and 0.2-0.5 cms thick. Hence, from the analyses that we carried out in this thesis, we can conclude that for chips used in the pulp mills, internal diffusion resistance controls the rate of reaction.

## CONCLUSIONS.

From the results of this work, we can conclude the following:

1. Analysis of the rate data using the dimensionless numbers indicates that the rate of reaction is influenced by both internal diffusion and chemical reaction resistances for all chip sizes under study.
2. The rate data, when analyzed using shrinking core models fit best for internal diffusion. However, the data is not fit well by any of these models, which suggests that either the controlling regime changes during the pulping or that the assumptions on which the models are based do not apply in this situation.
3. Including a term to account for changes in the effective diffusivity of the pulping chemicals in wood chips during pulping does not improve the fit of Shrinking core models to the data.
4. From the activation energy determinations, one can conclude that the process is in the chemical regime for the chip sizes under study. However, as  $\ln(1/t)$  versus  $1/T$  plots for these chip sizes do not show good straight lines, there may be a shift in the controlling mechanism during pulping.

## BIBLIOGRAPHY.

1. Smook G A.; "Handbook of Pulp & Paper Technologists". Joint Textbook Committee of the Paper Industry; 1982.
2. Kettunen J., Virkola N., and Yrjala I.; 11, 1979, 685-700; Paperi ja Puu - Papper och Tra; "Effect of Anthraquinone on neutral sulfite and alkaline sulfite cooking of pine".
3. Wong A.; Private Communication.
4. Raubenheimer; Eggers S.; 34, 19-23 (10 A, 1980); Das Papier; "Some aspects of sulfite pulping of Softwoods", E.S.P.R.I., 11<sup>th</sup> European Meeting, May 1979, "Pulping with sulfite and anthraquinone".
5. Ingruber O., Stradal M., Histed J.; 83, T 342 - 349 (1982); Pulp & Paper Canada ; "Alkaline Sulfite - Anthraquinone pulping of Eastern Canadian woods".
6. C.I.P. Research Ltd; Hawkesbury, Ontario, Canada.
7. B.C.Research ; Air Pollution Control Technology, Project 2419, 1976.
8. Kettunen J., Railawa I., Ruhanen M.; 1982. Int'l Sulfite Pulping Conference, Toronto, Canada; "A case study to convert a kraft mill into a neutral sulfite anthraquinone mill".
9. Cooper and Jeffreys ; "Chemical kinetics and Reactors designing". 1<sup>st</sup> American Ed.; Englewood Cliffs, N.J., Prentice-Hall 1973.
10. Levenspiel O.; " Chemical Reaction Engineering - An introduction to the design of Chemical reactors". Wiley Int'l Ed, N.Y., London; 1962.
11. Hammes G.; "Principles of Chemical Kinetics". N.Y. Academic Press, 1978.
12. Schoon Nils Herman; R185-R193, 1982; Svensk Papperstidning; "Interpretation of rate equations from the kinetic studies of wood pulping and wood bleaching".
13. Wilder H., Han S.,; Jan.1962., Vol.45 No.1; Tappi; "A comparison of the kinetics of the neutral sulfite and kraft pulping processes".
14. Gustafson R., Snelcher C., McKean W., Finlayson B.; 22,1,1983; pp 87-96; Ind.Eng.Chem.Process Des.Dev.;



C & E News; "Theoretical Model of the Kraft Pulping process".

15. Johnstone and Thring ; "Pilot Plant Models and Scale Up methods in Chemical Engineering"; N.Y. Academic Press, 1958.
16. Treybal R.; "Mass Transfer Operations". Mc Graw-Hill Book Company, N.Y.; 4<sup>th</sup>. Ed., 1981.
17. Karter E., Bobalek E.; 54(11), 1971, pp 1882-1888; Tappi; "Role of Physico - chemical rate phenomenon in wood pulp chlorination".
18. McKibbins S.; Vol.43, No.10, 1960, pp 801-85; Tappi; "Application of Diffusion theory to the washing of Kraft wood chips".
19. Christensen G.; No.4, 1951, pp 430; Australian Journal of Applied Science.
20. Hartler Nils; No.7, 1982, Papper och Tra ; Penetrerings -och diffusions - forkallandena vid sulfatkoket.
21. Glasstone S., Laidler K., and Eyring H.; 1<sup>st</sup> ed., page 537, Mc-Graw - Hill Co., Inc., 1941; "The theory of Rate processes".
22. Wilder H., Daleski E., (Jr.); Vol. 48, No.5, May 1965; Tappi; "Delignification rate studies".
23. Olm L., and Tistad G., Nr. 15, 1979, Svensk Papperstidning ; " Kinetics of the initial stage of Kraft pulping".

## APPENDIX

The appendix section of this thesis work is divided into the following sections:

1. Sample Calculations:

a) Sample Calculation for Estimation of Biot Numbers.

b) Sample Calculation for Estimation of Damkohler Numbers.

c) Sample Calculation for  $f(X)$  versus  $t/R^2$  plot.

d) Sample Calculation for  $f(X)/\text{Effective Diffusivity}$  versus  $t/R^2$  plots.

2. Cooking Liquor preparation:

a. Finite Heat-Up Method of Pulping.

b. Isothermal Method of Pulping.

3. Tables A-1 to A-31.

## 1. SAMPLE CALCULATIONS.

Sample calculations for Estimation of Biot Numbers ( $B_i$ ):

$$B_i = (k_L * l) / D \quad (57)$$

$$k_L = 1.17 * R_e^{-.415} * U_{ave} * S_c^{-.667} \text{ (Trickle Bed filter). ... (58)}$$

Since, we do not know which dimension, if any, dominates the transport within chips,

$$l = 6 / (S/V) - \text{equivalent diameter ( sphere )}.$$

$$D = 5.7 * 10^{-2} * T^{1/2} * \exp((-4870/(R*T)) [(-.02*[L]) + (.13*[OH]^{.55}) + 0.58]) \quad \dots (59)$$

The Sample calculation is carried out for the biggest chip size ( $d_e = 0.72 \text{ cms}$ ),  $T = 435^\circ \text{K}$ ,  $L = 27.2$  ( % on wood ).

$$\text{pH of liquor} = 11.34.$$

$$[\text{OH}]^- = 10^{11.34 - 14.00} = 0.00219 \text{ moles/liter}.$$

Substituting the values of  $[L]$ ,  $[\text{OH}]^-$ , and  $T$ , in equation (59),

$$D = 0.000171 \text{ cm}^2/\text{min}.$$

$$S_c = \mu / (\rho * D) \quad \dots (60)$$

From the literature survey (24), at  $298^\circ \text{K}$ , and 0.3 % solids concentration,

$$\mu_{\text{liquor}} = 0.9 \text{ cP} = 0.9 * 10^{-2} \text{ g/( cm-sec )}$$

$$\rho_{\text{liquor}} = 1.0 \text{ g/cm}^3 = \rho_{\text{water}}$$

Substituting these values into equation (60),

$$S_c = 3160.$$

Superficial Velocity ( $U_{ave}$ ):

$$U_{ave} = \frac{\text{Volumetric flow rate}}{\text{Cross Sectional Area of digester}} \dots (61)$$

Cross Sectional Area of Digester

$$= \frac{\pi * (\text{diameter of digester})^2}{4} \dots (62)$$

diameter of digester = 6.25" = 15.62 cms.

Substituting this value into equation (62),

$$\text{Cross Sectional Area of Digester} = 191.52 \text{ cm}^2$$

Volumetric flow rate of liquor = 20 lit/min

(manually measured)

$$= 333.33 \text{ cm}^3/\text{sec.}$$

Thus,  $U_{ave} = 1.74 \text{ cms/sec.}$

$$\text{Reynolds Number} = Re = \frac{d * U_{ave} * \rho}{\mu} \dots (63)$$

diameter of particle = Equivalent diameter,  $d_e$

$$d = d_e = 6 / (S/V) = 6/8.3 = 0.72 \text{ cms.}$$

Substituting the value of  $d, U_{ave}, \rho, \mu$  in equation (63),

$$Re = 139.2$$

Substituting the values of  $Re, U_{ave},$  and  $S_c$  into

equation (58),

$$k_L = 1.17 * (139.2)^{-0.415} * (1.74) (3160)^{-0.667}$$

$$\text{or } k_L = 0.00121 \text{ cms/sec.}$$

Substituting these values into equation (56),

$$B_i = 306.$$

Sample Calculation for Estimation of Damkohler Numbers:

Sample # 1 ( $d_e = 0.72$  cms).

Constant Temperature =  $162^{\circ}\text{C} = 435^{\circ}\text{K}$ .

thickness = 0.352 cms.

Delignification Rate data :

Lignin, L (% on wood)	Time (mins)
27.2	0
25.2	10
24.3	20
16.7	30
9.6	60

Initial Increment rate  $= (-dL/dt)_{\text{init.}}$

$$= (27.2 - 25.2) / (10 - 0)$$

$$= 0.195 \text{ \% on wood/mins}$$

Final Increment rate  $= (-dL/dt)_{\text{fin.}}$

$$= (16.70 - 9.69) / (60 - 30)$$

$$= 0.234 \text{ \% on wood/mins}$$

$$\text{Damkohler Number, } D_k = ([L] * D_a) / \{ (-dL/dt) * l^2 \}$$

..... (64)

where,  $l$ , diffusion path length

= equivalent diameter ( $d_e$ ) = 0.72 cms

and  $D$ , diffusivity of  $[\text{OH}]^-$  in the wood chips,  
is given by equation (59).

Substituting the values of  $R$ ,  $T$ ,  $[L]$ ,  $[\text{OH}]^-$  into  
equation (59),

$$(D)_{\text{init.}} = 0.000256$$

$$\text{and } (D)_{\text{fin.}} = 0.00136$$

$$[L]_{\text{init.}} = (27.2 + 25.2)/2 = 26.2$$

$$[L]_{\text{fin.}} = (16.7 + 9.6)/2 = 13.15$$

From equation (64), writing equations for  $(D_k)_{\text{init.}}$  and  $(D_k)_{\text{fin.}}$ , we get

$$(D_k)_{\text{init.}} = ( [L]_{\text{init.}} * (D)_{\text{init.}} ) / ( (-dL/dt)_{\text{init.}} * l^2 ) \quad \dots\dots(65)$$

$$(D_k)_{\text{fin.}} = ( [L]_{\text{fin.}} * (D)_{\text{fin.}} ) / ( (-dL/dt)_{\text{fin.}} * l^2 ) \quad \dots\dots(66)$$

Substituting the above values into equations (65)

and (66), we get,

$$(D_k)_{\text{init.}} = 0.066.$$

$$(D_k)_{\text{fin.}} = 0.147.$$

Sample Calculation for  $f(X)$  versus  $t/R^2$  plot:

Sample rate data :

chip size,  $d_e = 0.72$  cms.

Constant temperature =  $435^\circ\text{K}$

thickness =  $0.352$  cms.

Temperature ( $^\circ\text{K}$ )	Lignin, L (% on wood)	time, t (mins.)
	27.2	0
435	25.2	10
	24.3	20
	16.7	30
	9.6	60

$$\begin{aligned}\text{Fractional Conversion, } X &= (L_0 - L) / L_0 \\ &= (27.2 - 25.2) / 27.2 \\ &= 0.072\end{aligned}$$

For a spherical geometry,

$$f(X) = [ 1 - (3*(1-X))^{2/3} + (2*(1-X)) ] \dots (67)$$

Substituting the value of  $X = 0.072$ , in equation (67),

$$f(X) = 0.002$$

$R$  = radius of sphere, (as all the chips are approximated as spheres ), = equivalent diameter / 2

Equivalent diameter, (i.e., diameter of a sphere with same  $S/V$  ratio as an irregular particle), is then calculated as follows:



For a sphere,

$$\begin{aligned} S/V &= (4*\pi*R^2)/((4/3)*\pi*R^3) = 3/R \\ &= 6/\text{equivalent diameter.} \end{aligned}$$

Thus, equivalent diameter =  $6/(S/V)$ .

and Radius =  $3/(S/V)$ .

This has been used as an estimate of equivalent particle diameter because at the pH of the cook (pH=11.34) used in the experimental work, transport through chips in all directions is important.

Hence,  $R = d_e/2 = 0.360$  cms.

Hence,  $t/R^2 = 10/((0.36)^2) = 77$  mins/cm<sup>2</sup>.

Sample Calculation for the plots of  $f(X)/\text{Effective Diffusivity}$  versus  $t/R^2$ .

Calculation of Effective Diffusivity ( $D/Do$ ):

Sample # 1 ;  $d_e = 0.72$  cms ;  $S/V = 8.32$   $\text{cm}^{-1}$ .

Temperature =  $171^\circ\text{C} = 444^\circ\text{K}$

length = 2.625 cms.

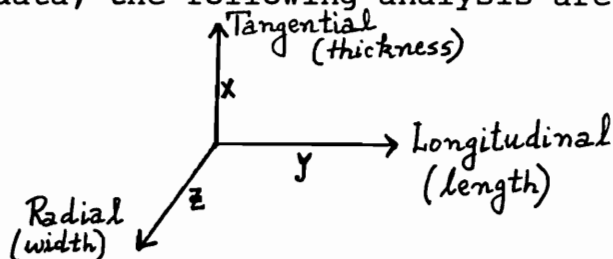
width = 1.050 cms.

thickness = 0.353 cms.

Sample rate data:

Lignin, L (% on wood)	time, t (mins)
27.2	0
25.16	10
20.14	20
14.34	30
11.02	60

Using the data, the following analysis are carried out:



Calculation of  $Do$  - "Hydroxyl ion diffusivity" in the absence of porous solid

$$Do = 5.7 \cdot 10^{-2} \cdot (T)^{1/2} \cdot \exp(-4870/(R \cdot T)) \quad \dots (68)$$

Substituting the value of Temperature,  $T=444^\circ\text{K}$ , in the equation (67), we get

$$Do = 0.0048 \text{ cm}^2/\text{min}.$$

Calculation of D, Diffusivity of  $[\text{OH}]^-$  in wood chips:

According to Gustafson's Equation,

$$\text{Diffusivity , } D = 5.7 \cdot 10^{-2} \cdot (T)^{1/2} \cdot \exp(-4870/(R \cdot T)) \cdot ((-0.02 \cdot [L]) + (.13 \cdot [\text{OH}] \cdot 55) + 0.58) \dots (69)$$

pH of liquor = 11.34.

Thus,  $[\text{OH}]^- = 0.0022$  mols/lit.

At  $t = 10$  mins,  $L(\% \text{ on wood}) = 25.16(\% \text{ on wood})$

Substituting these numbers in equation (69),

$$D = 0.000391 \text{ cm}^2/\text{min.}$$

Calculation of  $(D \cdot t)/l^2$ , where  $l$ , is the chip dimension

For longitudinal direction,

$$(D \cdot t)/l^2 = (D_0 \cdot t) \cdot (D)/(l^2 \cdot D_0) \dots (70)$$

where,  $D/D_0 = \text{Effective Diffusivity.}$

The effective diffusivity is read from Table 2 of the appendix section. As our Softwood chip mix had various species combined, hence, an average value of 0.47 was read from the longitudinal part of the table.

Hence, for the longitudinal direction,

substituting the values of  $D_0$ ,  $t$ ,  $l$ , and  $(D/D_0)$  into equation (70),

$$(D \cdot t)/l^2 = \frac{(0.0048 \cdot 10)}{(2.625)^2} \cdot 0.47$$

$$\begin{aligned} \text{For tangential direction, } (D \cdot t)/l^2 &= (0.000391 \cdot 10)/(0.3525)^2 \\ &= 0.0314 \end{aligned}$$

$$\begin{aligned} \text{For radial direction, } (D \cdot t)/l^2 &= (0.000391 \cdot 10)/(1.050)^2 \\ &= 0.0035 \end{aligned}$$

Use of table 2 and equation (70) was only made

for the biggest chip dimension (Longitudinal direction), and for tangential and radial directions,  $(D*t)/l^2$  was calculated by direct substitutions of the values of  $D$ ,  $t$ , and  $l$  only.

Calculation of  $E_{ax}$ ,  $E_{ay}$ ,  $E_{az}$  and  $E_a$ :

Use of Figure 3 is made to read the values of  $E_{ax}$ ,  $E_{ay}$ , and  $E_{az}$  values using the slab geometry for radial, longitudinal, and tangential directions respectively. For longitudinal directions, at  $(D*t)/l^2=0.00328$ ,  $E_{ay}=0.808$   
 For radial directions, at  $(D*t)/l^2=0.00350$ ,  $E_{ax}=0.807$   
 For tangential direction, at  $(D*t)/l^2=0.0314$ ,  $E_{ay}=0.752$ .

$$E_a = E_{ax}*E_{ay}*E_{az} = 0.808*0.807*0.752$$

$$E_a = 0.490. \quad \dots (71)$$

Calculation of  $D$  from  $(D*t)/a^2$ :

As all the chip sizes are approximated as spheres, hence,  $r$  - radius of sphere = equivalent diameter/2  

$$= 0.72/2 = 0.36 \text{ cms.}$$

At  $E_a = 0.490$ , from figure 3,

$$(D*t)/a^2 = 0.017 \quad \dots (72)$$

as,  $a = 0.36 \text{ cms}$ , hence, from equation (72),

$$D = 0.00022 \text{ cm}^2/\text{min.} \quad \dots (73)$$

Calculation of Effective Diffusivity ( $D/Do$ ):

This value of  $D$ , as obtained in equation (73) is then divided by the value of  $Do$  obtained in equation (68).

$$\text{Hence, } D/Do = 0.00022/0.0048 = 0.046$$

$t/R^2$  is obtained by dividing time by  $(\text{Radius})^2$

$f(X)$  values are calculated as shown in the last sample calculations of  $f(X)$  versus  $t/R^2$ . This value of  $f(X)$  is then divided by  $D/D_0$ , and plotted against the calculated  $t/R^2$  values.

## 2. Cooking Liquor Preparation.

### a. Finite Heat - Up Method of Pulping.

System: ASAQ pulping process.

pH of liquor: 11.34

Chemicals used:  $\text{Na}_2\text{SO}_3$ ,  $\text{Na}_2\text{CO}_3$ , and Anthraquinone.

$$\text{Na}_2\text{SO}_3 : \text{Na}_2\text{CO}_3 = 75 : 25$$

$$\text{Liquor} : \text{Wood} = 7 : 1$$

$$\text{Wood} : \text{Chemicals} = 100 : 20$$

$$\text{Chemicals} : \text{Liquor} = 20 : 700$$

$$= 0.0286 \text{ gm of } \text{Na}_2\text{SO}_3 \text{ and}$$

$$\text{Na}_2\text{CO}_3 \text{ are in 1 gm of liquor.}$$

Total amount of liquor = 7.5 kg. = 7500 g of liquor.

Thus, in 7500 g. of liquor, use  $(7500 \cdot 0.0286) = 214.5 \text{ g}$  of  $\text{Na}_2\text{SO}_3$  and  $\text{Na}_2\text{CO}_3$ , as  $\text{Na}_2\text{O}$ .

As the ratio of  $\text{Na}_2\text{SO}_3 : \text{Na}_2\text{CO}_3 = 75 : 25$ ,

hence, 160.9 g  $\text{Na}_2\text{SO}_3$  are present as  $\text{Na}_2\text{O}$ ,

and, 53.6 g  $\text{Na}_2\text{CO}_3$  are present as  $\text{Na}_2\text{O}$ .

$$\text{or } 160.9 \text{ g } \text{Na}_2\text{SO}_3 \cdot \frac{126 \text{ (Molecular wt. of } \text{Na}_2\text{SO}_3)}{62 \text{ (Molecular wt. of } \text{Na}_2\text{O})}$$

$$= 327 \text{ g } \text{Na}_2\text{SO}_3 \text{ are present as } \text{Na}_2\text{SO}_3$$

$$\text{Similarly, } 53.6 \text{ g } \text{Na}_2\text{CO}_3 \cdot \frac{106 \text{ (Molecular wt. of } \text{Na}_2\text{CO}_3)}{62 \text{ (Molecular wt. of } \text{Na}_2\text{O})}$$

$$= 92 \text{ g } \text{Na}_2\text{CO}_3 \text{ are present as } \text{Na}_2\text{CO}_3.$$

Anthraquinone (AQ) used was 0.3 % on wood basis.

$$\frac{0.3 \text{ g AQ} \cdot (100 \text{ g dry wood}) \cdot (7500 \text{ g liquor})}{(100 \text{ g dry wood}) \cdot 700 \text{ g liquor}}$$

$$= 3.21 \text{ g AQ.}$$

## b. Isothermal method of Pulping.

System: ASAQ process.

$$\text{Na}_2\text{SO}_3 : \text{Na}_2\text{CO}_3 = 75 : 25$$

$$\text{Liquor} : \text{Wood} = 7 : 1$$

$$\text{Wood} : \text{Chemicals} = 100 : 20$$

$$\text{Chemicals} : \text{Liquor} = 20 : 700$$

= 0.0286 g  $\text{Na}_2\text{SO}_3$  and  $\text{Na}_2\text{CO}_3$  are  
present in 1 g of liquor.

Total amount of liquor used = 9300 g of liquor.

Hence, in 9300 g of liquor, use  $(9300 \times 0.0286) = 266$  g  
of  $\text{Na}_2\text{SO}_3$  and  $\text{Na}_2\text{CO}_3$ .

$$\text{As } \text{Na}_2\text{SO}_3 : \text{Na}_2\text{CO}_3 = 75 : 25$$

$266 \times 0.75 = 199.5$  g of  $\text{Na}_2\text{SO}_3$  are present as  $\text{Na}_2\text{O}$

and  $266 \times 0.25 = 66.5$  g of  $\text{Na}_2\text{CO}_3$  are present as  $\text{Na}_2\text{O}$ .

$$\text{Thus, } 199.5 \text{ g } \text{Na}_2\text{SO}_3 \times \frac{126 \text{ (Molecular wt. of } \text{Na}_2\text{SO}_3)}{62 \text{ (Molecular wt. of } \text{Na}_2\text{O)}}$$

$$= 405.43 \text{ g of } \text{Na}_2\text{SO}_3 \text{ are present as } \text{Na}_2\text{SO}_3.$$

$$\text{Similarly, } 66.5 \text{ g } \text{Na}_2\text{CO}_3 \times \frac{106 \text{ (Molecular wt. of } \text{Na}_2\text{CO}_3)}{62 \text{ (Molecular wt. of } \text{Na}_2\text{O)}}$$

$$= 113.70 \text{ g of } \text{Na}_2\text{CO}_3 \text{ are present as } \text{Na}_2\text{CO}_3.$$

Anthraquinone (AQ) used was 0.3 % on wood basis:

$$\text{Thus, } \frac{0.3 \text{ g AQ}}{100 \text{ g dry wood}} \times \frac{(100 \text{ g dry wood})}{700 \text{ g liquor}} \times (9300 \text{ g liquor})$$

$$= 3.98 \text{ g AQ was used.}$$

Table A-1. Pulping data # 1 of "Finite Heat-Up  
method of pulping";

Maximum Temperature = 438<sup>o</sup>K;

Time at maximum temperature = 0 minutes.

Chip size,					
(de, cms.)	0.72	0.43	0.28	0.20	0.11
[L] <sub>0</sub> (% onwood)	27.23	26.83	27.80	26.14	26.10
Moisture Content					
( % )	6.65	7.53	6.91	6.76	7.54
Yield (%)	88.02	85.62	86.02	81.92	81.02
Lignin(% on Pulp)	27.54	25.41	23.49	25.17	24.29
Lignin(% on Wood)	24.24	21.76	20.21	20.62	19.68
% delignification	11	19	27	21	25



Table A-2. Pulping data # 2 of "Finite Heat-Up  
method of pulping";

Maximum Temperature = 438<sup>o</sup>K ;

Time at maximum temperature = 20 minutes.

-----					
Chip Size,					
(de, cms.)	0.72	0.43	0.28	0.20	0.11
[L] <sub>0</sub> , % on wood	27.23	26.83	27.80	26.14	26.10
Moisture Content					
( % )	6.65	7.53	9.91	6.76	7.54
Yield (%)	79.40	74.80	74.20	72.80	73.00
Kappa Number	165	137	148	145	146
	±2.4	±0.9	±2.4	±2.9	±1.8
Lignin (% on pulp)	18.54	15.98	17.01	16.77	16.80
	±.18	±.10	±.24	±.32	±.16
Lignin (% on wood)	14.72	11.95	12.26	12.20	12.62
	±.14	±.09	±.18	±.23	±.12
% Delignification	45.94	55.46	55.89	53.33	51.65
-----					

Table A-3. Pulping data # 3 of "Finite Heat-Up  
method of pulping";

Maximum Temperature = 438<sup>o</sup>K;

Time at maximum temperature = 60 minutes.

-----					
Chip size					
(de, cms)	0.72	0.43	0.28	0.20	0.11
[L] <sub>o</sub> (% on wood)	27.23	26.83	27.80	26.14	26.10
Moisture Content					
( % )	6.65	7.53	6.91	6.76	7.54
Yield (%)	70.00	63.60	64.30	63.20	67.00
Kappa Number	140	114	122	121	116
	±2.2	±2.8	±1.7	±1.5	±0.9
Lignin,					
(% on pulp)	16.21	13.79	14.53	14.45	14.02
	±.17	±.23	±.12	±.12	±.10
Lignin,					
(% on wood)	11.35	8.77	9.34	9.13	9.39
	±.12	±.14	±.08	±.07	±.06
% Delignification	58.32	67.31	66.40	65.07	64.02
-----					

Table A-4. Pulping data # 4 of "Finite Heat-Up  
method of pulping";

Maximum Temperature = 438<sup>o</sup>K;

Time at maximum temperature = 180 minutes.

---

Chip size,					
(de, cms)	0.72	0.43	0.28	0.20	0.11
[L] <sub>o</sub> (% on wood)	27.23	26.83	27.80	26.14	26.10
Yield (%)	53.54	50.66	50.64	50.72	54.78
Kappa Number	73.90	71.50	64.90	70.70	76.20
	± 1	±1.5	±1.5	±1.1	±1.7
Lignin					
(% on pulp)	10.07	9.84	9.23	9.77	10.30
	±.11	±.09	±.14	±.08	±.20
Lignin					
(% on wood)	5.39	4.98	4.67	4.95	5.63
	±.06	±.04	±.07	±.04	±.11
% Delignification	80.20	81.44	83.20	81.06	78.43

Table A-5. Pulping data # 1 of "Isothermal method of pulping"; Constant Temperature = 435°K.

Time at constant temperature = 10 minutes.

---

Chip size					
(de, cms.)	0.72	0.43	0.28	0.20	0.11
[L] <sub>0</sub> (% on wood)	27.23	26.83	27.80	26.14	26.10
Moisture Content					
( % )	6.65	7.53	6.91	6.76	7.54
Yield ( % )	91.90	89.70	91.40	85.20	82.90
Lignin					
(% on pulp)	27.50	28.04	26.91	27.24	27.14
Lignin					
(% on wood)	25.28	25.15	24.60	24.90	22.50
% Delignification	7.16	6.26	11.50	4.74	13.79

---

Table A-6. Pulping data # 2 of "Isothermal method of pulping"; Constant Temperature = 435°K.

Time at constant temperature = 20 minutes.

-----					
Chip size					
(de, cms.)	0.72	0.43	0.28	0.22	0.11
[L] <sub>0</sub> (% on wood)	27.23	26.83	27.80	26.14	26.10
Moisture Content					
( % )	6.65	7.53	6.91	6.76	7.54
Yield ( % )	87.60	83.50	85.40	79.00	76.20
Kappa Number				185	144
				±2.7	±2.2
Lignin					
(% on pulp)	27.81	24.94	24.29	20.43	16.59
				±.22	±.17
Lignin					
(% on wood)	24.36	20.82	20.74	16.14	12.64
				±.17	±.13
% Delignification	10.54	22.40	25.39	38.26	51.57
-----					

Table A-7. Pulping data # 3 of "Isothermal method of  
pulping"; Constant Temperature = 435°K;  
Time at constant temperature = 30 minutes.

-----					
Chip size					
(de, cms.)	0.72	0.43	0.28	0.20	0.11
[L] <sub>0</sub> (% on wood)	27.23	26.83	27.80	26.14	26.10
Moisture Content					
( % )	6.65	7.53	6.91	6.76	7.54
Yield (%)	81.30	76.90	78.20	71.40	73.00
Kappa Number		135	139	146	136
		±2.7	±2.2	±1.5	±2.5
Lignin					
(% on pulp)	20.49	15.81	16.16	16.80	15.90
		±.28	±.21	±.13	±.26
Lignin					
(% on wood)	16.66	12.16	12.64	11.99	11.59
		±.21	±.16	±.09	±.19
% Delignification	38.82	54.67	54.53	54.13	55.60
-----					

Table A-8. Pulping data # 4 of "Isothermal method of pulping"; Constant Temperature = 435°K;  
Time at constant temperature = 60 minutes.

-----					
Chip size					
(de, cms)	0.72	0.43	0.28	0.20	0.11
[L] <sub>0</sub> (% on wood)	27.23	26.83	27.80	26.14	26.10
Moisture Content					
( % )	6.65	7.53	6.91	6.76	7.54
Yield ( % )	68.60	65.10	64.40	62.16	63.20
Kappa Number	118	125	122	112	113
	$\pm 1.6$	$\pm 0.7$	$\pm 1.4$	$\pm 1.0$	$\pm 0.5$
Lignin					
(% on pulp)	14.13	14.80	14.56	13.60	13.73
	$\pm 0.9$	$\pm .02$	$\pm .13$	$\pm .06$	$\pm .05$
Lignin					
(% on wood)	9.69	9.63	9.38	8.45	8.68
	$\pm .06$	$\pm .01$	$\pm .08$	$\pm .04$	$\pm .03$
% Delignification	64.41	64.11	66.26	67.67	66.74
-----					

Table A-9. Pulping data # 5 of "Isothermal  
method of pulping"; Constant Temperature  
= 444°K; Time at constant temperature = 10  
minutes.

-----					
Chip size					
(de, cms.)	0.72	0.43	0.28	0.20	0.11
[L] <sub>0</sub> (% on wood)	27.23	26.83	27.80	26.14	26.10
Moisture Content					
( % )	6.65	7.53	6.91	6.76	7.54
Yield ( % )	89.00	87.40	88.40	78.40	75.70
Kappa Number				163	153
				±1.6	±2.3
Lignin					
(% on pulp)	28.26	24.79	28.59	18.41	17.46
				±.16	±.21
Lignin					
(% on wood)	25.16	21.66	25.27	14.44	13.22
				±.12	±.16
% Delignification	7.60	19.27	9.10	44.76	49.35
-----					



Table A-10. Pulping data # 6 of "Isothermal method  
of pulping"; Constant Temperature = 444<sup>o</sup>K  
Time at constant temperature = 20 minutes.

-----					
Chip size					
(de, cms)	0.72	0.43	0.28	0.20	0.11
[L] <sub>0</sub> (% on wood)	27.23	26.83	27.80	26.14	26.10
Moisture Content					
( % )	6.65	7.53	6.91	6.76	7.54
Yield ( % )	82.60	80.80	76.90	73.20	70.60
Kappa Number			163	147	145
			±1.6	±2.0	±2.5
Lignin					
(% on pulp)	24.38	22.97	18.32	16.85	16.70
			±.07	±.13	±.22
Lignin					
(% on wood)	20.14	18.56	14.08	12.23	11.76
			±.05	±.09	±.15
% Delignification	26.04	30.82	49.35	52.83	50.42
-----					

Table A-11. Pulping data # 7 of "Isothermal method of pulping"; Constant Temperature = 444°K.

Time at constant temperature = 30 minutes.

-----					
Chip size					
(de, cms.)	0.72	0.43	0.28	0.20	0.11
[L] <sub>0</sub> (% on wood)	27.23	26.83	27.80	26.14	26.10
Moisture Content					
( % )	6.65	7.53	6.91	6.76	7.54
Yield ( % )	77.90	80.40	71.50	69.10	64.50
Kappa Number	163		130	135	124
	±2.0		±2.1	±2.2	±0.8
Lignin					
(% on pulp)	18.41	23.23	15.31	15.79	14.75
	±.2		±.19	±.21	±.07
Lignin					
(% on wood)	14.34	18.68	10.94	10.91	9.51
	±.15		±.13	±.14	±.04
% Delignification	47.34	30.37	60.65	58.26	63.56
-----					

Table A-12. Pulping data # 8 of "Isothermal method of pulping"; Constant Temperature = 444°K.

Time at constant temperature = 60 minutes.

-----					
Chip size					
(de, cms.)	0.72	0.43	0.28	0.20	0.11
[L] <sub>0</sub> (% on wood)	27.23	26.83	27.80	26.14	26.10
Moisturé Content					
( % )	6.65	7.53	6.91	6.76	7.54
Yield ( % )	66.80	64.10	63.60	61.20	61.60
Kappa Number	143	115	118	110	111
	±1.8	±2.7	±1.8	±1.41	±0.8
Lignin					
(% on pulp)	16.49	13.94	14.17	13.45	13.57
	±.13	±.28	±.15	±.14	±.11
Lignin					
(% on wood)	11.02	8.93	9.02	8.23	8.36
	±.08	±.18	±.09	±.08	±.07
% Delignification	59.53	66.72	67.55	68.51	67.77
-----					

Table A-13. Pulping data # 9 of "Isothermal method of  
pulping"; Constant Temperature = 453°K

Time at constant temperature = 10 minutes.

-----					
Chip size					
(de, cms.)	0.72	0.43	0.28	0.20	0.11
[L] <sub>0</sub> (% on wood)	27.23	26.83	27.80	26.14	26.10
Moisture Content					
( % )	6.65	7.53	6.91	6.76	7.54
Yield ( % )	81.30	77.80	78.80	72.80	67.80
Kappa Number		119	129	144	121
		±2.0	±3.8	±2.2	±2.4
Lignin					
(% on pulp)	16.40	14.30	15.28	16.68	14.46
		±.20	±.42	±.26	±.21
Lignin					
(% on wood)	13.34	11.11	12.04	12.14	9.80
		±.15	±.33	±.19	±.14
% Delignification	51.0	58.59	56.69	53.56	62.45
-----					

Table A-14. Pulping data # 10 of "Isothermal method of pulping"; Constant Temperature = 453°K

Time at constant temperature = 20 minutes.

-----					
Chip size					
(de, cms.)	0.72	0.43	0.28	0.20	0.11
[L] <sub>0</sub> (% on wood)	27.23	26.83	27.80	26.14	26.10
Moisture Content					
( % )	6.65	7.53	6.91	6.76	7.54
Yield ( % )	86.22	67.11	66.00	61.89	60.67
Kappa Number		117	116	113	105
		<u>±</u> 1.1	<u>±</u> .9	<u>±</u> 1.3	<u>±</u> 2.3
Lignin					
(% on pulp)	28.42	14.15	14.08	13.67	12.96
		<u>±</u> .16	<u>±</u> .16	<u>±</u> .07	<u>±</u> .20
Lignin					
(% on wood)	24.51	9.49	9.29	8.46	7.86
		<u>±</u> .10	<u>±</u> .10	<u>±</u> .04	<u>±</u> .12
% Delignification	9.98	64.33	66.58	67.63	69.88
-----					

Table A-15. Pulping data # 11 of "Isothermal method of  
 pulping"; Constant Temperature = 453<sup>o</sup>K  
 Time at constant temperature = 30 minutes.

-----					
Chip size					
(de, cms.)	0.72	0.43	0.28	0.20	0.11
[L] <sub>0</sub> (% on wood)	27.23	26.83	27.80	26.14	26.10
Moisture Content					
( % )	6.65	7.53	6.91	6.76	7.54
Yield ( % )	72.20	68.60	66.80	63.60	63.00
Kappa Number	133	132	110	131	120
	±1.2	±1.1	±1.5	±1.1	±2.2
Lignin					
(% on pulp)	15.63	15.55	13.44	15.38	14.37
	±.15	±.15	±.14	±.07	±.20
Lignin					
(% on wood)	11.28	10.67	8.98	9.78	9.05
	±.10	±.10	±.09	±.04	±.12
% Delignification	58.58	60.23	67.70	62.58	65.31
-----					

Table A-16. Pulping data # 12 of "Isothermal method of pulping"; Constant Temperature = 453°K  
Time at constant temperature = 75 minutes.

-----					
Chip size					
(de, cms.)	0.72	0.43	0.28	0.20	0.11
[L] <sub>0</sub> (% on wood)	27.23	26.83	27.80	26.14	26.10
Moisture Content					
( % )	6.65	7.53	6.91	6.76	7.54
Yield ( % )	54.90	52.00	52.90	51.55	52.44
Kappa Number	90	71	63	56	52
	±1.4	±0.7	±1.1	±1.7	±1.3
Lignin					
(% on pulp)	11.58	9.76	9.06	8.42	8.05
	±.14	±.03	±.12	±.19	±.16
Lignin					
(% on wood)	6.35	5.07	4.79	4.34	4.22
	±.07	±.01	±.06	±.09	±.08
% Delignification	76.70	81.10	82.17	83.39	83.83
-----					

Table A-17. Lignin versus Kappa Calibration.

Pulp #	1	2	3	4	5	6
Kappa	101	127	75	99	150	56
Yield (%)	66	75	60	75	65	55
Lignin (% on pulp)	13.39	14.00	10.07	13.81	17.01	7.61
Lignin (% on wood)	8.88	10.47	6.04	10.30	11.04	4.18



Table A-18. Shrinking Core Models data for the  
analysis of Wilder & Daleski's delignification  
rate data (22); Temperature of pulping  
= 423°K; Reference time,  $t_a = 105$  mins.

Lignin, L (% on wood)	time, t (mins)	Frac. Conversion $X_c = (L_0 - L) / L_0$	t/ $t_a$	Film Diff.
28.8	0	0	0	0
23.6	5	.18	.05	.23
20.5	15	.29	.14	.37
15.8	35	.45	.33	.58
11.8	55	.59	.52	.76
9.6	75	.67	.71	.86
6.5	105	.77	1.00	1.00

Lignin, L (% on wood)	time, t (mins.)	Internal Diffusion	Chemical Reaction	Uniform Conc.
28.8	0	0	0	0
23.6	5	.054	.23	.13
20.5	15	.14	.37	.23
15.8	35	.34	.58	.40
11.8	55	.58	.76	.60
9.6	75	.74	.86	.74
6.5	105	1.00	1.00	1.00

Table A-19. Shrinking Core Models for the analysis of  
Olm and Tistad's delignification rate data.  
Operating Temperature = 313<sup>o</sup>K.  
ta = 14 minutes.

Lignin, L (% on wood)	time, t (mins)	t/ta	Frac. Conversion Xc=(Lo-L)/Lo		2 Dim.Slab
			Xc/Xa	Int.Diff.	
29.25	0	0	0	0	0
26.84	5	.36	.08	.56	.31
25.23	10	.71	.13	.88	.78
25.03	12.5	.89	.14	.98	.97
24.92	14.0	1.00	.15	1.00	1.00
Xc	Long Cyl.	Sphere	Long Cyl.	Sphere	Uniform
	Int.Diff.	Int.Diff.	Chem.Reac.	Chem.Reac.	Conc.
0	0	0	0	0	0
.08	.31	.31	.54	.55	.54
.13	.78	.78	.88	.88	.87
.14	.97	.97	.97	.98	.98
.15	1.00	1.00	1.00	1.00	1.00

Table A-20. Shrinking Core Models for the analysis of  
the finite heat-up method of pulping data .  
chip size,  $d_e = 0.72$  cms ; Temperature  
=  $438^\circ\text{K}$ .  $t_a = 180$  minutes.

Lignin, L (% on wood)	time, t (mins.)	Frac. Conv. (X)	(Xc/Xa)	2 Dim Slab Int.Diff.	Long Cyl. Int.Diff.	
24.20	0	0	0	0	0	
14.70	20	.39	.11	.50	.25	
11.30	60	.53	.33	.68	.46	
5.40	180	.78	1.00	1.00	1.00	
Frac. Conv. (Xc)	Long Cyl. Int.diff.	Long Cyl. Chem.Reac	Sphere Int.Diff.	Sphere Chem.Reac.	Uniform Conc.	
0	0	0	0	0	0	
.39	.20	.41	.18	.38	.33	
.53	.37	.58	.37	.56	.50	
.78	1.00	1.00	1.00	1.00	1.00	

Table A-21. Shrinking Core Models for the analysis of the Isothermal method of pulping data: chip size,  $d_c = 0.43$  cms ; Temperature =  $438^\circ\text{K}$ ; Long Cylinder Geometry; Reference time,  $t_a = 180$  minutes.

Lignin, L (% on wood)	time, t (mins.)	Frac. Conversion $X_c = (L_0 - L) / L_0$	t/ $t_a$	Film Diff.	Int. Diff.
20.21	0	0	0	0	0
12.30	20	0.39	0.11	0.51	0.21
9.34	60	0.54	0.33	0.70	0.42
4.67	180	0.77	1.00	1.00	1.00

Frac. Conv. $X_c = (L_0 - L) / L_0$	Chemical Reaction	Uniform Conc.
0	0	0
0.39	0.42	0.34
0.54	0.62	0.53
0.77	1.00	1.00

Table A-22. Shrinking Core Models for the analysis of  
 Isothermal method of Pulping data; chip  
 size,  $d_e = 0.72$  cms ; Temperature =  $444^\circ\text{K}$ .  
 $t_a = 60$  minutes;  $t_o = 10$  minutes.

Lignin, L (% on wood)	time, t (mins.)	Frac. Conversion $X_c = (L_o - L) / L_o$	t-t <sub>o</sub>	X <sub>c</sub> /X <sub>a</sub>	2 dim.Slab Int.Diff.	
25.16	10	0	0	0	0	0
20.14	20	.20	.20	.36	.13	
14.34	30	.43	.40	.77	.59	
11.02	60	.56	1.00	1.00	1.00	
X <sub>c</sub>	Long Cyl. Int.Diff.	Long Cyl. Chem.Reac.	Sphere Int.Diff.	Sphere Chem.Reac	Uniform Conc.	
0	0	0	0	0	0	0
.20	.11	.31	.1	.30	.27	
.43	.55	.73	.53	.71	.68	
.56	1.00	1.00	1.00	1.00	1.00	

Table A-23. Shrinking Core Models for the analysis of the Isothermal method of pulping data:

chip size,  $d_e = 0.11$  cms ; Temperature

=  $435^\circ\text{K}$ ; Spherical geometry;

$t_a = 60$  minutes;  $t_o = 10$  minutes.

Lignin, L (% on wood)	time, t (mins)	Frac.Conversion $X_c = (L_o - L) / L_o$	$\frac{(t - t_o)}{(t_a - t_o)}$	Film Diff.	Int. Diff.
22.50	10	0	0	0	0
12.60	20	0.44	0.2	0.72	0.46
11.60	30	0.48	0.4	0.78	0.56
8.70	60	0.61	1.00	1.00	1.00
Xc	Chem. Reac.	Uniform Conc.			
0	0	0			
.44	.65	.62			
.48	.72	.69			
1.00	1.00	1.00			

Table A-24. Table # 1 of "Accounting for time variable diffusivity". Isothermal method of pulping. chip size,  $d_e = 0.72$  cms;  $R^2 = 0.13$  cm<sup>2</sup>.

---


$$f(X) = (1 - (3*(1-X)^{2/3}) + (2*(1-X)))$$

Frac.Conversion,  $X_c = (L_0 - L) / L_0$

Temp. (°K)	Lignin, L (% on wood)	time, t (mins)	Xc	f(X)	t/R <sup>2</sup>	r <sup>2</sup>
	27.23	0	0	0	0	
	25.28	10	.07	.002	77	
435	24.36	20	.10	.004	154	.902
	16.70	30	.39	.062	231	
	9.69	60	.64	.206	463	
	27.23	0	0	0	0	
	25.16	10	.08	.003	77	
444	20.14	20	.26	.026	154	.944
	14.34	30	.47	.097	231	
	11.00	60	.59	.169	463	
	27.23	0	0	0	0	
	13.34	10	.51	.116	77	
453	24.51	20	.10	.56	154	.912
	11.28	30	.59	.162	231	
	6.35	75	.77	.331	576	

---

Table A-25. Table # 2 of "Accounting for time variable diffusivity"; Isothermal method of pulping; chip size,  $d_e = 0.72$  cms;  $R^2 = 0.13$  cm<sup>2</sup>.

---

Frac. Conversion,  $X_c = (L_0 - L) / L_0$   
 $f(X) = (1 - (3 * (1 - X)^{2/3}) + (2 * (1 - X)))$

Temp. Lignin, L	time, t	$X_c$	$f(X)$	$D_0$	$D/D_0$	$f(X)$	$t/R^2$	$r^2$
(°K)	(% on wood)	(mins)				(D/D <sub>0</sub> )		
27.23	0	0	0	.0044	*	0	0	
25.28	10	.07	.002	.0044	.044	.04	77	
435	24.36	20	.10	.0044	.042	.09	154	.93
	16.70	30	.39	.0044	.085	.73	231	
	9.69	60	.64	.0044	.124	1.66	463	
27.23	0	0	0	.0048	*	0	0	
25.16	10	.08	.003	.0048	.046	.06	77	
444	20.14	20	.26	.0048	.067	.39	154	.96
	14.34	30	.47	.0048	.097	1.00	231	
	11.02	60	.59	.0048	.114	1.79	463	
27.23	0	0	0	.0054	*	0	0	
13.34	10	.51	.116	.0054	.115	1.00	77	
453	24.51	20	.10	.0054	.039	14.28	154	.87
	11.28	30	.59	.0054	.112	1.45	231	
	6.35	75	.77	.0054	.146	2.27	576	

---

\* Calculation of the following point was not carried out, as  $f(X)/(D/D_0) = 0$ , at time,  $t = 0$  mins.



Table A-26. Table # 3 of "Accounting for time variable diffusivity". Isothermal method of pulping; chip size,  $d_e = 0.43$  cms;  $R^2 = .046$  cm<sup>2</sup>.

---

Frac. Conversion,  $X_c = (L_0 - L) / L_0$

$f(X) = (1 - (3*(1-X)^{2/3}) + (2*(1-X)))$

Temp (°K)	Lignin, L (% on wood)	time, t (mins)	X	f(X)	Do	D/Do	$\frac{f(X)}{(D/Do)}$	t/R <sup>2</sup>	r <sup>2</sup>
	26.83	0	0	0	.0044	*	0	0	
	25.15	10	.06	.002	.0044	.01	.13	217	
435	20.82	20	.22	.019	.0044	.05	.36	435	.88
	12.16	30	.55	.137	.0044	.10	1.30	652	
	9.63	60	.64	.203	.0044	.12	1.66	870	
	26.83	0	0	0	.0048	*	0	0	
	21.66	10	.19	.01	.0048	.02	.56	217	
444	18.60	20	.31	.04	.0048	.06	.65	435	.90
	18.70	30	.30	.04	.0048	.06	.62	652	
	8.93	60	.67	.22	.0048	.09	2.52	870	
	26.83	0	0	0	.0054	*	0	0	
	11.11	10	.59	.16	.0054	.11	1.14	217	
453	9.5	20	.64	.20	.0054	.12	1.67	435	.74
	10.7	30	.60	.17	.0054	.11	1.49	652	
	5.1	74	.81	.39	.0054	.15	2.57	1630	

---

\* Calculation of the following point was not carried out as  $f(X)/(D/Do) = 0$ , as  $f(X) = 0$ , at time,  $t = 0$ .

Table A-27. Table # 4 of "Accounting for time variable diffusivity". Isothermal method of pulping; chip size,  $d_e = 0.28$  cms;  $R^2 = .020$   $\text{cm}^2$ .

---

Frac.Conversion,  $X_c = (L_0 - L) / L_0$   
 $f(X) = (1 - (3 * (1 - X)^{2/3}) + (2 * (1 - X)))$

Temp. (°K)	Lignin, L (% on wood)	time, t (mins)	$X_c$	$f(X)$	$D_0$	$D/D_0$	$\frac{f(X)}{(D/D_0)}$	$t/R^2$	$r^2$
	27.80	0	0	0	.0044	*	0	0	
	24.60	10	.11	.005	.0044	.031	.161	495	
435	20.70	20	.25	.025	.0044	.052	.480	990	.92
	12.60	30	.55	.139	.0044	.098	1.418	1485	
	9.40	60	.66	.225	.0044	.114	1.973	1980	
	27.80	0	0	0	.0048	*	0	0	
	25.3	10	.09	.003	.0048	.026	.115	495	
444	14.10	20	.49	.107	.0048	.086	1.244	990	.81
	10.94	30	.61	.175	.0048	.110	1.600	1485	
	9.0	60	.67	.230	.0048	.117	1.960	1980	
	27.80	0	0	0	.0054	*	0	0	
	12.04	10	.57	.137	.0054	.094	1.583	495	
453	9.30	20	.66	.223	.0054	.114	1.956	990	.83
	8.98	30	.67	.234	.0054	.118	1.983	1485	
	4.80	75	.83	.415	.0054	.120	3.458	3710	

---

\* Calculation of the following point was not carried out as  $f(X)/(D/D_0) = 0$ , as  $f(X) = 0$ , as time,  $t = 0$

Table A-28. Table # 5 of "Accounting for time variable diffusivity". Isothermal Method of pulping; chip size,  $d_e = 0.20$  cms;  $R^2 = 0.01$  cm<sup>2</sup>.

---

Frac. Conversion,  $X_c = (L_0 - L) / L_0$

$f(X) = (1 - (3 * (1 - X)) + (2 * (1 - X)))$

Temp. (°K)	Lignin, L (% on wood)	time, t (mins)	Xc	f(X)	Do	D/Do	$\frac{f(X)}{(D/Do)}$	t/R <sup>2</sup>	r <sup>2</sup>
26.14		0	0	0	.0044	*	0	0	
24.90		10	.05	.001	.0044	.028	.03	1000	
435	16.10	20	.39	.061	.0044	.076	.80	2000	.91
	12.0	30	.54	.131	.0044	.094	1.39	3000	
	8.4	60	.68	.236	.0044	.122	1.93	6000	
26.14		0	0	0	.0048	*	0	0	
	14.40	10	.45	.09	.0048	.09	1.00	1000	
444	12.30	20	.53	.13	.0048	.10	1.30	2000	.76
	10.90	30	.58	.16	.0048	.11	1.48	3000	
	8.23	60	.68	.24	.0048	.12	1.97	6000	
26.14		0	0	0	.0054	*	0	0	
	12.14	10	.53	.13	.0054	.10	1.30	1000	
453	8.46	20	.68	.23	.0054	.12	1.94	2000	.78
	9.78	30	.62	.19	.0054	.11	1.66	3000	
	4.34	75	.83	.43	.0054	.15	2.92	7500	

---

\* Calculation of the following point was not carried

out as  $f(X)/(D/Do) = 0$ , as  $f(X) = 0$  at time,  $t = 0$

Table A-29. Table # 6 of "Accounting for time variable diffusivity". Isothermal method of pulping; chip size,  $d_e = 0.11$  cms;  $R^2 = 0.003$   $\text{cm}^2$ .

---

Frac.Conversion,  $X_c = (L_0 - L) / L_0$   
 $f(X) = (1 - (3 * (1 - X)^{2/3}) + (2 * (1 - X)))$

Temp. (°K)	Lignin, L (% on wood)	time, t (mins.)	$X_c$	$f(X)$	$D_0$	$D/D_0$	$\frac{f(X)}{(D/D_0)}$	$t/R^2$	$r^2$
	26.10	0	0	0	.0044	*	0	0	
	22.50	10	.14	.01	.0044	.04	.15	3333	
435	12.60	20	.52	.09	.0044	.10	.84	6666	.87
	11.60	30	.55	.14	.0044	.11	1.32	9999	
	8.70	60	.67	.22	.0044	.14	1.63	20000	
	26.10	0	0	0	.0048	*	0	0	
	13.20	10	.49	.11	.0048	.11	.99	3333	
444	11.80	20	.55	.14	.0048	.12	1.18	6666	.85
	9.50	30	.63	.20	.0048	.13	1.51	9999	
	8.36	60	.68	.24	.0048	.14	1.70	20000	
	26.10	0	0	0	.0054	*	0	0	
	9.80	10	.62	.19	.0054	.13	1.46	3333	
453	7.90	20	.70	.25	.0054	.14	1.77	6666	.72
	9.05	30	.65	.21	.0054	.13	1.61	9999	
	4.22	75	.84	.44	.0054	.17	2.62	20000	

---

\* Calculation of this point was not carried out as

$f(X)/(D/D_0) = 0$  , as  $f(X) = 0$  at time,  $t = 0$  mins.

Table A-30. Table to calculate Activation Energies of  
Olm and Tistad's delignification rate data (23).

Temp. (°K)	Lignin, L (% on wood)	time (mins)	$1/T \cdot 10^5$ (°K <sup>-1</sup> )	time for L = 25.70	ln(1/t)
413	29.25	0	242	8.40	-2.13
	26.84	5			
	25.23	10			
	25.03	12.5			
	24.92	14.0			
403	29.25	0	248	10.00	-2.30
	26.83	5			
	25.71	10			
	25.33	12.5			
	25.27	14.0			
393	29.25	0	254	12.5	-2.52
	26.41	5			
	26.07	10			
	25.76	12.5			
	25.53	14.0			

Table A-31. Table to calculate Activation Energy of the  
isothermal method of pulping data .

chip size,  $d_e = 0.28$  cms.

Temperature (°K)	Lignin, L (% on wood)	time, t (mins.)
435	27.8	0
	24.6	10
	20.7	20
	12.6	30
	9.4	60
444	27.8	0
	25.3	10
	14.1	20
	10.9	30
	9.0	60
453	27.8	0
	12.0	10
	9.3	20
	8.9	30
	4.8	75

Table A-31 (contd.)

Lignin, L (% on wood)	time, t (mins.)	1/t	ln(1/t)	Temp. T (°K)	1/T*10 <sup>5</sup> (°K <sup>-1</sup> )
	36	.028	-3.60	453	229.8
12	27	.037	-3.30	444	225.2
	10	.100	-2.30	435	220.7
-----					
	25	.040	-3.20	453	229.8
17	18	.055	-2.90	444	225.2
	7	.143	-1.95	435	220.7
-----					
	19	.053	-2.95	453	229.8
21	15	.066	-2.71	444	225.2
	5	.200	-1.61	435	220.7
-----					